

UC Irvine

UC Irvine Electronic Theses and Dissertations

Title

Engineering Physically Active and Genetically Specific Nanoantibiotics

Permalink

<https://escholarship.org/uc/item/0w95m6p4>

Author

Edson, Julius Adebayo

Publication Date

2017

Peer reviewed|Thesis/dissertation

UNIVERSITY OF CALIFORNIA,
IRVINE

Engineering Physically Active and Genetically Specific Nanoantibiotics

DISSERTATION

submitted in partial satisfaction of the requirements
for the degree of

DOCTOR OF PHILOSOPHY

in Chemical and Biochemical Engineering

by

Julius Adebayo Edson

Dissertation Committee:
Professor Young Jik Kwon, Chair
Professor Szu-Wen Wang
Professor Claudia Benavente

2017

DEDICATION

To

all my family

even those not blood related

For

ample love, guidance and support

TABLE OF CONTENTS

	Page
LIST OF FIGURES	vii
LIST OF TABLES	xi
ACKNOWLEDGEMENTS	xii
CURRICULUM VITAE	xv
ABSTRACT OF THE DISSERTATION	xvi
CHAPTER 1: Background and Introduction	1
1.1. Rise of drug resistant infections	1
1.2. Drug-resistance mechanism	2
1.3. Intracellular infections	4
1.4. Genetic specificity in antimicrobial therapy	5
1.5. Using nanoantibiotics as a physically active gene delivery carrier	7
1.6. Chitosan as a physically active carrier	10
1.7. Scope of the dissertation	11
1.8. References	12
CHAPTER 2: Synthesis and characterization of acid-transforming chitosan	19
2.1. Introduction	19
2.1.1. Chitosan structure, size and effects of molecular weight	20
2.1.2. pH-responsive linkers	22
2.2. Experimental methods	22

2.2.1. General	22
2.2.2. ATC synthesis	23
2.2.3. Chemical characterization methods	23
2.3. Results and discussion	26
2.3.1. ATC synthesis	26
2.3.2. Acid-transformation of ATC to native chitosan	29
2.3.3. Effects of deacetylation and molecular weight on synthesis	31
2.3.4. Separation and purification of polymer	31
2.4. Conclusion	32
2.5. References	33
CHAPTER 3: Antimicrobial capacity of acid-transforming chitosan (ATC)	35
3.1. Background	35
3.2. Experimental details	36
3.2.1. Materials	36
3.2.2. RAW 264.7 cells infection with GFP <i>Salmonella Typhimurium</i>	37
3.2.3. Effect of pH on microbial toxicity	37
3.2.4. Preparation of ATC/siRNA polyplexes	37
3.2.5. Preparation of <i>E. coli Nissle</i> samples for transposon screening	38
3.2.6. Cytotoxicity of polymer on RAW 264.7 cells	39
3.2.6. Statistical analysis	40
3.3. Results and discussion	40
3.3.1. Antimicrobial efficacy of ATC and toxicity	40

3.3.2. Formation of ATC/pdrn polyplexes	43
3.3.3. Utilization of ATC/pdrn polyplexes to treat intracellular infection	46
3.3.4. Suggested antimicrobial mechanism using transposon insertion sequencing	48
3.4. Conclusion	51
3.5. References	52
CHAPTER 4: Gene delivery using ATC	56
4.1. Introduction	56
4.2. Experimental methods	59
4.2.1. Materials	59
4.2.2. Preparation of ATC polyplexes	59
4.2.3. Assays for nucleic acid complexation by ATC	60
4.2.4. Morphology of ATC polyplexes	61
4.2.5. Transfection using ATC/pDNA polyplexes	61
4.2.6. Silenced eGFP expression in HeLa cells by ATC/siRNA polyplexes	62
4.2.7. Cytotoxicity of ATC polyplexes on HeLa/eGFP cells	62
4.3. Results and discussion	63
4.3.1. Complexation and morphology of polyplexes	63
4.3.2. Efficient transfection of pDNA with low cytotoxicity	67
4.3.3. Efficient silencing of eGFP with low cytotoxicity	69
4.3.4. Use of ATC as a vector for other cargo	71
4.3.5. Use of ATC in combined therapeutic	71
4.4. Significance of findings	72

4.5. References	73
CHAPTER 5: Summary and future directions	77
5.1. Summary of dissertation	77
5.2 Future directions	79
5.2.1. Nanoparticles with multi-stimuli response	79
5.2.2. Modification of Linker Molecule	81
5.2.3. Designing nucleic acid targets against drug-resistance enablers	83
5.2.4. Challenges for nanoantibiotics	85
5.2.4.1. Toxicity	85
5.2.4.2. Large-scale manufacturing	87
5.2.5. Future directions for nanoantibiotics	89
5.3. References	93

LIST OF FIGURES

Page

Figure 1.1. A schematic illustration of resistance mechanisms against antimicrobial agents, including 1) inactivated antimicrobial agents by hydrolysis, group transfer, or reduction (alterers), 2) blocked drug uptake and activity by membrane modification and altered binding sites, respectively (blockers), and 3) reduced intracellular drug accumulation by actively pumping through the membrane (three major expellers are shown). 3

Figure 1.2. Nanoantibiotics mechanisms versus conventional antibiotic mechanism. A schematic illustration of nanoantibiotics (nAbts) mechanism in comparison to conventional antibiotics mechanisms. 9

Figure 2.1. ATC synthesis scheme. The amine groups in chitosan backbone was phthalamide-protected and its primary hydroxyl groups were further conjugated with TFA-protected aminoethoxy branch with ketal linkage (TFA-AE-k). The de-protection of both Phth and generated the final product. 25

Figure 2.2. Molecular characterizations of chitosan, Phth-TFA-C, and ATC by (A) ^1H NMR, (B) FTIR, and (C) MALDI-TOF. 26

Figure 2.3. Acid-triggered transformation of ATC to chitosan (marked as C) at an acidic pH (10 mg/mL), confirmed by (A) ^1H NMR and (B) solubility changes upon acid-transformation and subsequent neutralization. 28

Figure 2.4. Hydrolysis kinetics of ATC at pH 5.0, 6.0, and 7.4. 29

Figure 2.5. Inverted microscope images of chitosan and ATC after incubation at pH 5.0 and neutralization as described in Figure 2.3B.	30
Figure 3.1. (A) ATC polymer against <i>S. typhimurium</i> varying pH conditions. (B) MTT assay of Chitosan and ATC on RAW 264.7 cells. (C) Comparison of the in vivo toxicity of Chitosan vs ATC.	42
Figure 3.2. ATC/pdrn characterizations at N/P = 100 shown through DLS data	43
Figure 3.3. RAW 264.7 cells infected for 1h (early-stage) with GFP <i>S. typhimurium</i> then treated with ATC/pdrn polyplexes at varying polymer concentrations, flow cytometry data with corresponding fluorescence images.	45
Figure 3.4. RAW 264.7 cells infected for 16h (prolonged) with GFP <i>S. typhimurium</i> then treated with ATC/pdrn polyplexes at varying polymer concentrations, flow cytometry data indicating the median fluorescence intensity (MFI) with corresponding fluorescence images	46
Figure 3.5. Colony count of <i>S. typhimurium</i> post treatment and cell lysis. (A) agar plate of titrated colonies, with the overall count (B) of the colonies compared side-by-side.	47
Figure 4.1. ATC/siRNA polyplex preparation, cellular uptake, acid-transformation in the endosome/lysosome, siRNA release into the cytoplasm, and gene silencing. Upon acid-hydrolysis in the mildly acidic endosome/lysosome, ATC loses the extended, flexible, and cationic branches, responsible for primary interaction with siRNA, leading to polyplex dissociation and facilitated siRNA release.	58

Figure 4.2. ATC/pDNA polyplexes prepared at different N/P ratios and their characterization by (A) DLS size measurement and zeta-potential analysis, (B) ethidium bromide (EtBr) exclusion assay, (C) gel retardation assay before and after acid-hydrolysis, and (D) TEM. 65

Figure 4.3. ATC/siRNA polyplexes prepared at different N/P ratios and their characterization by (A) DLS size measurement and zeta-potential analysis, (B) ethidium bromide (EtBr) exclusion assay, (C) gel retardation assay before and after acid-hydrolysis, and (D) TEM. 66

Figure 4.4. Transfection studies on HeLa cells, ATC/pDNA transfection at varying N/P ratios 67

Figure 4.5. Fluorescence microscope images and FACS data of ATC/siRNA Polyplexes on HeLa eGFP Cells after 72 hrs. Polyplexes at N/P ratio of 50 were used. 68

Figure 4.6. Transfection studies on HeLa cells. (A) ATC/pDNA transfection of GFP plasmid, (B) ATC/siRNA silencing of eGFP, (C) MTT assay of ATC/pDNA polyplexes, (D) MTT assay of ATC/siRNA polyplexes. 70

Figure 5.1. (a) Formation of a stimuli-responsive nanoantibiotics particle: a combined system can be created by combining conventional antibiotics with nanoantibiotics. (b) Proposed therapeutic effect of stimuli-responsive nanoantibiotics against intracellular infection. 80

Figure 5.2. Drug molecule conjugated linker synthesis reaction scheme 82

Figure 5.3 Manufacturing methods of nanoparticle. Nanoparticles can be manufactured in large scales either by bottom-up or top-down manufacturing methods. 88

Figure 5.4 Antibiotics market share in comparison to the overall pharmaceutical market size. 90

LIST OF TABLES

	Page
Table 2.1. pH-responsive functionalities	21
Table 3.1. <i>E. coli Nissle</i> transposon sequencing data	49
Table 5.1. Drug-resistance enablers for MDRMOs (common in bold)	84
Table 5.2 Examples of commercial nanoantibiotics products	91

ACKNOWLEDGEMENTS

There are so many people I would like to thank for their support during the process of completing this dissertation, but I will start with the most obvious person. My research advisor, Professor Young Jik Kwon, had been with me since the beginning of this process, and I have learned so much from him throughout. The work present in this dissertation would not be possible without his support, guidance, and friendship over the last five years. Though there were tons of headaches and frustrations along the way, I could not have asked for a better mentor that always pushed and pulled the very best out of me. Young not only helped me grow and develop as a scientist but also as a leader and a genuinely better person.

I would also like to thank my committee members, Professor Szu-Wen Wang and Professor Claudia Benavente. Szu was always there during all the phases of my graduate career, from my preliminary exams, all the way to my defense. I knew I could always depend on her to give me insightful criticism that made me strive to improve my science. Claudia has been an immense academic and emotional support during the past few years. She is always wonderfully sarcastic but never held back honest opinions, as one would expect from a true friend.

My next thanks go to my colleagues in BioTEL (Young's Lab). Besides being superb colleagues that strove to make a lasting impact on the scientific community, they are also my family. They were the people I see daily, joke around with, debate, fight, and support. They provide intellectual support when needed and emotional support openly.

They are truly some of the best people and scientist I know, and I cannot wait to see all their future successes (It will be amazing!!).

My colleagues in my cohort and my friends all over the university thank you for all the support you have freely given me these past few years. Though I cannot name all of you due to my attempt at brevity, know that you all mean the world to me, and you have my endless gratitude. And briefly, this includes you, Jackie, Christie, and Sandra. Jackie, our dinner dates, Christie, our procrastination coffee breaks, and Sandra our wine nights and TV binge.

An acknowledgment would not be complete with mentioning the support of my University, and the support of all the staff. I am sorry that I will not mention everyone (because I know I will forget to list so many) but thank you all immensely. Especially, the graduate division and DECADE community, you have all helped to make these past few years so enjoyable.

My friends and family outside my University, thank you all so much for your support. My siblings Joann, and Desmond, I love you both so much, and your support pushes me to do better daily. Dr. Ilona Kretzschmar, and Dr. Claude Brathwaite, I doubt I would have become a scientist today without the both of you to guide me throughout my undergraduate career. Ron, Jodi, and Erin Arden thank you for accepting me into your family and always cheering for me throughout the years.

And finally, my final gratitude goes to my soon to be wife, Amy. I would start with just the simple fact that you are amazing (and not just because you keep me fed). You are one of the strongest, yet the gentlest person I know. I could not have asked for a

better partner in life and for all the support you have given me these past few years you have my endless gratitude and love. You allowed me to vent all my research frustrations and are there when I needed someone to bounce ideas off. You are a true definition of a partner, and I happily look forward to our future together. Thank you so much for everything!!

Thank you all for being a part of my journey!

“And so, does the destination matter? Or is it the path we take? I declare that no accomplishment has substance nearly as great as the road used to achieve it. We are not creatures of destinations. It is the journey that shapes us. Our callused feet, our backs strong from carrying the weight of our travels, our eyes open with the fresh delight of experiences lived.”

-- Brandon Sanderson

CURRICULUM VITAE

Julius Adebayo Edson

Education:

- 2017 University of California, Irvine
Ph.D., Chemical and Biochemical Engineering
- 2015 University of California, Irvine
M.S., Chemical and Biochemical Engineering
- 2012 The City College of New York
B.E., Chemical Engineering

Field of study:

Acid-responsive polymers for antibiotic and gene therapy applications

Publications:

1. Edson, J.A., Kwon, Y.J. (2014), RNAi for silencing drug resistance in microbes toward development of nanoantibiotics. *J. Control. Release*, 189: 150-157.
2. Kemp, J., Edson, J., Kwon, Y.J. (2014), Nano-antibiotics: nanotechnology in fighting against infectious diseases. *Handbook of Nanobiomedical Research*: 373-405.
3. Hong, C.A., Cho, S.K., Edson, J.A., Kim, J., Ingato, D., Pham, B., Chuang, A., Fruman, D., Kwon Y.J. (2016), Viral/Nonviral chimeric nanoparticles to synergistically suppress leukemia proliferation via simultaneous gene transduction and silencing. *ACS Nano*, 10(9): 8705-8714.
4. Edson, J.A., Kwon, Y.J., (2016), Design, challenge, and promise of stimuli-responsive nanoantibiotics. *Nanoconvergence*, 3:26.

ABSTRACT OF THE DISSERTATION

Engineering Physically Active and Genetically Specific Nanoantibiotics

By

Julius Adebayo Edson

Doctor of Philosophy in Chemical and Biochemical Engineering

University of California, Irvine, 2017

Professor Young Jik Kwon, Chair

Drug-resistant infectious bacteria are a pressing societal challenge with conventional antibiotics are becoming less effective at treating bacterial infections. More specifically, gram-negative intracellular infection provides an additional challenge. An innovative therapy for combating these emerging superbugs requires a paradigm-shift in therapy development. Therefore, a combinatory therapy of nanoantibiotics and gene therapy was developed. Chitosan, has been heralded as a material with applications in gene therapy, antimicrobials, wound healing, and various biomedical fields due to its availability, nontoxicity, and biodegradability, therefore, it was a highly suitable nanoantibiotic. However, the efficacy of chitosan is restricted due to the lack of aqueous solubility and limited response to biological triggers.

The focus of my work has been to engineer chitosan as an improved gene delivery vector while maintaining the antimicrobial properties. This was achieved by conjugating an amino branch to the primary hydroxyl group via a temporary, acid-cleavable ketal linkage to created acid-transforming chitosan (ATC). The temporary conjugated

aminoethoxy branch onto chitosan increased the hydrophilicity, maintained antimicrobial efficacy, and promoted cytosolic release in the mildly acidic endosome. The change in hydrophilicity and solubility of ATC was confirmed by dissolving ATC in deionized water and observing a complete dissipation. Acid-triggered reduction of ATC to native chitosan was achieved by incubation at an endosomal pH 5.0, and analyzed by NMR, MALDI-TOF, and FTIR. The antimicrobial capabilities of ATC were explored, and the possible mechanism of action was determined using transposon insertion sequencing. The efficacy of the free polymer was observed against *S. typhimurium*, an intracellular pathogen, alone at varying pH conditions which lead to a positive correlation between pH and effects the polymer had on the microbe. Additionally, ATC polyplexes were applied to RAW 264.7 cells infected with *S. typhimurium* expressing GFP and resulted in a decrease in the levels of bacteria found within the cells as confirmed by flow cytometry. This highlighted the key advantage of using an antimicrobial vector against difficult intracellular infections. Improved cytosolic release, which led to improvement in gene delivery, was confirmed by the complexation of ATC with pDNA, and siRNA to form acid-responsive DNA/ATC (D/ATC) and siRNA/ATC (R/ATC) nanoparticles (NPs), The results indicated transfection of 30% and silencing of 85%, for both D/ATC and R/ATC, respectively.

In summary, this dissertation provides a comprehensive study from synthesis to application of acid-transforming chitosan as a potential synergistic treatment of drug-resistant microbes.

Chapter 1: Background and Introduction

1.1 Rise of drug-resistant infections

Infectious diseases remain a major cause of death worldwide with an estimated 23,000 death toll annually in the United States alone ¹. Drug-resistant microbes infect an additional 2 million people, leading to sickness. A 2014 report from the United Kingdom estimates the death toll of an antibiotic-resistance crisis to be about 300 million deaths globally, with a loss of up to \$100 trillion to the global economy ². Dire state of affairs has made treatment of infectious diseases a top priority of the US government ^{1,3}. Recently, various drug-resistant microorganisms, such as vancomycin-resistant *Staphylococcus aureus* (VRSA), methicillin-resistant *S. aureus* (MRSA), carbapenem-resistant Enterobacteriaceae (CRE), and multi-drug resistant *Mycobacterium tuberculosis* (MDR-TB) have increased due to prevalent overuse and misuse of antibiotics ^{2,4-6}. Developed countries have the largest occurrences of multidrug-resistant microorganisms (MDRMOs), which are attributed to high availability and abuse of conventional antibiotics in agriculture and the human health sectors ⁶. Furthermore, intracellular infections such as TB provide additional therapeutic challenges.

Variations of antibiotic agents developed after the discovery of penicillin have treated a variety of microbial infections by interfering with the integrity of the cell wall or membrane, hindering DNA or RNA synthesis, or disrupting protein or amino acid synthesis ⁷⁻¹⁰. While antibiotics are effective for a short period, their overt misuse of has driven microbes to evolve and acquire resistance against many conventional antimicrobial agents ¹¹. Moreover, the continuing attempt to develop new antimicrobial drugs has been

outpaced by the emergence of drug-resistance microbes despite few successes (i.e., teixobactin) ^{9,12–14}. Resistance to antibiotics is acquired by one of two distinct manners, microevolution or horizontal gene transfer ^{10,15–17}. Microevolution leads to the survival and growth of the mutated genetic line itself. In contrast, horizontal gene transfer occurs when plasmids are exchanged between microbial species, resulting in propagated antibiotics resistance between multiple species ^{16,18}. Drug resistance in microbes is achieved by various mechanisms, including inactivation or modification of antimicrobial drugs, alteration of drug target sites, or reduction of drug accumulation by actively expelling antimicrobial drugs across the cell membrane (Figure 1.1). These methods collectively contribute to developing resistance to current antimicrobial therapy ¹⁰.

1.2 Drug-resistance mechanisms

An effective mechanism for developing resistance against antimicrobial drugs is to modify or alter their structure to an inactive form via hydrolysis, group transfer, or reduction ¹⁵, (Figure 1.1). The hydrolysis of β -lactam antibiotics is of significant concern for its frequent clinical use as the first line of defense against common infections. Group transfer mechanism includes acylation, phosphorylation, thiolation, glycosylation, nucleotidylation, and ribosylation. Other mechanisms usually consist of chemical inactivation by oxidation ¹⁹. Another facilitator of drug resistance formation is the modification of the drug target site. Many antimicrobial agents target molecular sites that are vital for microbial growth and survival. Modification of such target sites by random mutations under antibiotic pressure leads to resistance (Figure 1.1). Mutations in RNA polymerase and DNA gyrase results in resistance to rifamycins and quinolones ²⁰. Furthermore, mutated transpeptidase MecA makes *S. aureus* resistant to methicillin as

well as most other lactam antibiotics²⁰. Finally, actively pumping out antimicrobial agents across the membranes with the use of transporter proteins is another very common way for microbes to acquire drug resistance²¹. Five families of prokaryotic efflux systems involved in drug efflux have been identified: ATP-binding cassette (ABC), major facilitator superfamily (MFS), resistance-nodulation-division (RND), multi-antimicrobial extrusion (MATE), and small multi-drug resistance (SMR). While the ABC transporters are ATP-dependent, the other drug transporters require proton motif force^{22–24} (Figure 1.1). All of these mechanisms are facilitated by some protein within the microbe.

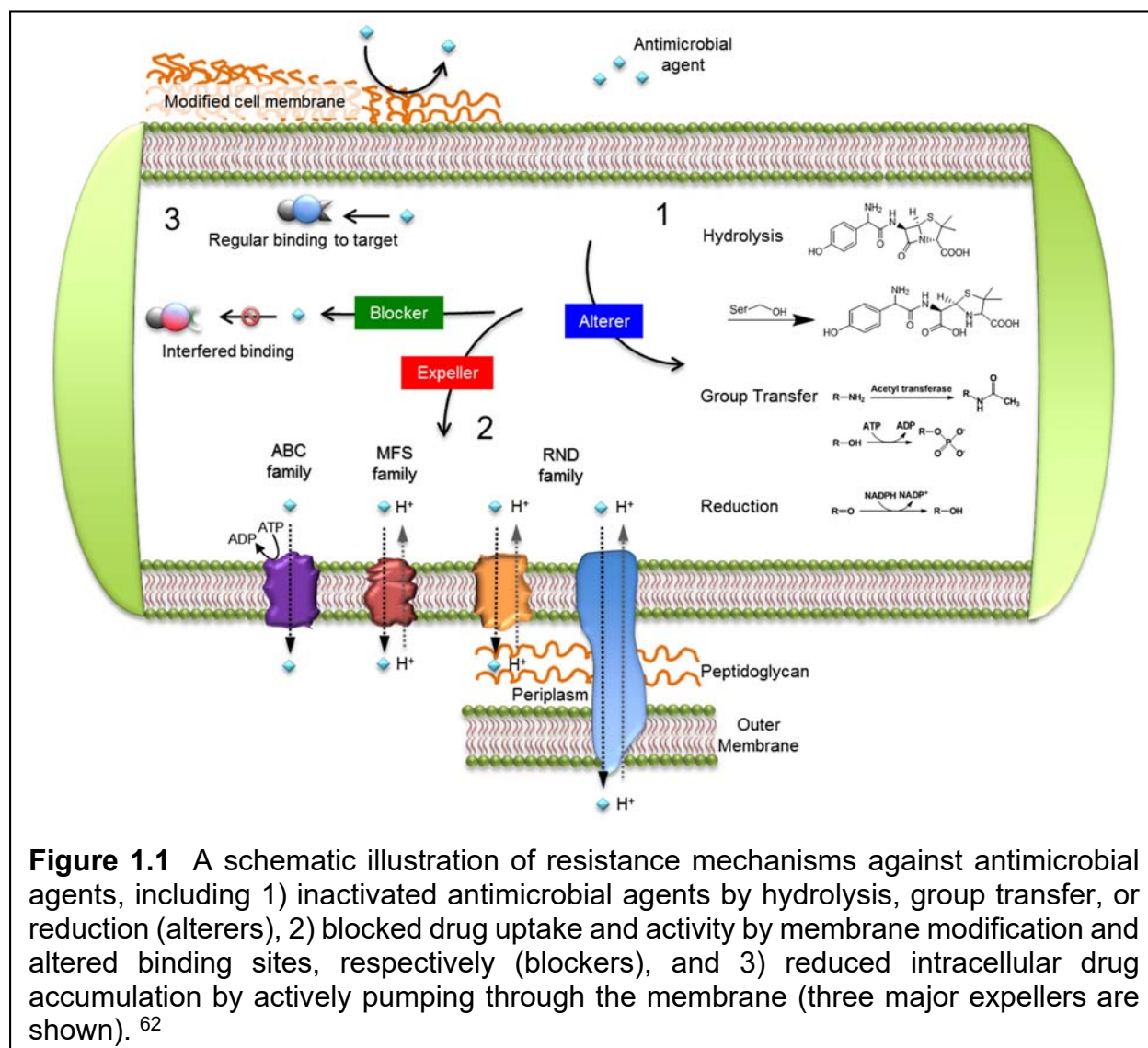


Figure 1.1 A schematic illustration of resistance mechanisms against antimicrobial agents, including 1) inactivated antimicrobial agents by hydrolysis, group transfer, or reduction (alterers), 2) blocked drug uptake and activity by membrane modification and altered binding sites, respectively (blockers), and 3) reduced intracellular drug accumulation by actively pumping through the membrane (three major expellers are shown).⁶²

1.3 Intracellular infections

Intracellular bacteria are infectious microorganisms that replicate within host cells, usually mononuclear phagocytes (MPs). This allows the bacteria to evade host humoral defense mechanisms and aids in the survival and persistence of infection ²⁵. Any host cell is suitable for most intracellular infection, but MPs are especially favorable for certain intracellular bacteria because they consume microorganisms and other foreign bodies, also, they have a long lifespan ²⁵.

Intracellular microorganisms can be classified by the following four characteristics: the exploitation of intracellular survival mechanisms, the role of T-lymphocytes in pathogenesis, the formation of granulomas at the infected tissue, and chronic infection caused by the inability to eradicate granulomas. The obligatory identifier of intracellular bacteria is the capacity to enter host cells, but some extracellular bacteria perform this function as well ²⁵.

M. tuberculosis (Mtb) best fulfills the definition of an intracellular bacteria ²⁵ and is quickly becoming a global health problem. The bacteria cause tuberculosis (TB) which is estimated to affect 60 million people globally ²⁶, with 9 million new cases appearing annually ²⁶, and 1.5 million people dying from the disease giving it the highest morbidity rate amongst infectious diseases. Even with the advent of antibiotics, persistent infections and the emergence of drug-resistant strains remain a challenge to treat. Mtb primarily infects the lung first and occurs with a single 5 µm droplet containing about three tubercle bacilli. Current treatment includes the use of nitroimidazoles, fluoroquinolones such as moxifloxacin, and pyrazinamide, to which various resistances are have developed. ²⁶⁻²⁸.

1.4 Genetic specificity in antimicrobial therapy

Common antimicrobial agents, from β -lactams to fluoroquinolones, eradicate microbes by interfering with their key biological processes. Formation of drug-resistance intervenes with the eradication of these microbes. Therefore, new strategies to combat drug-resistant microbes by impairing the drug-resistance facilitators (Figure 1.1), particularly with high genetic specificity are in demand^{29,30}. Silencing the expression and activity of drug-resistance enablers by delivering antimicrobial RNA is of great interest in treating drug-resistant infections. RNA interference (RNAi)-mediated antimicrobial therapy can synergistically and selectively remove drug-resistant microbes when co-administered with common antimicrobial drugs. Despite the high promise in treating drug-resistant microbes, RNAi is under-investigated in antimicrobial research and rarely utilized in the clinical trials for MDMRO treatment³¹. Limited use of RNAi in antimicrobial therapy is mainly attributed to the recent discovery of the prokaryotic gene silencing pathway, requiring further elucidation of detailed mechanisms for designing effective antimicrobial RNAs.

RNAi was first observed in plants and then various other eukaryotic organisms such as *Caenorhabditis elegans* and even mammalian systems^{30,32}. Recognition and processing of double-stranded RNA (dsRNA) within a cell eventually leads to the production of small interfering RNA (siRNA) of 20 to 30 nucleotides that are incorporated into a complex known as the RNA-induced silencing complex (RISC) in eukaryotes^{30,33}. This complex is responsible for deleting target mRNAs by complementary base pairing. An analogous gene silencing mechanism mediated by the prokaryotic clustered regularly interspaced short palindromic repeat (CRISPR) was also reported³⁴. CRISPR-mediated

gene silencing, which is typically used as a mechanism for bacteria to develop resistance against foreign nucleic acids, can be employed as a method to silence the target drug-resistance-enabling pathways in prokaryotes³⁴. In general, RNAi in both eukaryotic and prokaryotic systems is a similar process of internalization of short silencing RNA molecules, integration to a large silencing protein complex, and eventual degradation of target mRNA³⁵. While siRNA-RISC complex binds and degrades target mRNA with a complementary sequence in eukaryotes, Cas RAMP module (Cmr) complex, a multi-subunit ribonucleoprotein,^{36,37} in combination with CRISP RNA (crRNA; previously referred to as prokaryotic silencing RNA or psiRNA) cleaves the target mRNA at two well defined sites starting from the 3' end in prokaryotes^{34,38–40}. The Cmr complex binds with crRNA with an additional 5' tag of 8 nucleotides (guide sequence) and then cleaves the target mRNA with a complementary target sequence that encodes a drug-resistance enabler as shown *in vitro* with β -lactamase^{36,41}. The target mRNA is cut at the location complementary to 14 nucleotides downstream of the 3' end of crRNA³⁶.

Introduction of small silencing RNA (siRNA for eukaryotes and crRNA for prokaryotes) complementary to drug-resistance enabler-encoding mRNA can be an effective and targeted way to tackle the resistance against common antimicrobial drugs^{39,42}. For example, using crRNA against expellers, MsrA or LmrA, re-sensitizes MRSA and *E. coli* to conventional antibiotic treatment^{22,43}. Additionally, the degradation of target mRNA by delivering crRNA in *Sulfolobus solfataricus*⁴⁴ and *Synechocystis sp.*⁴⁵ has also been reported. In contrast to ample examples of eukaryotic gene silencing^{46–49}, achieving gene silencing in prokaryotes has not been attempted until recently^{38,50–53}. A group from Tel Aviv University School of Medicine were able to sensitize streptomycin resistant *E.*

coli to antibiotics by silencing the gene *ndm1* and *ctx-M-15* using the CRISPR-Cas system

54.

1.5 Using nanoantibiotics as a physically active gene delivery carrier

A pivotal limiting factor in the clinical use of gene therapy is the efficient delivery of nucleic acids. siRNA and crRNA are subject to degradation by nucleases and immune response *in vivo* ⁴⁹. Effective and safe carriers for antimicrobial RNAs share some characteristics required for the nanoscale vectors developed for gene therapy: protection of nucleic acids during circulation, selective internalization by target cells/microbes, and efficient cytosolic release. The additional antimicrobial activity of the carrier itself can be advantageous and specifically desirable for antimicrobial RNA delivery to treat intracellular pathogens. For example, some classes of materials have been discovered to possess antimicrobial capabilities such as producing reactive oxygen species (ROS), disrupting cell membrane, inducing DNA damage, or interrupting trans-membrane electron transport, all of which microbes would not easily develop resistance against via genetic mutations ⁵⁵.

Nanoantibiotics (nAbts) are nanomaterials that have an antimicrobial activity or improve the efficacy and safety of antibiotics administration ⁵⁵. NAbts possess many advantages over conventional antibiotics, including but not limited to production, storage, durability, and versatility. Preparation of antimicrobial nanoparticles may be cheaper, faster, and more adaptable with the added advantage of a long shelf life ^{55,56}. They are typically composed of either naturally occurring antibacterial substances, metals and metal oxides, carbon-based nanomaterials, or nanoemulsions ^{57,58}. Moreover, the

persistent misuse and overuse of current antimicrobials can also be attributed to the lack of patient compliance ⁵⁹⁻⁶¹. NAbts provide the added advantage of a site-specific, sustained release that can be administered in a single dose. While most conventional antibiotics are a systematic release of therapeutics that require multiple doses.

The improved antimicrobial efficacy can be attributed to high surface area to volume ratios and unique chemical-physical properties. Some proposed antimicrobial mechanisms of nAbts include: 1) generation of reactive oxygen species (ROS) that age bacterial intracellular components, 2) compromise the bacterial cell wall/membrane, 3) interruption of energy transduction, and 4) inhibition of enzyme activity and DNA synthesis ^{55,56}, as shown in Figure 1.2. In comparison, conventional antibiotic agents have treated a diverse multitude of microbes via interference with the integrity of the cell wall or membrane, hindrance DNA or RNA synthesis, or disruption of protein or amino acid synthesis (Figure 1.2) ⁶². While there is some overlap present, such as inhibition of nucleic acid synthesis and compromising cell wall integrity, the mechanisms by which these occur are vastly different. While conventional antibiotics interfere on the molecular scale, nAbts physically disrupt key biological processes. This allows for a unique method of destroying microbes with a combination of both mechanisms.

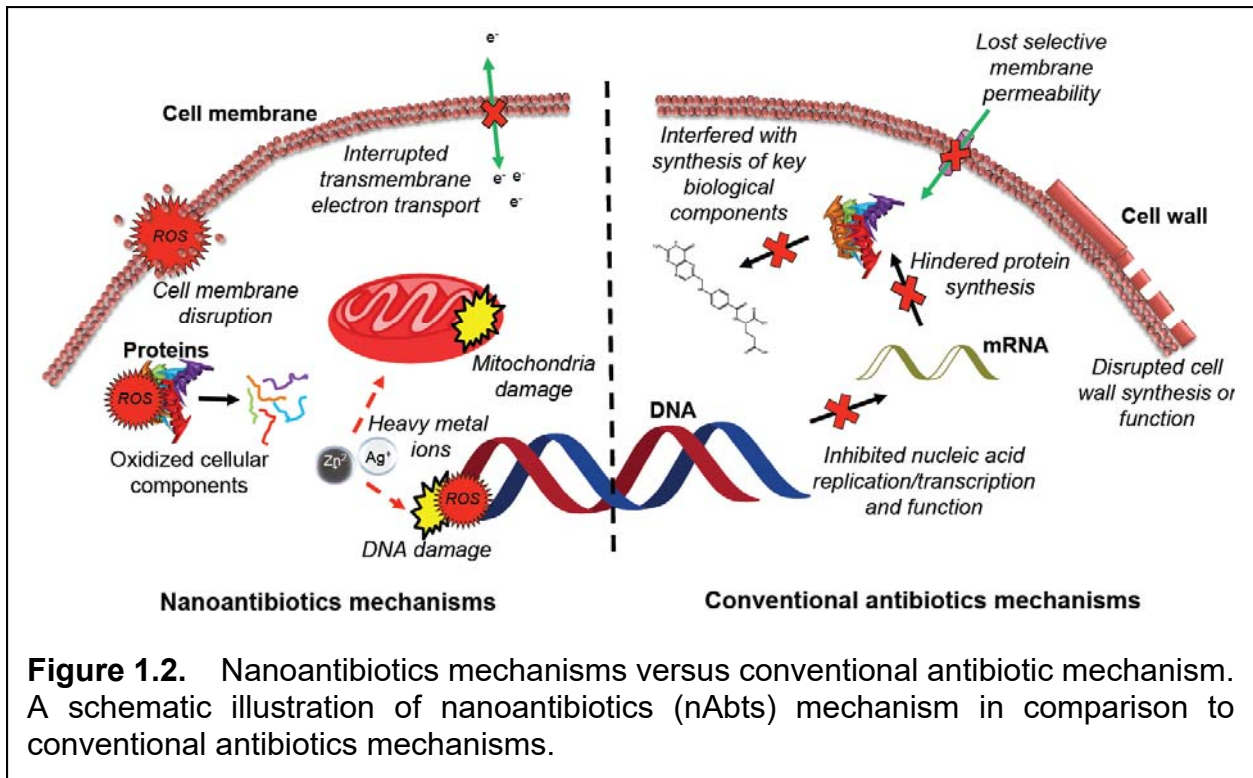


Figure 1.2. Nanoantibiotics mechanisms versus conventional antibiotic mechanism. A schematic illustration of nanoantibiotics (nAbts) mechanism in comparison to conventional antibiotics mechanisms.

1.6 Chitosan as a physically active carrier

NABts come in different shapes and sizes, all of which have been continuously documented^{55,58,63–65}. Nanoantibiotic polymers typically need to be formulated into nanoparticles for full usage of the therapeutic antimicrobial properties. These polymers do hinder the growth of bacteria through one of the nABts mechanisms. Chitosan is chosen as a vector for various reason. Chitosan, an *N*-deacetylated chitin product, possesses excellent innate antimicrobial properties⁶⁶ and enzymatically degrades into oligosaccharides. Chitosan physically targets the bacterial surface and damages the cell membrane via strong electrostatic interactions between the cationic amines on the chitosan and the anionic phosphoryl groups of the microbe membranes^{67–69}. Chitosan has been shown to adequately complex nucleic acids^{69,70} and damages the cell membranes of *S. aureus*^{71,72}.

The threatening challenges concerning the increasing rate of drug-resistant microbes can be addressed by an innovative therapeutic strategy of combining nucleic acids against drug-resistance enablers and antimicrobial nanomaterials. Further understanding of the prokaryotic gene silencing process, selection of novel materials that are antimicrobial and capable of carrying antimicrobial nucleic acids, and development of safe and efficient administration methods will not only improve the conventional ineffective antimicrobial treatments but also assist in preventing the formation of further resistances. Furthermore, engineering nanoantibiotics using silencing mechanisms does not negate the use of conventional therapies using small molecules. Rather, gene-based strategies provide additional synergistic therapies that will allow for more effective treatment of bacterial infections.

1.7 Scope of the dissertation

In this dissertation, the use of a pH-responsive polymer as an antimicrobial gene delivery platform was explored. The key design parameter was to have the delivery vehicle play an active role in the therapy. Various types of antimicrobial could have been selected, but very few met the design criteria for gene therapy. Furthermore, due to the overlapping pathways of gene delivery and intracellular infections, the design was focused on bacteria that invade mammalian cells. The motivation behind **Chapter 1** is to highlight the challenges with drug-resistant formation caused by conventional antibiotics and to demonstrate a possible strategy to circumvent the current problems with antimicrobial resistance by using nanoantibiotics as a delivery vector for gene therapy. This will be achieved by the combination of the gene-based system to combat drug-resistance with an engineered vector capable of efficiently delivering a genetic payload in addition to supporting the therapeutic process.

Chapter 2 provides details of the synthesis of acid-transforming chitosan (ATC). Chitosan was selected as our vector because it had many of the desired properties for the therapeutic. However, the use of the polymer was met with various hurdles such as aqueous solubility, and challenges with endosomal escape. This chapter provides the synthesis scheme used to create the acid-responsive variant of chitosan. The modified polymer overcame the hurdles presented in the unmodified polymers. Additionally, this chapter discusses the challenges involved in the separation and purification of the modified polymer.

Chapter 3 explored the antimicrobial capabilities of ATC and determined the possible mechanism for the antimicrobial efficacy of ATC and chitosan. The efficacy was observed against the bacteria alone at varying pH conditions to see the effects had on the polymer and microbe. Additionally, the mechanism of action of ATC was hypothesized using preliminary data from transposon insertion sequencing. The utility of ATC polyplexes in the eradication of an intracellular infection was also demonstrated. The investigation into the death of bacteria within a macrophage and the possible target sites that would be most efficacious for the application of ATC polyplexes.

The motivation for **Chapter 4** is to demonstrate the gene delivery capabilities of ATC polymer. Various polyplexes were created using different genetic materials pDNA, and siRNA. These polyplexes were characterized by morphology, surface charge, and complexation efficiency. Additionally, in this chapter, the transfection efficiency was observed using flow cytometry.

Chapter 5 describes the summary of developing acid-transforming chitosan as an antimicrobial gene delivery vector from chemical synthesis to final formulation of the therapeutic and concluded with perspectives and future directions of the work.

1.8. References

- (1) Arias, C. a; Ph, D.; Murray, B. E. **2015**, 1168–1170.
- (2) Wang, H.; Lozano, R.; Davis, A.; ... *Lancet (London, England)* **2015**, 385 (9963), 117–171.

- (3) Fauci AS; Marston HD. *Jama* **2014**, 2520, 454–461.
- (4) Levy, S. B. *The antibiotic paradox : how the misuse of antibiotics destroys their curative power*, 2nd ed.; Perseus Pub: Cambridge MA, 2002.
- (5) English, B. K.; Gaur, A. H. *Adv. Exp. Med. Biol.* **2010**, 659, 73–82.
- (6) Gaash B. *Indian J. Pract. Dr.* **2008**, 5 (1), 03–04.
- (7) Schmidt, B.; Ribnicky, D. M.; Poulev, A.; Logendra, S.; Cefalu, W. T.; Raskin, I. *Metabolism.* **2008**, 57 (SUPPL. 1).
- (8) Clardy, J.; Fischbach, M. a; Walsh, C. T. *Nat. Biotechnol.* **2006**, 24 (12), 1541–1550.
- (9) Hancock, R. E. W. *Nat. Rev. Drug Discov.* **2007**, 6 (1), 28–28.
- (10) Tenover, F. C. *Am. J. Infect. Control* **2006**, 34 (5 SUPPL.).
- (11) Holden, M. T. G.; Feil, E. J.; Lindsay, J. a; Peacock, S. J.; Day, N. P. J.; Enright, M. C.; Foster, T. J.; Moore, C. E.; Hurst, L.; Atkin, R.; Barron, A.; Bason, N.; Bentley, S. D.; Chillingworth, C.; Chillingworth, T.; Churcher, C.; Clark, L.; Corton, C.; Cronin, A.; Doggett, J.; Dowd, L.; Feltwell, T.; Hance, Z.; Harris, B.; Hauser, H.; Holroyd, S.; Jagels, K.; James, K. D.; Lennard, N.; Line, A.; Mayes, R.; Moule, S.; Mungall, K.; Ormond, D.; Quail, M. a; Rabinowitsch, E.; Rutherford, K.; Sanders, M.; Sharp, S.; Simmonds, M.; Stevens, K.; Whitehead, S.; Barrell, B. G.; Spratt, B. G.; Parkhill, J. *Proc. Natl. Acad. Sci. U. S. A.* **2004**, 101 (26), 9786–9791.
- (12) Ling, L. L.; Schneider, T.; Peoples, A. J.; Spoering, A. L.; Engels, I.; Conlon, B. P.;

- Mueller, A.; Hughes, D. E.; Epstein, S.; Jones, M.; Lazarides, L.; Steadman, V. A.; Cohen, D. R.; Felix, C. R.; Fetterman, K. A.; Millett, W. P.; Nitti, A. G.; Zullo, A. M.; Chen, C.; Lewis, K. *Nature* **2015**, *517* (7535), 455–459.
- (13) Katz, M. L.; Mueller, L. V; Polyakov, M.; Weinstock, S. F. *Nat. Biotechnol.* **2006**, *24* (12), 1529–1531.
- (14) Sheridan, C. *Nat. Biotechnol.* **2006**, *24* (12), 1494–1496.
- (15) Alekshun, M. N.; Levy, S. B. *Cell* **2007**, *128* (6), 1037–1050.
- (16) Meynell, E.; Meynell, G. G.; Datta, N. *Bacteriol. Rev.* **1968**, *32* (1), 55–83.
- (17) Brinton, C. C.; Baron, L. *CRC Crit. Rev. Microbiol.* **1971**, *1* (1), 105–160.
- (18) van der Horst, M. a.; Schuurmans, J. M.; Smid, M. C.; Koenders, B. B.; ter Kuile, B. H. *Microb. Drug Resist.* **2011**, *17* (2), 141–147.
- (19) Wright, G. D. *Adv. Drug Deliv. Rev.* **2005**, *57* (10), 1451–1470.
- (20) Lambert, P. A. *Adv. Drug Deliv. Rev.* **2005**, *57* (10), 1471–1485.
- (21) Paulsen, I. T.; Skurray, R. A. *Gene* **1993**, *124* (1), 1–11.
- (22) Van Bambeke, F.; Glupczynski, Y.; Plésiat, P.; Pechère, J. C.; Tulkens, P. M. *J. Antimicrob. Chemother.* **2003**, *51* (5), 1055–1065.
- (23) Juranka, P. F.; Zastawny, R. L.; Ling, V. *FASEB J.* **1989**, *3* (14), 2583–2592.
- (24) Veen, H. van; Callaghan, R.; Soceneantu, L.; Sardini, A.; Konings, W. N.; Higgins, C. F. *Nature* **1998**, *391* (February), 580–584.
- (25) Kaufmann, S. H. E. *Annu. Rev. Immunol.* **1993**, *11* (1), 129–163.

- (26) Pálfi, G.; Dutour, O.; Perrin, P.; Sola, C.; Zink, A. *Tuberculosis*. 2015, pp S1–S3.
- (27) Maslov, D. A.; Zaïchikova, M. V.; Chernousova, L. N.; Shur, K. V.; Bekker, O. B.; Smirnova, T. G.; Larionova, E. E.; Andreevskaya, S. N.; Zhang, Y.; Danilenko, V. N. *Tuberculosis* **2015**, *95* (5), 608–612.
- (28) Juréen, P.; Werngren, J.; Toro, J.-C.; Hoffner, S. *Antimicrob. Agents Chemother.* **2008**, *52* (5), 1852–1854.
- (29) Bartlett, J. G. *Clin. Infect. Dis.* **2011**, *53* (SUPPL. 1), 4–7.
- (30) Hannon, G. J. *Nature* **2002**, *418* (6894), 244–251.
- (31) Ginn, S. L.; Alexander, I. E.; Edelstein, M. L.; Abedi, M. R.; Wixon, J. J. *Gene Med.* **2013**, *15* (2), 65–77.
- (32) Fire, A.; Xu, S.; Montgomery, M. K.; Kostas, S. A.; Driver, S. E.; Mello, C. C. *Nature* **1998**, *391* (6669), 806–811.
- (33) Harborth, J.; Elbashir, S. M.; Vandeburgh, K.; Manninga, H.; Scaringe, S. a; Weber, K.; Tuschl, T. *Antisense Nucleic Acid Drug Dev.* **2003**, *13* (2), 83–105.
- (34) Wiedenheft, B.; Sternberg, S. H.; Doudna, J. a. *Nature* **2012**, *482* (7385), 331–338.
- (35) van der Oost, J.; Brouns, S. J. J. *Cell* **2009**, *139* (5), 863–865.
- (36) Hale, C. R.; Majumdar, S.; Elmore, J.; Pfister, N.; Compton, M.; Olson, S.; Resch, A. M.; Glover, C. V. C.; Graveley, B. R.; Terns, R. M.; Terns, M. P. *Mol. Cell* **2012**, *45* (3), 292–302.

- (37) Hatoum-Aslan, a.; Maniv, I.; Marraffini, L. a. *Proc. Natl. Acad. Sci.* **2011**, *108* (52), 21218–21222.
- (38) Hale, C. R.; Zhao, P.; Olson, S.; Duff, M. O.; Graveley, B. R.; Wells, L.; Terns, R. M.; Terns, M. P. *Cell* **2009**, *139* (5), 945–956.
- (39) Hale, C.; Kleppe, K.; Terns, R. M.; Terns, M. P. *RNA* **2008**, *14* (12), 2572–2579.
- (40) Rusk, N. *Nat. Methods* **2012**, *9* (3), 220–221.
- (41) Zhang, J.; Rouillon, C.; Kerou, M.; Reeks, J.; Brugger, K.; Reimann, J.; Cannone, G.; Liu, H.; Albers, S.; Naismith, H.; Spagnolo, L.; White, M. F. *Mol Cell* **2012**, *45* (3), 303–313.
- (42) Eidem, T. M.; Roux, C. M.; Dunman, P. M. *Wiley Interdiscip. Rev. RNA* **2012**, *3* (3), 443–454.
- (43) Griffith, J. K.; Baker, M. E.; Rouch, D. A.; Page, M. G. P.; Skurray, R. A.; Paulsen, I. T.; Chater, K. F.; Baldwin, S. A.; Henderson, P. J. F. *Curr. Opin. Cell Biol.* **1992**, *4* (4), 684–695.
- (44) Zebec, Z.; Manica, A.; Zhang, J.; White, M. F.; Schleper, C. *Nucleic Acids Res.* **2014**, *42* (8), 5280–5288.
- (45) Abe, K.; Sakai, Y.; Nakashima, S.; Araki, M.; Yoshida, W.; Sode, K.; Ikebukuro, K. *Biotechnol. Lett.* **2014**, *36* (2), 287–294.
- (46) Jiang, M.; Milner, J. *Oncogene* **2002**, *21* (39), 6041–6048.
- (47) Zhou, J.; Rossi, J. J. *Gene Ther.* **2011**, *18* (12), 1134–1138.

- (48) Volpe, T. *Science (80-.)*. **2002**, 297 (5588), 1833–1837.
- (49) Xu, D.-Q.; Zhang, L.; Kopecko, D. J.; Gao, L.; Shao, Y.; Guo, B.; Zhao, L. Humana Press, 2009; pp 1–27.
- (50) Bikard, D.; Hatoum-Aslan, A.; Mucida, D.; Marraffini, L. A. *Cell Host Microbe* **2012**, 12 (2), 177–186.
- (51) Barrangou, R.; Fremaux, C.; Deveau, H.; Richards, M.; Patrick Boyaval; Moineau, S.; Romero, D.; Horvath, P. *Science (80-.)*. **2007**, 315 (March), 1709–1712.
- (52) Yanagihara, K.; Tashiro, M.; Fukuda, Y.; Ohno, H.; Higashiyama, Y.; Miyazaki, Y.; Hirakata, Y.; Tomono, K.; Mizuta, Y.; Tsukamoto, K.; Kohno, S. *J. Antimicrob. Chemother.* **2006**, 57 (1), 122–126.
- (53) Karvelis, T.; Gasiunas, G.; Miksys, A.; Barrangou, R.; Horvath, P.; Siksnys, V. *RNA Biol.* **2013**, 10 (5), 841–851.
- (54) Yosef, I.; Manor, M.; Kiro, R.; Qimron, U. *Proc. Natl. Acad. Sci.* **2015**, 112 (23), 7267–7272.
- (55) Huh, A. J.; Kwon, Y. J. *J. Control. Release* **2011**, 156 (2), 128–145.
- (56) Zazo, H.; Colino, C. I.; Lanao, J. M. *J. Control. Release* **2016**, 224, 86–102.
- (57) Pelgrift, R. Y.; Friedman, A. J. *Adv. Drug Deliv. Rev.* **2013**, 65 (13), 1803–1815.
- (58) Zhu, X.; Radovic-Moreno, A. F.; Wu, J.; Langer, R.; Shi, J. *Nano Today* **2014**, 9 (4), 478–498.
- (59) Pechère, J. C. *Clin. Infect. Dis.* **2001**, 33 Suppl 3 (Supplement 3), S170-3.

- (60) Kardas, P.; Devine, S.; Golembesky, A.; Roberts, C. *Int. J. Antimicrob. Agents* **2005**, 26 (2), 106–113.
- (61) Okeke, I. N.; Lamikanra, A.; Edelman, R. *Emerg. Infect. Dis.* **1999**, 5 (1), 18–27.
- (62) Edson, J. A.; Kwon, Y. J. *Journal of Controlled Release*. Elsevier 2014, pp 150–157.
- (63) Lederberg, L. J.; Laureate, N. In *Handbook of Clinical Nanomedicine*; 2013; pp 15–21.
- (64) Wang, S.; Zheng, F.; Huang, Y.; Fang, Y.; Shen, M.; Zhu, M.; Shi, X. *ACS Appl. Mater. Interfaces* **2012**, 4, 6393–6401.
- (65) Doi, S. *MRS Proc.* **2013**, 1498, 127–132.
- (66) Kim, T. H.; Jiang, H. L.; Jere, D.; Park, I. K.; Cho, M. H.; Nah, J. W.; Choi, Y. J.; Akaike, T.; Cho, C. S. *Prog. Polym. Sci.* **2007**, 32 (7), 726–753.
- (67) Lee, D. W.; Lim, H.; Chong, H. N.; Shim, W. S. *Open Biomater. J.* **2009**, 1, 10–20.
- (68) Liu, H.; Du, Y.; Wang, X.; Sun, L. *Int. J. Food Microbiol.* **2004**, 95 (2), 147–155.
- (69) Chung, Y.; Su, Y.; Chen, C.; Jia, G.; Wang, H.; Wu, J. C. G.; Lin, J. *Acta Pharmacol. Sin.* **2004**, 25 (7), 932–936.
- (70) Mourya, V. K.; Inamdar, N. N. *React. Funct. Polym.* **2008**, 68 (6), 1013–1051.
- (71) Ravi Kumar, M. N. . *React. Funct. Polym.* **2000**, 46 (1), 1–27.
- (72) Aranaz, I.; Mengibar, M.; Harris, R.; Panos, I.; Miralles, B.; Acosta, N.; Galed, G.; Heras, A. *Curr. Chem. Biol.* **2009**, 3 (2), 203–230.

Chapter 2: Synthesis and characterization of acid-transforming chitosan

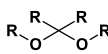
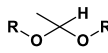
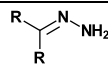
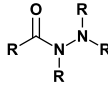
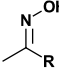
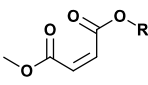
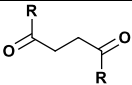
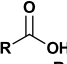
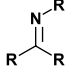
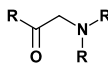
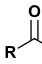
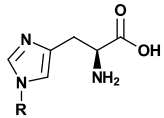
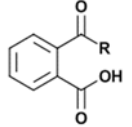
2.1. Introduction

Chitosan is an abundant, natural, biodegradable, antimicrobial material with no reported toxicity. Although it is a unique material used within numerous fields, ranging from pharmaceutical to food industry ¹, chitosan is difficult to use easily in most of those applications due to its lack of solubility in biologically relevant pH. Chitosan only readily dissolves in any solvent that is of a pH of 5.0 or lower. This pH is not within the range of normal biological pH (6-8). Accordingly, this limits the general use of chitosan as a drug delivery material. Currently, all attempts to overcome this limitation has been accomplished through varied mechanical and chemical modification share one commonality: the permanence of modification ^{1,2}. Chitosan has three modifiable sites, the primary, secondary hydroxyl, and the primary amine functionality. Various modifications to these sites over the years have produced chitosan for use in a multitude of industries. While the applications are broad, very few are used in healthcare. Additionally, while some of the known modifications have shown success in applications of gene delivery, long-term effects of those modifications in a clinical setting are still unknown. Therefore, we modified chitosan with the addition of a 2-aminoethoxy branch allowing for improved application in aqueous environments.

2.1.1. Chitosan structure, size, and effects of molecular weight

Chitosan can be obtained in various ranges of molecular weights, ranging from 10,000 g/mol to 800,000+ g/mol, depending on the processing and the origin of the chitin used to create chitosan. Many of chitosan's properties are attributed to molecular weight, with different properties associated with each molecular weight range³⁻⁵. Low molecular

Table 2.1. pH-responsive functionalities

Name	Structure	pH Range	References
Ketal		4-5	9,21,22
Acetal			9,21
Hydrazone			9
Hydrazide		<5	9
Oxime			9
Methyl maleate		5.5, 6.8	9
Succinyl			6,23
Carboxymethyl			6,21
Imine		5-7	9
Amino ester			24
Acetyl			6,25
Histidine		6-7	9
Phthalyl			6

weight chitosan and chitosan oligomers of 1kDa have shown higher antimicrobial activity against gram-negative bacteria, whereas larger oligomers have higher activity against gram-positive bacteria ⁴. It is suggested that molecular weight and degree of deacetylation (DD) have the greatest influence on the various properties of chitosan since both parameters affect the number of free amine and crystallinity of the polymer³. For the study, medium molecular weight (30,000-60,000 kDa) chitosan at 80% DA was used with the possibility of retaining the benefits determined from low and high molecular weight chitosan.

2.1.2. pH-responsive linkers

pH-responsive linkers have a unique advantage against microbes that thrive in highly acidic environments, whether extracellularly in the stomach (pH = 1-3) and gastrointestinal tract (pH = 5-8) or intracellular in the phagolysosomes (pH = 4.5-5) and macrophages ⁶⁻⁸. Additionally, chronic infections and wounds have pH values between 5.4 – 7.4 and are another potential site for the application of this therapy ⁷. Examples of microbes that thrive in an acidic environment include *Helicobacter pylori*, *Agrobacterium tumefaciens* or *Vibrio cholera* ^{6,7}. This specificity allows for a direct exploitation of the stimuli-response in certain tissues or a cellular compartment. The key element for pH-responsiveness is protonation/deprotonation caused by charge distribution over ionizable functional groups such as carboxyl or amino groups six listed in Table 2.1. Polymers that contain carboxylic, sulfonic acid or amino groups such as poly(L-histidine), poly(methacrylic acid) (PMAA), and poly(acrylic acid) (PAA) ⁹, have been commonly used for their pH-responsive functionalities. pH changes induce a phase transition in pH-

responsive polymers very abruptly, which can aid within intracellular compartments or with rapid release of drug cargos. ^{6,9}

2.2 Experimental methods

2.2.1 General

All chemicals were purchased from commercially available sources and used as received. Chitosan (MW 18–44 kDa, 80% degree of deacetylation) and 3-(4,5-dimethyl-2-thiazolyl)-2,5-diphenyltetrazoliumbromide (MTT) were purchased from Sigma-Aldrich (Milwaukee, WI). 2,2,2-Trifluoro-1-{2-[2-(1-methoxy-1-methylethoxy)ethoxy]ethylamino}-1-ethanone (trifluoroacetate [TFA]-protected aminoethoxy branch with ketal linkage, TFA-AE-k) was synthesized as previously reported ^{10,11}. Phthalic anhydride and hydrazine monohydrate were purchased from Acros Organics (Morris Plains, NJ).

2.2.2 ATC synthesis

Phthalimide-protected chitosan (Phth-C): Chitosan (1 g, 6 mmole pyranose) and phthalic anhydride (4 g, 20 mmole) were dissolved in 30 mL of 5% (v/v) deionized water in DMF and heated to 120 °C under nitrogen for 7 h. The reaction was stopped by mixing with 300 mL of deionized water and Phth-C was obtained after vacuum filtration in a fritted funnel, then dried under vacuum for 4 h at room temperature. Yield: 90%. FT-IR (KBr, cm^{-1}): 2950 – 2800 (alkyl), 1777 – 1670 (carbonyl), 1250 – 950 (pyranose), 728 (arom). ¹H NMR (500 MHz, $\text{DMSO-}d_6$, δ , ppm): 1.9 (m, acetyl), 3.0 – 5.2 (m, pyranose), 7.5 – 7.9 (m, N-phthaloyl). MALDI-TOF MS (m/z): 18,000 – 44,000.

Phth-C conjugated with TFA-protected aminoethoxy branches via ketal linkage

(Phth-TFA-AE-k-C): Phth-C (1 g, 1.91 mmole), pyridinium *p*-toluenesulfonate (PPTS) (2 g, 7.96 mmole), and TFA-AE-k (3 g, 10 mmole) were mixed in 20 mL anhydrous THF and 5Å sieves (10 g) for 3 h at 25 °C then the reaction was quenched by adding 5 mL triethylamine (TEA). Residual PPTS and unreacted TFA-AE-k were removed by repeated rinsing three times with 100 mL methanol (MeOH), then dried under vacuum for 4 h at room temperature, resulting in Phth-TFA-AE-k-C as tan-brown solid. Yield: 40%. FT-IR (KBr, cm^{-1}): 2950 – 2800 (alkyl), 1777 – 1670 (carbonyl), 1200 – 1000 (pyranose), 728 – 700 (arom). ^1H NMR (500 MHz, $\text{DMSO-}d_6$, δ , ppm): 1.3 (s, ketal), 1.9 (s, acetyl), 3.0 – 5.2 (m, pyranose), 7.5 – 7.9 (m, *N*-phthaloyl), 9.5 (s, acetamide). MALDI-TOF MS(m/z): 18,000 – 51,000.

Chitosan conjugated with aminoethoxy branches via ketal linkage (ATC): Phth-TFA-AE-C (1 g, 1.0 mmole) was added to 10 mL of 1 M NaOH and stirred at room temperature for 24 h for TFA-deprotection. After the precipitate was removed by centrifugation, the liquid fraction was added to 100 mL of 20% (v/v) hydrazine in deionized water and stirred at 90 °C for 16 h for Phth-deprotection. The final product, ATC as white-colored powder, was obtained after dialysis in deionized water for 24 h and freeze-drying (Freezone 2L, Labconco [Kansas City, MO]) for 18 h. Yield: 50%. FT-IR (KBr, cm^{-1}): 2950 – 2800 (alkyl), 1665 – 1650 (Carbonyl), 1200 – 900 (pyranose). ^1H NMR (500 MHz, D_2O , δ , ppm): 1.46 (s, ketal), 2.1 (s, acetyl), 3.3 – 4.0 (m, pyranose). MALDI-TOF MS (m/z): 11,000 – 50,000.

2.2.2 Chemical characterization methods

Proton nuclear magnetic resonance (^1H NMR) was recorded on Bruker (Billerica, MA) DRX500 spectrometer with a BBO probe as standard with 10 mg of ATC and chitosan samples in 1 mL DMSO- d_6 or $\text{D}_2\text{O}/\text{DCI}$. Fourier transform infrared (FT-IR) spectra were obtained on Jasco 4700 spectrophotometer (Oklahoma City, OK) between 4000 and 400 cm^{-1} with a resolution of 4 cm^{-1} on pressed 1% (w/w) ATC and chitosan samples in potassium bromide (KBr) windows. Matrix-assisted laser desorption/ionization (MALDI)-TOF measurements were completed on AB SCIEX (Redwood City, CA) TOF/TOF 5800 System with 10 mg/mL 2,5-dihydroxybenzoic acid in 50% (V/V) acetonitrile in deionized water (1% trifluoroacetic acid) as a matrix solution. The solubilities of ATC and chitosan were observed by dissolving them in pH 5.0 acetate buffer at $37\text{ }^\circ\text{C}$ for 4 h or DI water at a concentration of 10 mg/mL. ATC and chitosan solutions in pH 5.0 acetate buffer (1 mL) were then neutralized with 200 μL of NaOH (1 M in DI water) to show reduced ATC to native chitosan with lowered solubility. Half-lives of ATC at different pHs were calculated using the Arrhenius equation where A and A_0 represented the integrations of ketal linkage peaks (1.46 ppm) in ^1H NMR spectrum. ATC (10 mg) was dissolved in 1 mL of acetate (pH 5.0 and pH 6.0, adjusted by NaOH) and Tris-HCL (pH 7.4) buffer in D_2O , respectively, and incubated at $37\text{ }^\circ\text{C}$ for various periods of time.

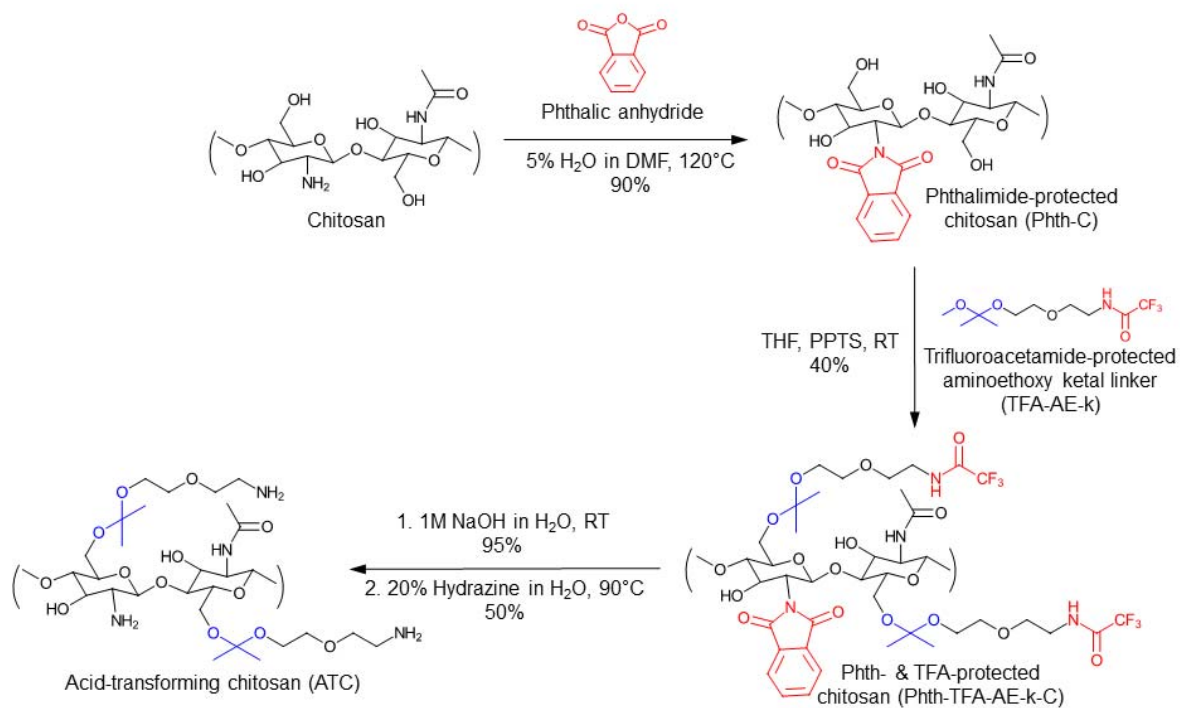
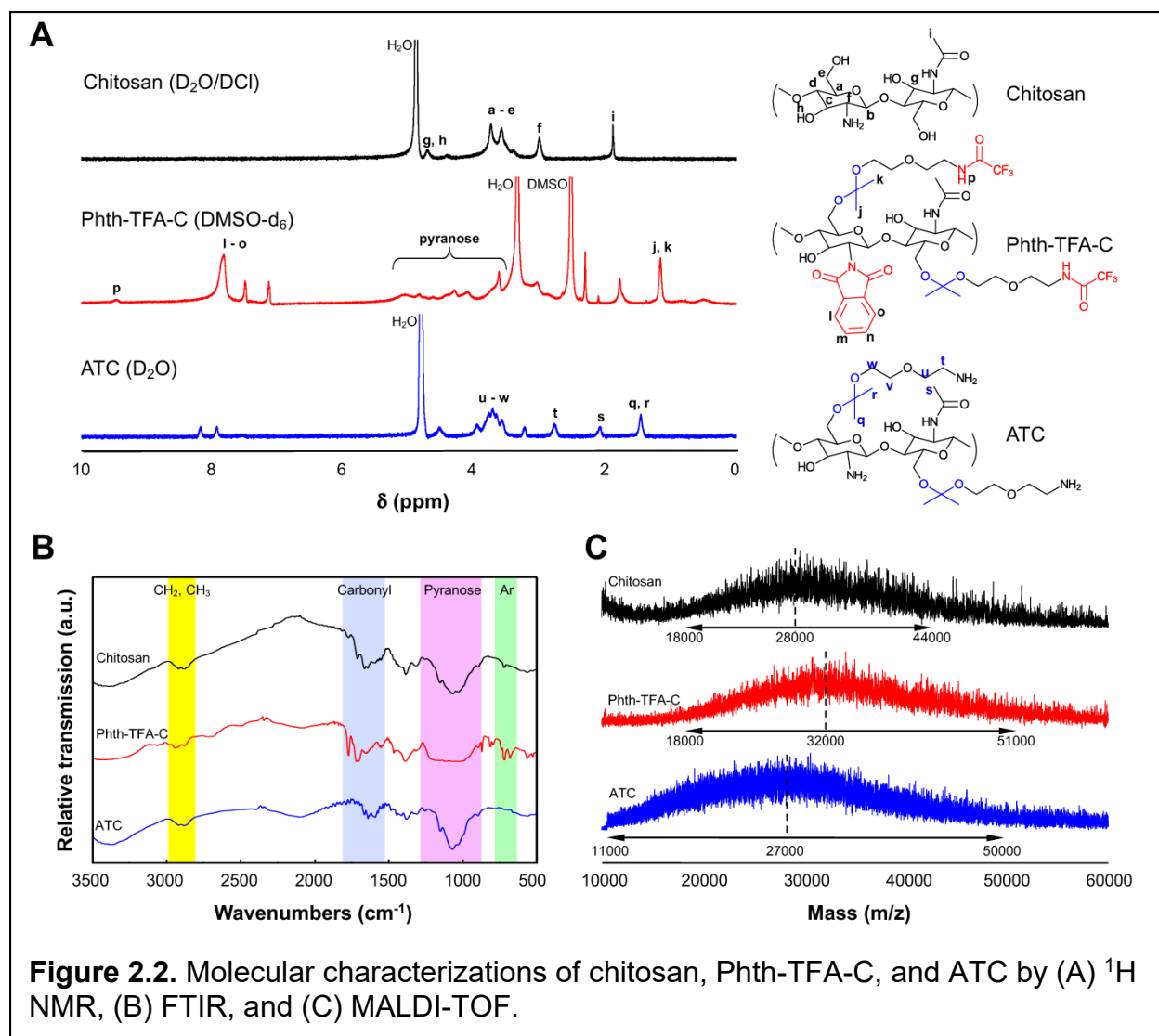


Figure 2.1. Synthesis of ATC. The amine groups in chitosan backbone was phthalamide-protected and its primary hydroxyl groups were then conjugated with TFA-protected aminoethoxy ketal (TFA-AE-k). ATC was obtained after the deprotection of both Phth and TFA.

2.3 Results and discussion

2.3.1 ATC Synthesis

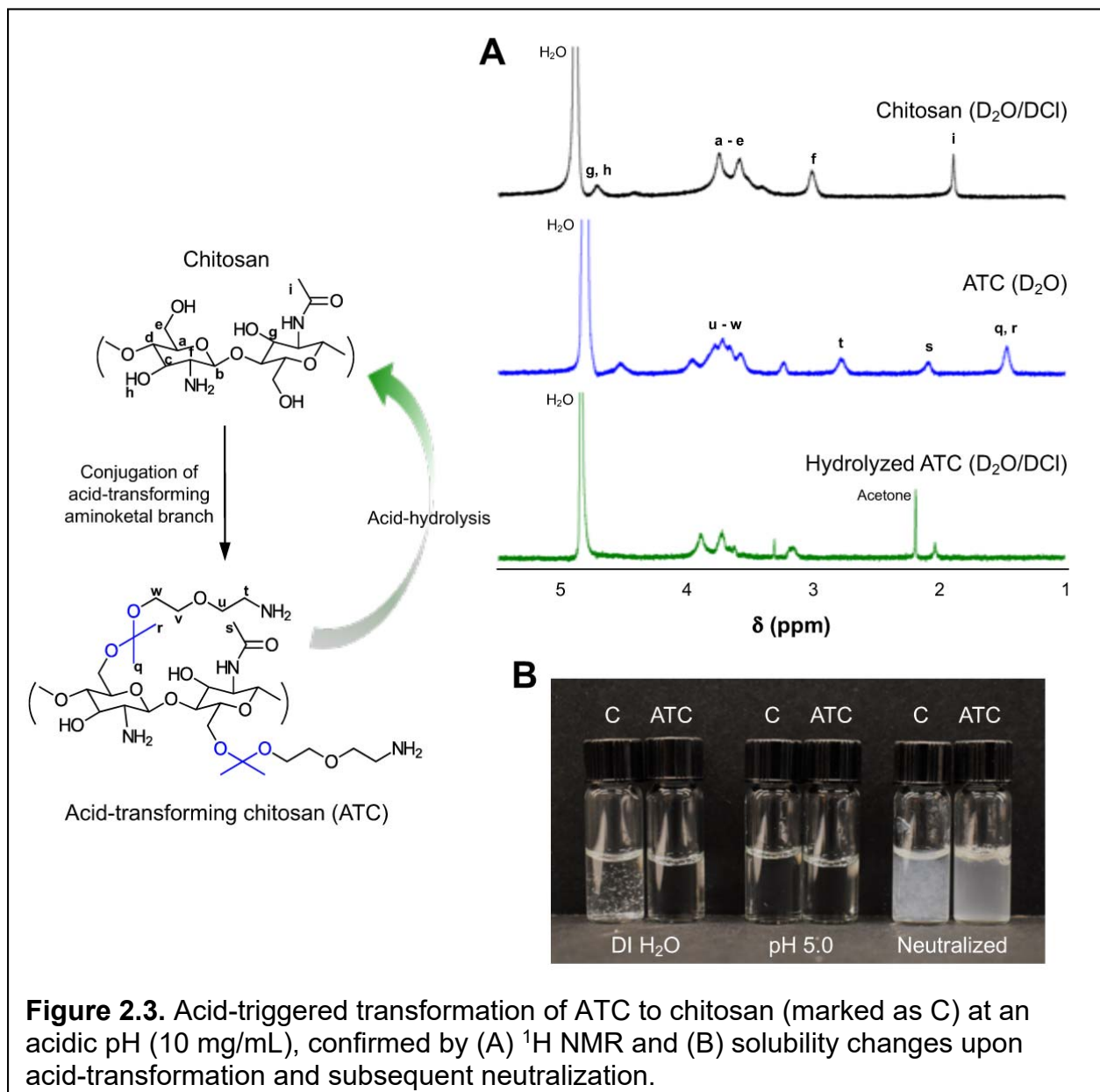
Chitosan was conjugated with acid-cleavable, cationic side chains to synthesize acid-transforming chitosan (ATC) with improved aqueous solubility, siRNA complexation, and siRNA release into the cytoplasm upon acid-hydrolysis of the ketal linkage in the mildly acidic endosome. Successful ATC synthesis was confirmed by the peak at 1.4 ppm, indicative of the dimethyl ketal linkage, and disappearance of the peaks for the



phthalimide and TFA groups at 7.8 ppm and 9.5 ppm, respectively in ^1H NMR spectra (Figure 2.2A). Comparison of the dimethyl ketal (1.4 ppm) with pyranose (3.5 – 3.8 ppm) peak integrations determined that approximately 13% of primary hydroxyl groups were conjugated with the acid-cleavable, cationic side chain. FTIR also confirmed the alkyl (yellow), carbonyl (blue), pyranose (pink), and aromatic (green) groups (Figure 2.2B). The peaks representing carbonyl, pyranose, and aromatic groups exhibited noticeable changes at the protected intermediate but no visible peak shifts were observed in the alkyl region. Chitosan has stronger CH_2 and CH_3 vibrations than the conjugated aminoethoxy branch which could have caused the lack of significant vibrational change in the alkyl region ^{12,13}.

Molecular characterizations of chitosan offer significant technical challenges primarily due to its poor aqueous solubility ¹⁴. While chitosan requires an acidic solvent, ATC should avoid an acidic solvent for characterization. Therefore, it was essential to use the combination of multiple molecular characterization methods such as ^1H NMR, FTIR, and MALDI-TOF a in characterizing ATC and its intermediates (Figure 2.2). MALDI-TOF provided an estimated range of the molecular weight of chitosan, the intermediate, and ATC (Figure 2.2C). The dashed line was used to indicate the peak of the curvature. Between chitosan and phth-TFA-C, the peak shifted from 28,000 to 32,000 m/z. The shift was attributed to conjugation of TFA-AE-k to chitosan as confirmed by conjugation efficiency (i. e. $\sim 13\%$) as calculated by ^1H NMR. After removal of the phth and TFA protecting groups, the MALDI-TOF peak shifted back to 27,000 m/z. The average molecular weight of ATC was lower than chitosan but the molecular weight distribution of ATC (11,000 – 50,000 m/z) was wider than that of chitosan (18,000 – 44,000 m/z). This

could be attributed by significant differences between chitosan and ATC in solubility for separation and purification during synthesis as well as sample preparation for characterization. The molecular weights estimated by MALDI-TOF could be complemented by other methods such as gel permeation chromatography (GPC) and provide crucial information for understanding and predicting its molecular behaviors and



interactions with nucleic acids; however, ATC and its intermediates tend to aggregate in a column, interfering with obtaining an accurate molecular weight measurement.

2.3.2 Acid-transformation of ATC to native chitosan

Acid-triggered ATC transformation to chitosan was demonstrated by changes in molecular structure and solubility at various pHs (Figure 2.3). After incubation at pH 5.0 for 16 h, the peaks for the ketal linkage (1.4 ppm, q, r) disappeared, the broad peak at 3.5-4.0 ppm (u-w) reduced to two distinct peaks upon the loss of aminoethoxy side chain, and a sharp peak at 2.2 ppm for acetone, a by-product of ketal hydrolysis, appeared (Figure 2.3A). Acid-transformation of ATC to chitosan was also obvious in solubility

changes (Figure 2.3B). While chitosan rapidly precipitates in water, ATC was instantaneously and fully dissolved in water. At an endosomal pH of 5.0, chitosan became soluble but precipitated severely upon neutralization, while hydrolyzed ATC at pH 5.0 became insoluble without visible precipitation upon neutralization. The half-lives of

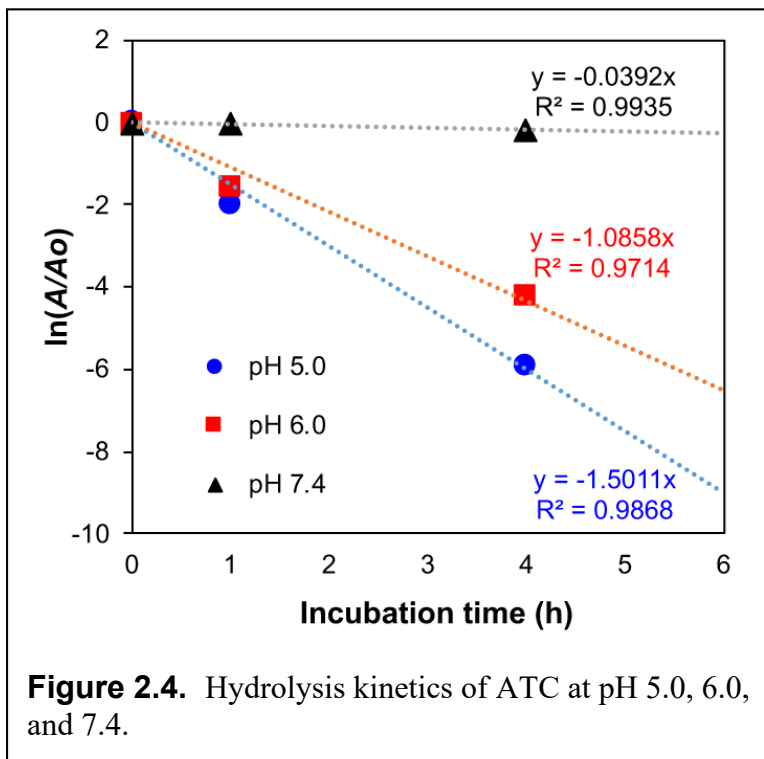
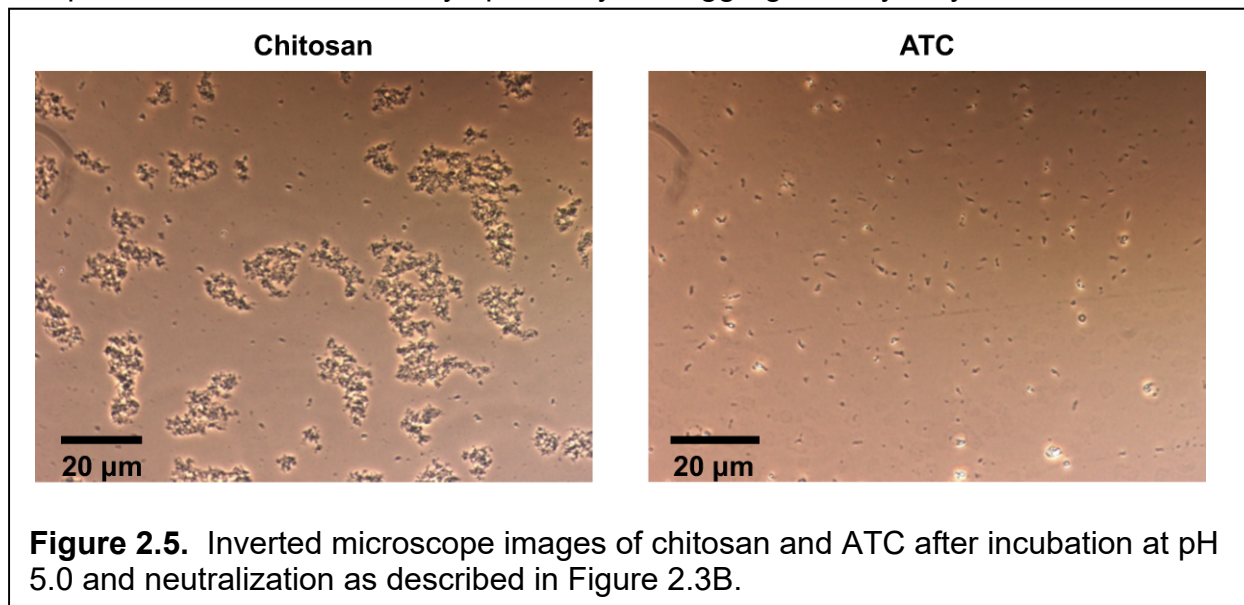


Figure 2.4. Hydrolysis kinetics of ATC at pH 5.0, 6.0, and 7.4.

ATC at pH 5.0, 6.0 and 7.4 were calculated to be 0.48, 0.64, and 17.7 h, respectively (Figure 2.4). Neutralization of acid-incubated ATC reduced its solubility due to acid-

hydrolysis of ketal linkages of aminoethoxy side chains. This observation indicates molecular changes of ATC during extracellular and intracellular processes; ATC is water-soluble during extracellular transport and cellular uptake, gets acid-hydrolyzed in the endosome/lysosome and undergoes transformation, and is released as chitosan into the cytoplasm. Interestingly, ATC solution incubated at pH 5.0 and further neutralized became a homogeneous suspension of small particulates (575 +/- 42 nm), while much larger aggregates (1110 +/- 425 nm) of chitosan treated in the same way (Figure 2.5). This observation implies faster clearance of hydrolyzed ATC by reticuloendothelial system (RES) and enzymatic degradation^{15,16} as well as lower risk of causing adverse effects such as embolism^{17,18} than native chitosan. The results shown in Figure 2.3 implicate efficient siRNA complexation by ATC with improved aqueous solubility and molecular interactions with cationic side chains, rapid siRNA release upon acid-hydrolysis of cationic side chains in the mildly acidic endosome/lysosome and avoided re-complexation of siRNA in the cytoplasm by self-aggregated, hydrolyzed ATC.



2.3.3 Effects of deacetylation and molecular weight on synthesis

Properties of chitosan are heavily dependent on the degree of de-acetylation, changing the number of free primary amines, and the molecular weight of the polymer. In most cases, natural chitosan has an extremely heterogeneous molecular weight. Depending on the source of chitosan, the heterogeneity of changes ^{19,20}. The molecular weight of chitosan can range from 10 kDa to 100,000 kDa with polydispersity index greater than 3. This polydispersity presents a challenge in the synthesis of ATC. Chitosan was refined and purified before use by the manufacturer to overcome the variability. These purified, source chitosan were provided with a narrower range of molecular weight and specific deacetylation values. When used in the reaction, the higher molecular weight and higher de-acetylation values typically required longer reaction times and higher concentrations of catalyst. This was expected since the larger chain lengths, and increased number of amines will have a direct effect on the products for each step of the synthesis.

2.3.4 Separation and purification of polymer

The final yield of ATC obtained was highly dependent on the deprotection conditions and the recovery of pure ATC after the separation process. Separating conjugated ATC from unconjugated was relatively straightforward due to the increased water solubility when conjugated. Unmodified chitosan precipitates easily in aqueous conditions. The major challenge involved in the separation process is that it is done in water through dialyzing. Specifically, ATC did not have a long shelf life in aqueous conditions and would start reverting to chitosan after 24 h at room temperature. However,

dialysis post deprotection took 24 h minimum to complete. Thus some product was lost during purification. Additionally, ATC appeared to have a maximum solubility in water at around 7 mg/ml. Solutions with higher concentrations of ATC precipitates, which led to the possible loss of product during the separation process. For a generation of large amounts of ATC, large volumes would need to be generated to account for the solubility limit. There is a possibility that modifying the linker molecule to a longer alkyl chain or increasing the conjugation further could improve the solubility limit. However, those changes may also impact the properties of antimicrobial or gene therapy applications.

2.4 Conclusion

The modification of chitosan with an acid-responsive linker to form acid-transforming chitosan (ATC) was accomplished and fully characterized. This modification was shown to be temporary, and chitosan is regenerated upon acid hydrolysis. While the synthesis worked, the efficiency was relatively low, yielding with only milligram quantities of ATC recovered after each reaction process. For future applications, the synthesis scheme will need to be revisited and optimized to allow for higher yields. Another alternative would be to change the reaction process from a batch type reaction to a continuous reaction. Additionally, it would be ideal to have the linker molecule play an active role in the therapeutic process so future studies will include the possibility of conjugating conventional antibiotics via the linker molecule.

2.5 References

- (1) Mourya, V. K.; Inamdar, N. N. *React. Funct. Polym.* **2008**, *68* (6), 1013–1051.
- (2) Mourya, V. K.; Inamdar, N. N.; Tiwari, A. *Adv. Mater. Lett.* **2010**, *1* (1), 11–33.
- (3) Ravi Kumar, M. N. . *React. Funct. Polym.* **2000**, *46* (1), 1–27.
- (4) Aranaz, I.; Mengibar, M.; Harris, R.; Panos, I.; Miralles, B.; Acosta, N.; Galed, G.; Heras, A. *Curr. Chem. Biol.* **2009**, *3* (2), 203–230.
- (5) Srinivasulu K; N. Dhiraj Kumar. *IMPACT Int. J. Res. Eng. Technol. (IMPACT IJRET)* **2014**, *2* (2), 85–96.
- (6) Balamuralidhara, V., Pramodkumar, T. M., Srujana, N., Venkatesh, M. P., Gupta, N. V., Krishna, K. L., & Gangadharappa, H. V. *American Journal of Drug Discovery and Development*. 2011, pp 24–48.
- (7) Kondo, G.; Oda, T.; Suzuki, A.; Tokuyama, M.; Oppenheim, I.; Nishiyama, H. In *AIP Conference Proceedings*; AIP, 2008; Vol. 982, pp 458–463.
- (8) Schmaljohann, D. *Adv. Drug Deliv. Rev.* **2006**, *58* (15), 1655–1670.
- (9) Fleige, E.; Quadir, M. A.; Haag, R. *Adv. Drug Deliv. Rev.* **2012**, *64* (9), 866–884.
- (10) Cho, S. K.; Kwon, Y. J. *J. Control. Release* **2011**, *150* (3), 287–297.
- (11) Shim, M. S.; Kwon, Y. J. *Bioconjug. Chem.* **2009**, *20* (3), 488–499.
- (12) Lawrie, G.; Keen, I.; Drew, B.; Chandler-Temple, A.; Rintoul, L.; Fredericks, P.; Grøndahl, L. *Biomacromolecules* **2007**, *8* (8), 2533–2541.
- (13) Pranoto, Y.; Rakshit, S. K.; Salokhe, V. M. *LWT - Food Sci. Technol.* **2005**, *38* (8),

859–865.

- (14) Byrd, H. C. M.; McEwen, C. N. *Anal. Chem.* **2000**, 72 (19), 4568–4576.
- (15) Lim, S. M.; Song, D. K.; Oh, S. H.; Lee-Yoon, D. S.; Bae, E. H.; Lee, J. H. *J. Biomater. Sci. Polym. Ed.* **2008**, 19 (4), 453–466.
- (16) Reifarth, M.; Hoepfener, S.; Schubert, U. S. *Adv. Mater.* **2018**, 1703704.
- (17) Cao, Y.; Ding, Y.; Zhang, L.; Shi, G.; Sang, X.; Ni, C. *J. Appl. Polym. Sci.* **2018**, 135 (4), 45731.
- (18) Hong, S.-C.; Yoo, S.-Y.; Kim, H.; Lee, J. *Mar. Drugs* **2017**, 15 (3), 60.
- (19) Zvezdova, D. *Synth. Charact. chitosan from Mar. sources Black Sea* **2010**, 3, 65–69.
- (20) Rinaudo, M. *Prog. Polym. Sci.* 2006, pp 603–632.
- (21) Shim, M. S.; Kwon, Y. J. *Adv. Drug Deliv. Rev.* **2012**, 64 (11), 1046–1059.
- (22) Wong, S.; Shim, M. S.; Kwon, Y. J. *J. Mater. Chem. B* **2014**, 2 (6), 595.
- (23) Cobo, I.; Li, M.; Sumerlin, B. S.; Perrier, S. *Nat. Mater.* **2015**, 14 (2), 143–159.
- (24) Bui, Q. N.; Li, Y.; Jang, M. S.; Huynh, D. P.; Lee, J. H.; Lee, D. S. *Macromolecules* **2015**, 48 (12), 4046–4054.
- (25) Felber, A. E.; Dufresne, M. H.; Leroux, J. C. *Adv. Drug Deliv. Rev.* **2012**, 64 (11), 979–992.

Chapter 3: Antimicrobial capacity of acid-transforming chitosan (ATC)

3.1. Background

Intracellular bacteria are infectious microorganisms that replicate within host cells, usually mononuclear phagocytes (MPs) ¹. This allows the bacteria to evade host humoral defense mechanisms and aids in the survival and persistence of infection ². *Salmonella typhimurium* is an example of a pathogenic gram-negative intracellular bacterium. *S. typhimurium*, generally infect humans and many other mammalian species, most specifically domestic animals ³. *Salmonella* invades cells by injecting effector proteins into the host cell then triggering cytoskeletal rearrangement ⁴. The bacterium further persists within a vacuole (~pH 7.4) after escaping the endosomal compartment (~pH 5.0). Intracellular bacteria such as *Salmonella* persists and hide well within cells, making their treatment challenging due to the added biological barrier. However, there is a possibility of treating these infections by hijacking the gene delivery pathway, through the application of nanoparticle vectors that are engineered for enhanced cellular uptake and intracellular release. The most suitable vector would be a non-viral vector (reduced immunogenicity) with some antimicrobial capabilities.

Chitosan is a natural polysaccharide, with broad-spectrum antimicrobial efficacy against both gram-positive and gram-negative bacteria ⁵. In our previous work, we improved on key limitations of chitosan (limited solubility in aqueous solution and inefficient nucleic acid complexation and release) with the synthesis of acid-transforming chitosan (ATC). ATC was shown to be aqueous soluble, but more significantly was the

regeneration of chitosan upon acid hydrolysis. The regenerated chitosan presented an opportunity to apply the antimicrobial material to an intracellular infection where both the gene silencing pathway and the acid-responsive properties can be utilized. Therefore, in the work presented we confirmed ATC's antimicrobial efficacy against an intracellular gram-negative infection (*S. typhimurium*). In confirmation of the antimicrobial efficacy of ATC, objectives were evaluated: antimicrobial capacity of the polymer at various pHs to simulate possible intracellular conditions; formation of ATC polyplexes to treat intracellular infections in vitro; elucidation of ATC's antimicrobial mechanism with the aid of transposon insertion sequencing.

3.2 Experimental details

3.2.1. Materials

All chemicals were purchased from commercially available sources and used as received. Chitosan (M_w 18–44 kDa, 95% deacetylated) was purchased from Heppe Medical Chitosan (Halle, Germany) and 3-(4,5-dimethyl-2-thiazolyl)-2,5-diphenyltetrazolium bromide (MTT) and Gentamicin were purchased from Sigma-Aldrich (Milwaukee, WI). Raw 264.7 and HeLa cells (ATCC, Rockville, MD) and were cultured in Dulbecco's modified Eagle's medium (DMEM) (MediaTech, Herndon, VA) with 10% fetal bovine serum (FBS) (Hyclone, Logan, UT) and 1% antibiotics (100 units/mL penicillin; 100 µg/mL streptomycin) (MediaTech). Libraries of *E. coli* Nissle (ECN 150923) and *S. typhimurium* (MZ0921) bacterial strains were obtained from the lab of Professor Michael McClelland (University of California, Irvine) and grown in LB broth at 37°C, with antibiotics

added at the following concentrations: 100 µg/ml ampicillin, 60 µg/ml kanamycin, as indicated.

3.2.2. RAW 264.7 cells infection with GFP *Salmonella Typhimurium*

GFP *Salmonella* (MZ0921) was grown for 16h in LB broth in 60 µg/mL antibiotics to 10⁹ CFU. In DMEM *Salmonella* was diluted 4-fold to 10⁵ CFU. 10 µL of bacteria was diluted in 10 mL of fresh LB. Followed by further dilution of 20 µL into 20 mL of DMEM with 10% FBS 400 µL of inoculant was added to each well then incubated for 30 min. After 30 min, the inoculant was removed and washed twice with PBS. 400 µL of DMEM with 100 µg/mL gentamicin was added to each well and incubated for 1 h at 37 °C. The media was removed, and wells washed once with PBS. 400 µL of DMEM with 100 µg/mL gentamicin and 60 µg/mL kanamycin was added to the cells and incubated for 1 h. 10% 10x DMEM and 10x PBS and FBS were added to the polyplex solutions. Media was removed, and wells were washed once with PBS.

3.2.3 Effect of pH on microbial toxicity

5 µL and 10 µL of 1 M acetic acid buffers at pH 5, 5.5, and 6 were added to each well in a 24 well plate. 100 µL of sample was then added to each well and mixed on an orbital shaker for 5 mins. 100 µL of bacteria in LB broth was added followed with 24 h growth at 37 °C incubator

3.2.4. Preparation of ATC/pdrn polyplexes

Polyplexes at N/P of 100 were created from 500 µL of the polymer at concentrations of 100, 500, and 1000 µg/ml ATC in DI water was added dropwise to 500 µL of 34.07 µg of pdrn, followed by vortexing and incubation at room temperature for 30

min to form ATC/pdrn polyplexes. The resulting polyplex solution was diluted with an additional 800 μL of DI water. Mean particle diameter (Z-average) with a polydispersity index (PDI) and zeta potential of various ATC/pdrn polyplexes were measured by dynamic light scattering (DLS) particle analysis using a Zetasizer Nano ZS (Malvern, UK) at 25 °C and angle of 90°. The viscosity (0.887 mPA/s) and refractive index (1.33) of water at 25 °C were used to analyze the data.

3.2.5. Preparation of *E. coli* Nissle samples for transposon screening

For the log phase: 100 μL of ECN 150923, stored in the -80 °C (@ 10⁹ CFU) was added to 10 mL of LB w/ 10 μL of kanamycin (60 mg/mL) final concentration 60 $\mu\text{g}/\text{mL}$) and grown overnight. 100 μL was then taken and added to 10 mL of LB (60 $\mu\text{g}/\text{mL}$ kanamycin), allowed to reach OD of 0.3. A 100 μL aliquot of the 0.3 OD was mixed by pipetting with 40 μL of 50% glycerol to make 20% glycerol and frozen in -80 for titering. 500 μL of bacteria was added to a 24 well plate, and 500 μL of the compound was added to each well. The plate was stored in an incubator at 37 degrees with 200 rpms of shaking. After 1 h a 100 μL aliquot of each was mixed with 40 μL of 50% glycerol to make 20% glycerol and frozen in -80 for titering. The remaining was transferred to a 10-mL conical tube, centrifuged at 1500 rpm to make a pellet, the supernatant was thrown away. The pellet was washed in 5 mL LB again, and then centrifuged again, the supernatant removed, then resuspended in 3 mL of LB with kanamycin, and grown overnight. The purpose was to remove the compound and grow the bacteria without selection. After growth, a 1 mL aliquot was mixed with 400 μL of 50% glycerol to make 20% glycerol and frozen in -80 °C for sequencing.

For stationary phase: 100 μL of ECN 150923, stored in the $-80\text{ }^{\circ}\text{C}$ (10^9 CFU) was added to 10 mL of LB w/ 10 μL of kanamycin (60 mg/mL) final concentration 60 $\mu\text{g}/\text{mL}$) and grown overnight. A 100 μL aliquot of stationary bacteria was mixed with 40 μL of 50% glycerol to make 20% glycerol and frozen in -80 for titering. 500 μL of stationary bacteria was added to a 24 well plate, and 500 μL of the compound was added to each well. The plate was stored in an incubator at 37 degrees with 200 rpms of shaking. After 1 h a 100 μL aliquot of each was mixed with 40 μL of 50% glycerol to make 20% glycerol and frozen in -80 for titering. The remaining was transferred to a 10-mL tube, centrifuged at 1500 rpm to make a pellet, the supernatant was thrown away. The pellet was washed in 5 mL LB again and then centrifuged again, the supernatant removed, then resuspended in 3 mL of LB with kanamycin, and grown overnight. Titrations were done on the library by sampling what went into the 24 wells and the content of each well at one hour. Sequencing was completed following procedures previously published ⁶.

3.2.6. Cytotoxicity of polymer on RAW 264.7 cells

Cells were seeded at a density of 9,000 cells per/well in a 96-well plate and incubated overnight. The culture medium was replaced with 200 μL of the polymer at various concentrations by serial dilution in FBS-free DMEM and incubated for 12h at 37 $^{\circ}\text{C}$. The medium was replaced with 200 μL of MTT solution (1 mg/mL in FBS-free DMEM). After 2 h of incubation at 37 $^{\circ}\text{C}$, the MTT solution was discarded from each well, and the cells were washed with PBS once. 200 μL of DMSO was added to each well to dissolve the MTT formazan crystals formed by live cells, and the plate was incubated at 37 $^{\circ}\text{C}$ for

5 min. The absorbance of formazan products was then measured at 561 nm wavelength using a microplate reader, Synergy HT (BioTEK, Winooski, VT, USA).

3.2.7. Statistical analysis

All Data were expressed as mean +/- standard deviation. chi-squared T(x) was used to evaluate data for significant differences between means. We accepted $p < 0.05$ as an indication that statistically significant differences exist between the means.

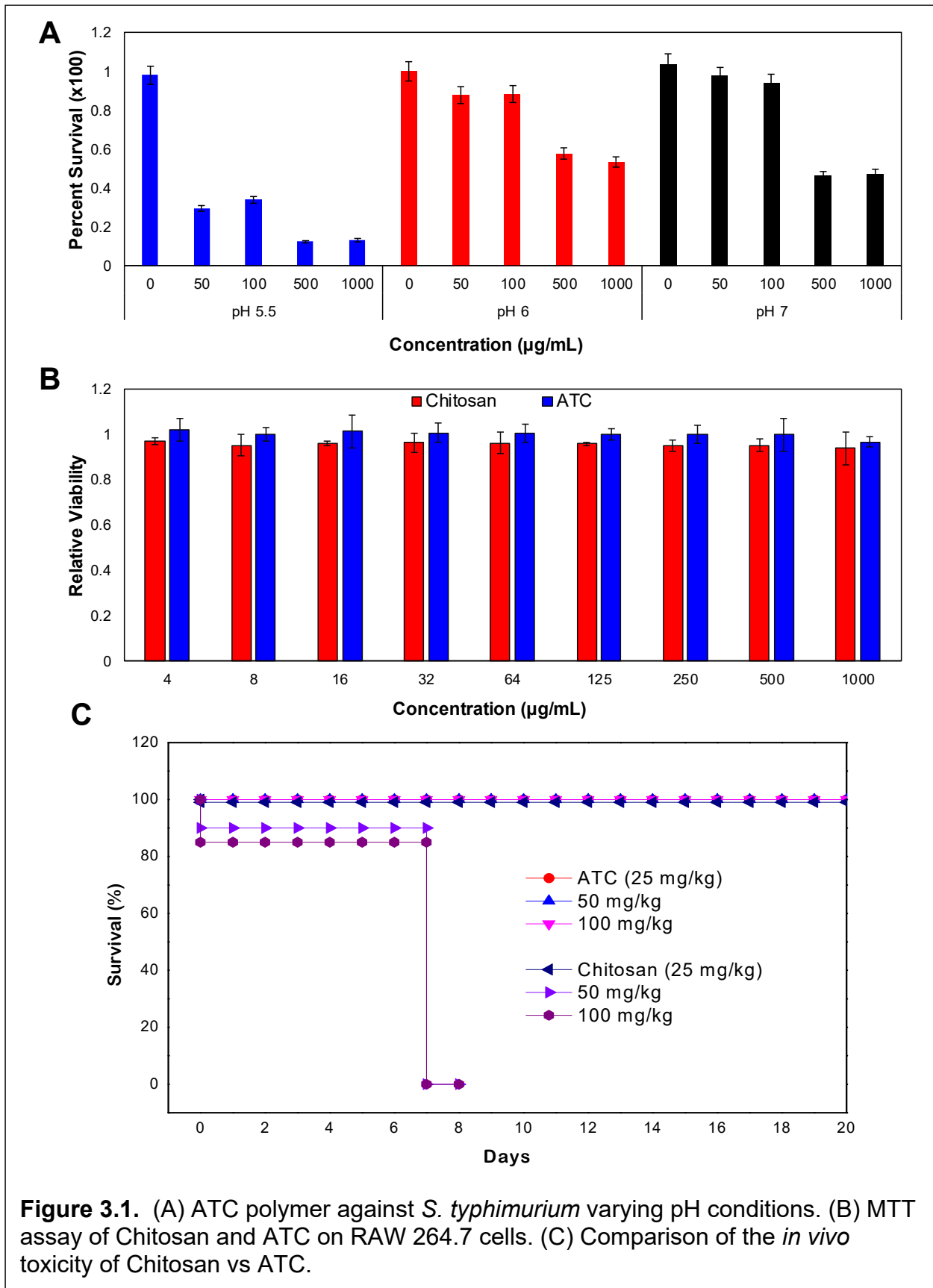
3.3 Results and discussion

3.3.1. Antimicrobial efficacy of ATC and toxicity of ATC

Intracellular pathogens can localize in cellular compartments such as early endosome, late endosome, or vacuoles^{1,7,8} protecting them from normal bactericidal activities of the host cell. Each of these compartments has a pH ranging from 5.3 or lower for late endosome to 7.4 for vacuoles⁹⁻¹¹. *S. typhimurium*, has been shown to transition from the late endosome to a specialized vacuole within the host cell^{12,13}. Therefore, in engineering an antimicrobial gene carrier against intracellular microbes like *S. typhimurium*, antimicrobial efficacy under a multitude of pH conditions is desired. To this end, antimicrobial efficacy of ATC against *S. typhimurium* at varied pH was confirmed prior to testing on intracellular infection (Figure 3.1A). *S. typhimurium* was incubated with ATC and 25 mM of buffer (pH 5.5, 6, or 7) for 24 h (Figure 3.1A). Less than 50% of microbes survived regardless of pH at ATC concentration greater than 500 $\mu\text{g}/\text{mL}$. At pH 5.5, the percent of surviving microbes decreases for all ATC concentrations but most significantly for concentrations of 50 and 100 $\mu\text{g}/\text{mL}$. It has been previously reported that

the antimicrobial efficacy of chitosan increased in an acidic pH ¹⁴, same can be expected for ATC. In an acidic pH the primary amines with pKa values ~ 6.5 become protonated, which is believed to favor interactions with microbial wall and membrane ¹⁵ without damage to mammalian cells.

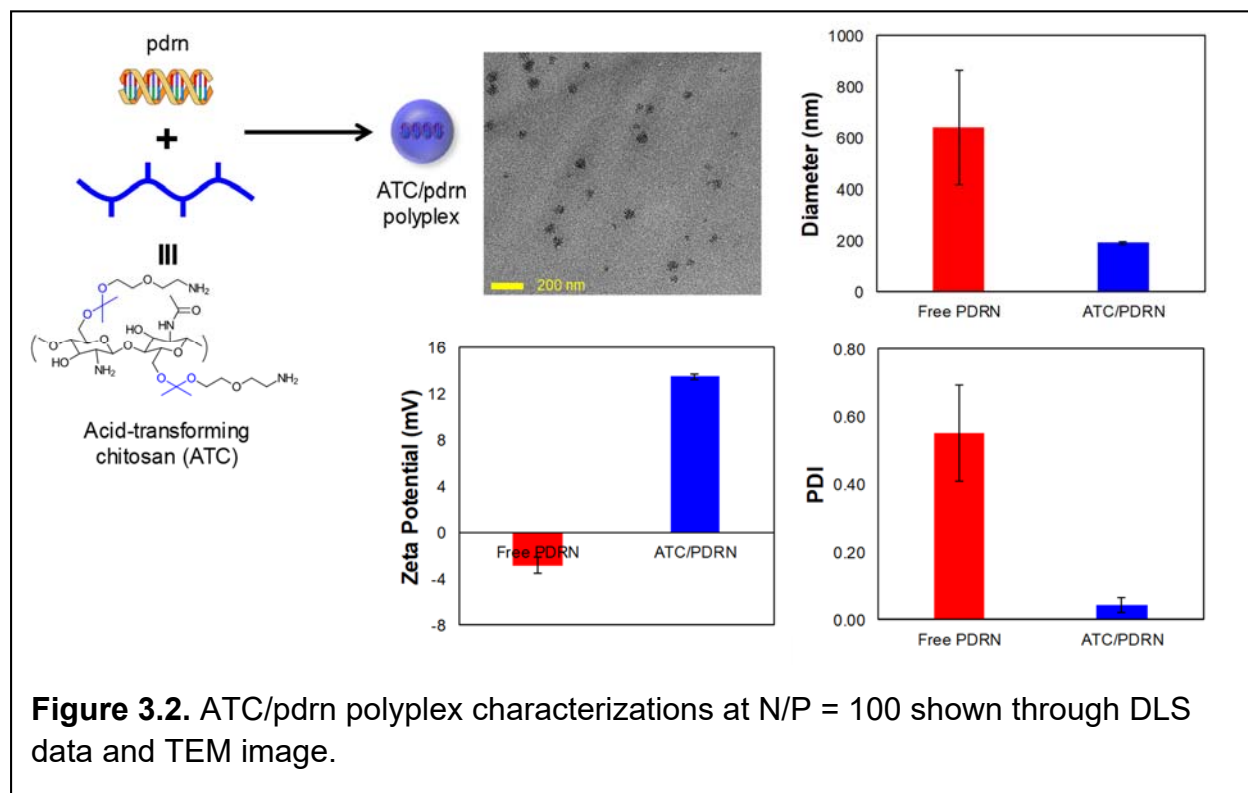
In vitro and *in vivo* toxicity is of high importance for the design of nanoantibiotic platform using ATC. Furthermore, since intracellular bacteria are within a host mammalian cell, ATC needs to maintain minimal toxicity to the host while effectively eradicating the infection. From the MTT assay of ATC against RAW 264.7 macrophage cells, no toxicity was observed at any of the concentrations (Figure 3.1B). ATC was compared to unmodified chitosan which no *in vitro* cellular toxicity was reported¹⁶. However, for *in vivo* studies, 50 mg/kg doses and higher of chitosan caused death (Figure 3.1C). The observed *in vivo* toxicity agreed what has been previously reported for chitosan¹⁶ when delivered intravenously. Blood aggregation was speculated as the cause of death¹⁷. Interestingly, although ATC was derived from chitosan, *in vivo* toxicity was not observed at similar dosages. This reduced toxicity was possibly because ATC is a water-soluble variant of chitosan, therefore, when administered intravenously was less likely to cause blood aggregation. In the design of the platform, limiting acute toxicity was given greater significance since the focus was on immediate eradication of a pathogenic bacteria. However,



possible long-term toxicities associated with chitosan and hence ATC, should be noted as well. While toxicities stemming from chronic use are only just starting to be explored, these toxicities are usually dose and concentration dependent^{18,19}. Some early studies have indicated some chronic *in vivo* toxicity against zebrafish models at dosages of 250 mg/L which is close to the lethal dose of 280 mg/L¹⁸. Furthermore, while these chronic toxicities should be considered, they are at doses much higher than doses of clinical significance.

3.3.2. Formation of ATC/pdrn polyplexes

ATC displayed excellent antimicrobial activity, however, in an uncomplexed form, traversing the cell membrane would be a problem. Therefore, cell uptake was facilitated

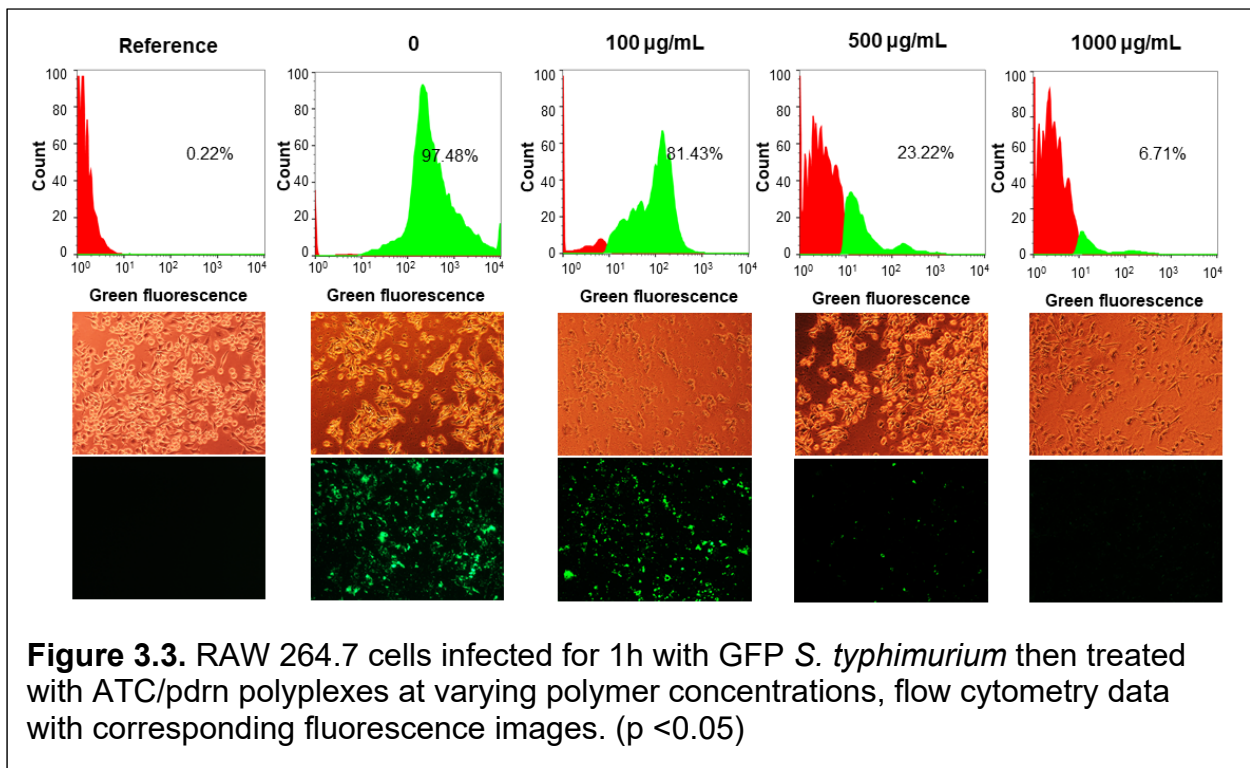


by creating a polyplex out of ATC with polydeoxyribonucleotide (pdrn) to form particles around 200 nm in diameter (Figure 3.2).

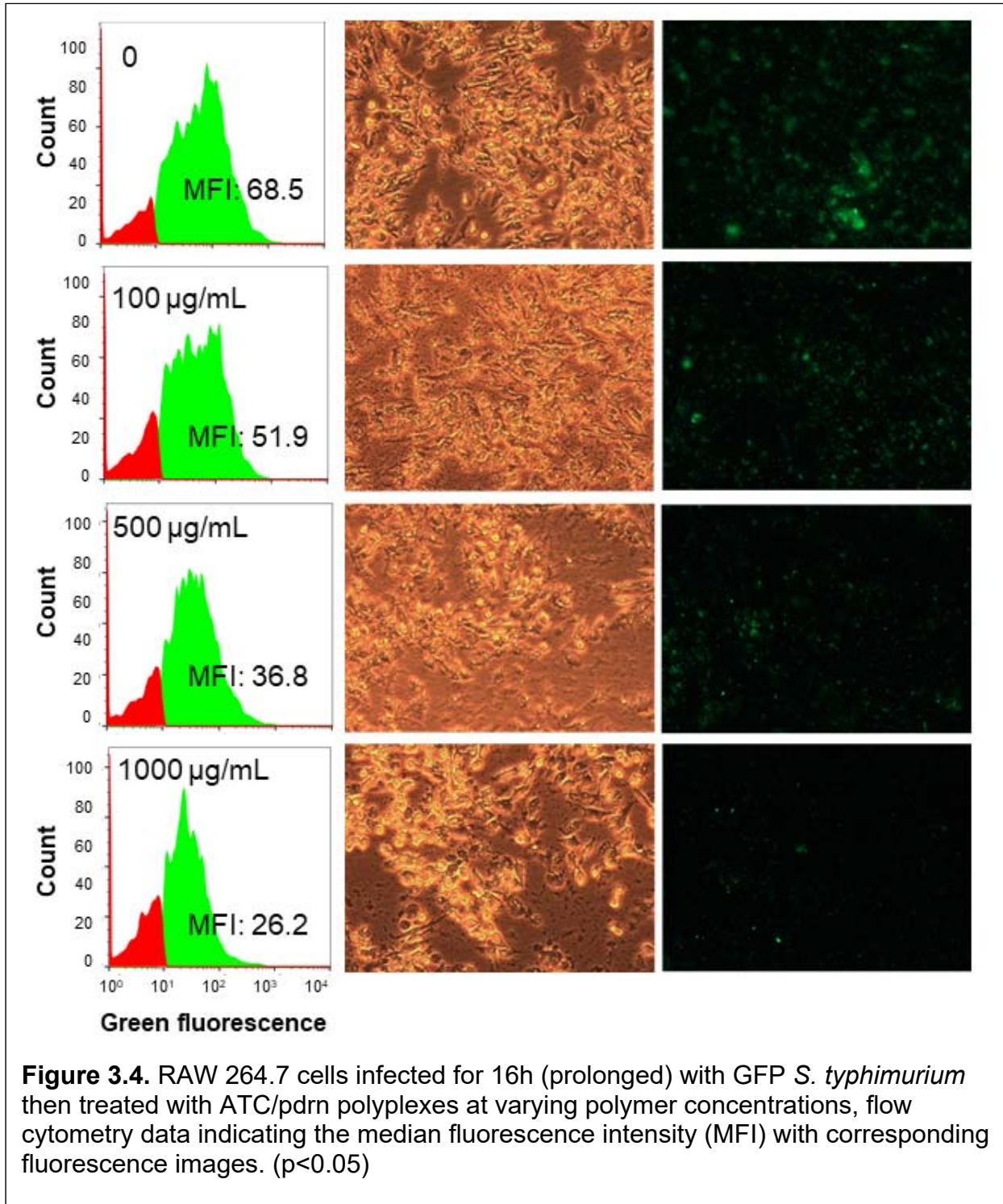
Pdrn was selected because it is comprised of negatively charged nucleic acids and lacks genetic specificity as it does not code for any specific proteins^{20,21}. Thus a polyplex can be simply formed through electrostatic interaction to test the intracellular antimicrobial activity of ATC. Polyplexes were created at an N/P ratio of 100 and created highly monodisperse particles with a PDI less than 0.1 (Figure 3.2). These particles also had a zeta potential of +13 mV. ATC/pdrn polyplexes were created and used without any additional purification. Due to the lack of further purification, there could have been possibility of excess uncomplexed material which were not expected to cause any problems for *in vitro* studies. However, for *in vivo* studies and future clinical applications, further purification will be desired. Removal of excess pdrn or ATC could be achieved by column chromatography.

3.3.3. Utilization of ATC/pdrn polyplexes to treat intracellular infection

Intracellular infections can occur in various cell types, but usually more prevalent in phagocytic cells²², hence the use of RAW 264.7. Furthermore, in most real-world applications, antibiotics are not used until the infection has prolonged, ATC polyplexes were applied to prolonged infections to highlight the versatility of ATC as a nanoantibiotic. Therefore, to demonstrate an early infection, where there were minimal bacteria per cell, RAW 264.7 cells were infected with GFP expressing *S. typhimurium* for 1 h then treated with ATC/pdrn polyplexes. Microbe death was confirmed using fluorescence microscopy and flow cytometry. For early-stage infection, the most significant results occurred at 500 and 1000 $\mu\text{g/mL}$ of ATC/pdrn polyplexes (Figure 3.3). Bacterial growth was hindered nearly 100% at concentrations of 1000 $\mu\text{g/mL}$, and minimal 100 $\mu\text{g/mL}$. This result was as expected and correlated with the antimicrobial efficacy observed with uncomplexed ATC. For a prolonged intracellular infection, RAW 264.7 cells were infected with GFP



expressing *S. typhimurium* where the bacteria grew for 16 h before ATC/pdrn polyplexes were introduced (Figure 3.4). There was significant reduction of up to 40% in bacteria as the concentration of polyplex increased. Even at low concentrations of polyplex, 100



mg/mL, there was a 9% reduction in the median fluorescence intensity compared to the control. Though this was a single dose study, continued treatment could yield a further reduction in bacteria growth. The antimicrobial capacity against early-stage intracellular infection was further emphasized in cell lysis data (Figure 3.5). Bacteria at 1000 $\mu\text{g/mL}$ of ATC were almost completely eliminated, and intracellular survival of colonies was almost negligible. From the colony count, 100 $\mu\text{g/mL}$ polyplexes showed about twice the reduction in *S. typhimurium* growth compared to the control than observed in the flow cytometry data and fluorescence images. It is possible that there were false positive fluorescent readings attributed to extracellular bacteria since it is expected highest antimicrobial activity would occur intracellularly.

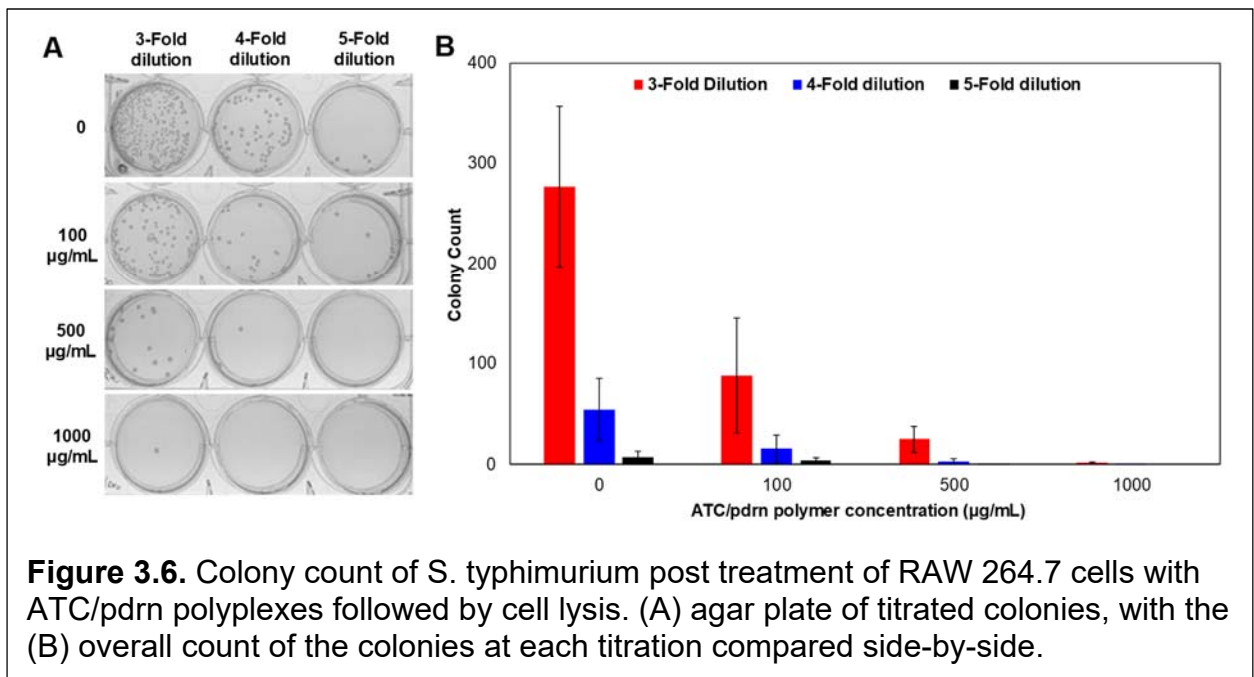


Figure 3.6. Colony count of *S. typhimurium* post treatment of RAW 264.7 cells with ATC/pdrn polyplexes followed by cell lysis. (A) agar plate of titrated colonies, with the (B) overall count of the colonies at each titration compared side-by-side.

3.3.4. Suggested antimicrobial mechanism using transposon insertion sequencing

One of the suggested mechanisms by which chitosan, and ATC, kills microbes involves charge-mediated transmembrane pore formation²³, however there is growing speculation that this is not the only mechanism. Therefore, to determine whether the antimicrobial efficacy is predicated on pore formation on the cell membrane or disruption of microbial intracellular processes^{5,24–26} an analysis of microbe fitness upon exposure to chitosan or ATC was performed on *E. coli Nissle* was used as a preliminary model (Table 3.1). Preliminary data of sequenced samples highlighted a myriad of genes that could have some significance in the mechanism of action. It is important to note that these genes were not upregulated or down-regulated in this assay instead only changes in the relative abundance of mutants. Some mutants are becoming more common while others are becoming rarer during the treatment. If a mutant became common, then knocking out the gene made the bacterium survive better in the presence of the treatment with the polymers. However, if the mutant became rarer upon treatment, then that means knocking out the gene caused the survival of the bacterium in the treatment to be worse. This event would have indicated that such gene might be involved in protecting the bacterium against the treatment. However, no such genes were found in the preliminary study. More replicates would need to be used in future studies to confirm whether such a gene existed. While an equal number of genes in the cytosol versus membrane appeared have been flagged, only a few are significant. The library used consisted of about 40,000 independent mutants which were constructed by electroporating the transposon into the bacteria. Each transposon, with a kanamycin resistance cassette and a barcode, located

Table 3.1. *E. coli* Nissle transposon sequencing data

Legend: Red= also in <i>S. Typhi</i> – cytosol Blue = also in <i>S. Typhi</i> - membrane Green = mutant more resistant than wild type to ATC and chitosan * = P value <0.05			Significant Sample	Log (Input before treatment / Output after treatment)					
				ATC 0.7 mg/ml	ATC 3.5 mg/ml	ATC 7.0 mg/ml	Chit 0.7 mg/ml	Chit 3.5 mg/ml	Chit 7.0 mg/ml
Gene	Function Location	ATC	Chit	Δ	Δ	Δ	Δ	Δ	Δ
MprA	transcriptional regulator/ repressor Cytosol	✓	✓	2.8*	3.0*	2.5*	3.6	2.9*	1.8*
EntB/ PhzD	Isochorismatase siderophore biosynthesis Cytosol	✓		2.8*	3.2*	2.6*	3.1	1.4	1.4
BioA	adenosylmethionine--8-amino-7-oxononanoate aminotransferase Cytosol	✓		2.7*	2.8*	2.5*	2.6	2.1*	1.5
ItaE	low-specificity L-threonine aldolase Cytosol	✓		2.8*	2.9*	2.5*	2.5	2.4*	1.2
PoxB	pyruvate dehydrogenase Cell Membrane	✓		2.7*	3.0*	2.5*	2.4	1.3	2.1*
YbcU	lambda Bor protein precursor Outer cell membrane	✓		2.9*	3.1*	2.6*	2.8	1.4	2.2*
YjiR	GntR family transcriptional regulator Cytosol	✓		3.2*	3.5*	3.1*	3.1	0.9	1.8
FlhA	flagellar biosynthesis protein Inner cell membrane	✓		2.6	2.9*	2.8*	-1.1	0.2	0.9
ClbM	MATE family efflux transporter:Na+-driven multidrug efflux pump Transmembrane	✓		2.9*	3.2*	2.7*	2.9	1.3	1.1
FecD	Iron(III) dicitrate transport system permease protein Inner cell membrane	✓		2.8*	2.8*	2.7*	-2.0	-0.2	0.7
GcvH	Glycine cleavage system H protein Cytosol	✓		2.9*	3.1*	2.6*	2.8	1.5	1.5

in a random place in just one bacterium. Then the library was selected for in kanamycin-containing media to generate 40,000 mutants with an identifiable barcode ⁶. After exposure to both chitosan and ATC, only a few features seemed to be disrupted. Furthermore, all significant data appears to have occurred primarily in the log phase samples as opposed to the stationary phase bacteria. There is a possibility that the exposure time to ATC was too short, hence why the log phase bacteria showed a response to chitosan and ATC as opposed to the stationary phase. At 1 h exposure to polymers, log phase bacteria were growing and proliferating at a much faster rate. Hence any changes in microbe fitness would be observed much faster. Samples will need longer exposure to the polymer, to observe possible changes in stationary phase.

ATC is derived from chitosan, and because of the stimuli-responsive modification, it should revert to chitosan upon acid hydrolysis. However, the initial results indicate there may be some mechanistic differences between the two polymers. Only one gene had significant fitness change for both chitosan and ATC (Table 3.1). The MprA gene is responsible for transcriptional regulation in the cytosol ^{27,28}. It is found in multiple organisms ^{29,30} and was the only gene with a positive increase in fitness for both samples. It was interesting that ATC showed a greater effect on the bacterium in comparison to chitosan. Additionally, the effect was consistent at all concentration levels of ATC, whereas chitosan only showed any significant effects at random concentrations. There is a possibility that since ATC was in a non-acidic solvent and chitosan was dissolved in an acidic buffer of pH 5, caused the difference in fitness readings. Early studies have indicated that acidic conditions around pH 5 influenced the growth of the microbe, hence the possibility of a negated effect of chitosan. Since chitosan cannot be solubilized in

solutions greater than pH 5 this effect will be considered in future studies by hydrolyzing ATC under mildly acidic conditions of pH 5.5, then analyzing for fitness changes.

E. coli Nissle was used in the preliminary studies, and future studies will transition to a more complex *S. typhimurium* library. It is expected that both bacteria will have similar fitness conditions since they are both gram negative with the capability of surviving intra or extracellularly^{31,32}. This was shown in the preliminary data where those genes that are found in both microbes are highlighted (Table 3.1). Interestingly, transposon insertion sequencing can also be used to highlight metabolic pathways^{6,33,34}. Sets of genes can be mapped under selection onto any known network of genes such as metabolic pathways. Therefore, if a set of genes under selection are enhanced in a specific part of the network, that would indicate that part of the network could be of relevance for the phenotype of the bacterium in the treatment. This can then be used to elucidate the mechanism of action of ATC and chitosan under varying conditions, as well as predict possible methods of drug resistance formation that may arise.

3.4. Conclusions

In this study, extracellular and intracellular treatment of *S. typhimurium* was demonstrated using acid-transforming chitosan (ATC). Antimicrobial efficacy of ATC was confirmed in the possible different pH conditions where the bacteria might be in the host cell, without observing any evidence of acute toxicity. Furthermore, polyplexes created from ATC were able to effectively eliminate intracellular infection. The mechanism by which ATC works has not been elucidated, however, preliminary results hinted at

antimicrobial activity on the bacterial membrane as well as interference with intracellular processes. Overall, it appeared that using ATC as antimicrobial polyplex is a viable and effective method for traversing extracellular and intracellular barriers to treat hardy gram-negative intracellular infections such as *Salmonella*.

3.5 References

- (1) Ribet, D.; Cossart, P. *Microbes and Infection*. Elsevier Masson March 1, 2015, pp 173–183.
- (2) Kaufmann, S. H. E. *Annu. Rev. Immunol.* **1993**, *11* (1), 129–163.
- (3) McClelland, M.; Sanderson, K. E.; Spieth, J.; Clifton, S. W.; Latreille, P.; Courtney, L.; Porwollik, S.; Ali, J.; Dante, M.; Du, F.; Hou, S.; Layman, D.; Leonard, S.; Nguyen, C.; Scott, K.; Holmes, A.; Grewal, N.; Mulvaney, E.; Ryan, E.; Sun, H.; Florea, L.; Miller, W.; Stoneking, T.; Nhan, M.; Waterston, R.; Wilson, R. K. *Nature* **2001**, *413* (6858), 852–856.
- (4) Gart, E. V; Suchodolski, J. S.; Welsh, T. H.; Alaniz, R. C.; Randel, R. D.; Lawhon, S. D.; Lawhon, S. D. *Front. Microbiol.* **2016**, *7*, 1827.
- (5) Verlee, A.; Mincke, S.; Stevens, C. V. *Carbohydr. Polym.* **2017**, *164*, 268–283.
- (6) de Moraes, M. H.; Desai, P.; Porwollik, S.; Canals, R.; Perez, D. R.; Chu, W.; McClelland, M.; Teplitski, M. *Appl. Environ. Microbiol.* **2017**, *83* (5).
- (7) Cossart, P.; Sansonetti, P. J. *Science* **2004**, *304* (5668), 242–248.

- (8) García-Del Portillo, F. *Microbes Infect.* **2001**, 3 (14–15), 1305–1311.
- (9) Huotari, J.; Helenius, A. *EMBO J.* **2011**, 30 (17), 3481–3500.
- (10) Hu, Y.-B.; Dammer, E. B.; Ren, R.-J.; Wang, G. *Transl. Neurodegener.* **2015**, 4 (1), 18.
- (11) Sonawane, N. D.; Thiagarajah, J. R.; Verkman, A. S. *J. Biol. Chem.* **2002**, 277 (7), 5506–5513.
- (12) Buchmeier, N. A.; Heffron, F. *Infect. Immun.* **1991**, 59 (7), 2232–2238.
- (13) Rathman, M.; Barker, L. P.; Falkow, S. *Infect. Immun.* **1997**, 65 (4), 1475–1485.
- (14) No, H. K.; Young Park, N.; Ho Lee, S.; Meyers, S. P. *Int. J. Food Microbiol.* **2002**, 74 (1), 65–72.
- (15) Friedman, A. J.; Phan, J.; Schairer, D. O.; Champer, J.; Qin, M.; Pirouz, A.; Blecher-Paz, K.; Oren, A.; Liu, P. T.; Modlin, R. L.; Kim, J. *J. Invest. Dermatol.* **2013**, 133 (5), 1231–1239.
- (16) Kean, T.; Thanou, M. *Advanced Drug Delivery Reviews.* 2010, pp 3–11.
- (17) Yang, J.; Tian, F.; Wang, Z.; Wang, Q.; Zeng, Y.-J.; Chen, S.-Q. *J. Biomed. Mater. Res. Part B Appl. Biomater.* **2008**, 84B (1), 131–137.
- (18) Wang, Y.; Zhou, J.; Liu, L.; Huang, C.; Zhou, D.; Fu, L. *Carbohydr. Polym.* **2016**, 141, 204–210.
- (19) Yuan, Z.; Li, Y.; Hu, Y.; You, J.; Higashisaka, K.; Nagano, K.; Tsutsumi, Y.; Gao, J. *Int. J. Pharm.* **2016**, 515 (1–2), 644–656.

- (20) Squadrito, F.; Bitto, A.; Irrera, N.; Pizzino, G.; Pallio, G.; Minutoli, L.; Altavilla, D. *Front. Pharmacol.* **2017**, *8*, 224.
- (21) Bitto, A.; Polito, F.; Altavilla, D.; Minutoli, L.; Migliorato, A.; Squadrito, F. *J. Vasc. Surg.* **2008**, *48* (5), 1292–1300.
- (22) Pizarro-Cerdá, J.; Cossart, P. *Cell*. Cell Press February 24, 2006, pp 715–727.
- (23) Liu, H.; Du, Y.; Wang, X.; Sun, L. *Int. J. Food Microbiol.* **2004**, *95* (2), 147–155.
- (24) Chung, Y.; Su, Y.; Chen, C.; Jia, G.; Wang, H.; Wu, J. C. G.; Lin, J. *Acta Pharmacol. Sin.* **2004**, *25* (7), 932–936.
- (25) Zheng, L. Y.; Zhu, J. F. *Carbohydr. Polym.* **2003**, *54* (4), 527–530.
- (26) Das, S. N.; Wagenknecht, M.; Nareddy, P. K.; Bhuvanachandra, B.; Niddana, R.; Balamurugan, R.; Swamy, M. J.; Moerschbacher, B. M.; Podile, A. R. *J. Biol. Chem.* **2016**, *291* (36), 18977–18990.
- (27) Lomovskaya, O.; Lewis, K. *Proc. Natl. Acad. Sci. U. S. A.* **1992**, *89* (19), 8938–8942.
- (28) del Castillo, I.; González-Pastor, J. E.; San Millán, J. L.; Moreno, F. *J. Bacteriol.* **1991**, *173* (12), 3924–3929.
- (29) He, H.; Zahrt, T. C. *J. Bacteriol.* **2005**, *187* (1), 202–212.
- (30) Kolter, R.; Siegele, D. A.; Tormo, A. *Annu. Rev. Microbiol.* **1993**, *47* (1), 855–874.
- (31) Leung, K. Y.; Finlay, B. B. **1991**, *88*, 11470–11474.
- (32) Zilberstein, D.; Agmon, V.; Schuldiner, S.; Padan, E. *J. Bacteriol.* **1984**, *158* (1),

246–252.

(33) van Opijnen, T.; Camilli, A. *Nat. Rev. Microbiol.* **2013**, *11* (7), 435–442.

(34) Chao, M. C.; Abel, S.; Davis, B. M.; Waldor, M. K. *Nat. Rev. Microbiol.* **2016**, *14* (2), 119–128.

Chapter 4: Gene delivery using ATC

4.1 Introduction

RNA interference (RNAi) enables the knockdown of a specific gene in a sequence-specific manner, offering tremendous opportunities for research and clinical translation to treating cancer, inflammatory diseases, genetic disorders, and more ^{1,2}. A key molecular event for successful RNAi is the binding of small interfering RNA (siRNA) with RNA-induced silencing complex (RISC) to form a complex that cleaves the mRNA with a complementary sequence ³. Due to its macromolecular size, anionic charge, and susceptibility to nuclease-mediated degradation, siRNA requires an efficient delivery carrier that traverses all the multiple extracellular and intracellular barriers before reaching a RISC ^{4,5}. However, intrinsic toxicity of delivery carriers, imperfect biocompatibility, and limited gene silencing efficiency for a desired period of time remain unresolved issues for siRNA delivery, particularly in clinical use ^{6,7}.

Chitosan, a biocompatible, cationic polysaccharide derived from the exoskeleton of arthropods and fungal cell walls, has been investigated for gene delivery ⁸⁻¹⁰. However, its dissolution only at a pH of 6.0 or lower ¹¹⁻¹³ due to its primary amines with a significantly lower pKa (e.g., 6.3) than the physiological pH range (e.g., 7.0-7.5), is a pivotal limitation in using chitosan irrespective of potentially broad applications ¹⁴. While nucleic acids can be polyplexed by chitosan at an acidic pH ¹⁵, a lowered charge density under physiological conditions ¹⁶⁻¹⁸ leads to the premature release of nucleic acids, thus reducing transfection efficiency. Upon endocytosis, the mildly acidic condition in the endosome protonates

chitosan again, elevates the electrostatic interactions between chitosan and nucleic acids, and subsequently hinders their release into the cytoplasm^{19,20}. Covalent modifications of chitosan in attempts to overcome these limitations permanently altered its structure and aided gene delivery with limited improvement^{14,21–23}. Irreversible conjugation of various functional groups onto the primary hydroxyl, the secondary hydroxyl, or primary amine groups has shown marginal improvement in gene delivery^{24,25} and long-term efficiency and safety of those changes, particularly in a clinical setting, are still unknown.

Stimuli-reversible modification overcomes chitosan's limitations without compromising the intrinsically attractive function. Ketal linkages rapidly cleave at a mildly acidic endosomal pH (~5.0) and have been intensively employed in the cytoplasmic release of biomacromolecules such as proteins and nucleic acids^{26,27}. In this study, we grafted a cationic, water-soluble branch onto the primary hydroxyl groups of chitosan via an acid-degradable ketal linkage resulting in acid-transforming chitosan (ATC). The chemical modification is designed to improve aqueous solubility and enhance molecular interactions with siRNA by adding flexible cationic branches extended from the rigid polymer backbone. Upon endocytosis, the ketal linker allows ATC for reversion to native chitosan in the mildly acidic endosome/lysosome, where the cationic branches are dissociated from the polymer backbone and release of siRNA is ensured. Subsequent release into the cytoplasm (Figure 1) is hypothesized to be enhanced by endosomal destabilization by a combination of the proton sponge effect by chitosan^{28,29} and increased osmotic pressure contributed by dissociated branches³⁰. We synthesized ATC and investigated its acid-transformation, followed by preparation of ATC/siRNA polyplexes and characterization for size, zeta-potential, and morphology. *In vitro* studies

demonstrated highly efficient gene silencing and significantly lowered cytotoxicity by ATC/siRNA polyplexes.

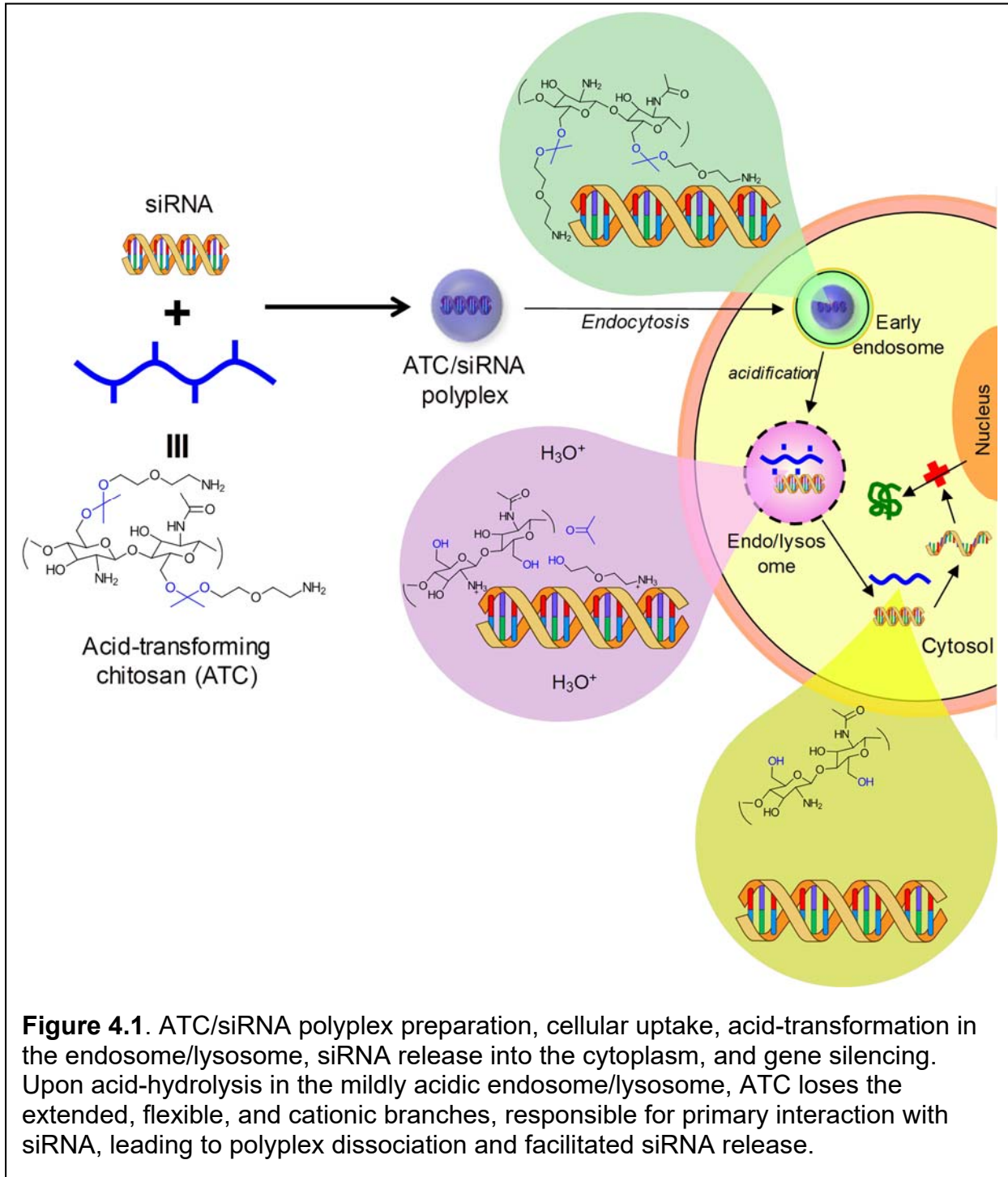


Figure 4.1. ATC/siRNA polyplex preparation, cellular uptake, acid-transformation in the endosome/lysosome, siRNA release into the cytoplasm, and gene silencing. Upon acid-hydrolysis in the mildly acidic endosome/lysosome, ATC loses the extended, flexible, and cationic branches, responsible for primary interaction with siRNA, leading to polyplex dissociation and facilitated siRNA release.

4.2 Experimental methods

4.2.1. Materials

All chemicals were purchased from commercially available sources and used as received. Chitosan (M_w 18–44 kDa, 95% degree of deacetylation) was purchased from Hepe Medical Chitosan (Halle, Germany) and 3-(4,5-dimethyl-2-thiazolyl)-2,5-diphenyltetrazolium bromide (MTT) was purchased from Sigma-Aldrich (Milwaukee, WI). Silencer® GFP siRNA (sense strand 5'-CAAGCUGACCCUGAAGUUCdTdT-3' and antisense strand 5'-GAACUUCAGGGUCAGCUUGdCdC-3'), and negative control siRNA with a scrambled sequence (sense strand 5'-AGUACUGCUUACGAUACGGdTdT-3' and antisense strand 5'-CCGUAUCGUAAGCAGUACUdTdT-3'), were purchased from Ambion (Austin, TX). HeLa cells (ATCC, Rockville, MD) were cultured in Dulbecco's modified Eagle's medium (DMEM) (MediaTech, Herndon, VA) with 10% fetal bovine serum (FBS) (Hyclone, Logan, UT) and 1% antibiotics (100 units/mL penicillin; 100 µg/mL streptomycin) (MediaTech, Herndon, VA). HeLa cells stably expressing GFP (HeLa/EGFP) were prepared by transducing them with retrovirus encoding enhanced green fluorescence protein (eGFP) and further sorting them by FACS, as described for the preparation of NIH 3T3/EGFP cells^{31,32}.

4.2.2. Preparation of ATC/siRNA polyplexes

Desired amounts of ATC in 100 µL DI water was drop-wise mixed with eGFP siRNA (1.5 µg) in 100 µL DI water to yield various N/P ratios, followed by a brief vortex and incubation at room temperature for 30 min to form ATC/siRNA polyplexes. The resulting polyplex solution was diluted with an additional 800 µL of DI water. Mean particle

diameter (Z-average) with a polydispersity index (PDI) and zeta potential of various ATC/siRNA polyplexes were measured by dynamic light scattering (DLS) particle analysis using a Zetasizer Nano ZS (Malvern, UK) at 25 °C and angle of 90°. The viscosity (0.887 mPA/s) and refractive index (1.33) of water at 25 °C were used to analyze the data.

4.2.3. Assays for nucleic acid complexation by ATC

The ability of ATC to complex siRNA was evaluated by a standard ethidium bromide (EtBr) exclusion assay. EtBr (1 µg) and siRNA (1 µg) were incubated in 40 µL of DI water for 15 min at room temperature. Desired amounts of ATC solution in 60 µL of DI water were added to achieve various N/P ratios and vortexed. After 30 min of incubation at room temperature, fluorescence intensity (λ_{ex} 320 nm and λ_{em} 600 nm) was measured using a fluorescence microplate reader (Synergy HT, BioTEK [Winooski, VT]). Reduced fluorescence intensity was used as a quantitative indicator of siRNA condensation in the polyplexes.

The ATC's siRNA complexation efficiency was also determined by agarose gel electrophoresis. Desired amounts of ATC dissolved in 100 µL DI water were vortexed with 1 µg of siRNA in 100 µL DI water to yield polyplexes at various N/P ratios. Polyplexes (18 µL mixed with 2 µL DNA loading dye [Thermo Fisher Scientific, Waltham, MA]) were loaded into each well of 1% (w/v) agarose gel. To demonstrate the dissociation of the siRNA from ATC upon acid-transformation, the polyplexes were mixed with an equal volume of pH 5.0 acetate buffer (100 mM acetic in DI water adjusted by 50 mM sodium acetate trihydrate) and further incubated for 4 h at 37 °C. The acid-transformation was quenched by adding 5 µL of 1 N NaOH into 20 µL samples and incubating the mixture for another 15 min. An 18 µL aliquot of the samples were mixed with 2 µL of loading dye,

and the resulting mixture solution was loaded on the agarose gel. Electrophoresis was carried out at a constant voltage of 45 V for 10 min then 100 V for 30 min in Tris-acetate-EDTA (TAE) buffer. Bands were then visualized under a UVP transilluminator (Analytik, Jena, Germany) at a wavelength of 365 nm.

4.2.4. Morphology of ATC/siRNA polyplexes

The morphology of various polyplexes were analyzed by transmission electron microscopy (TEM). ATC/siRNA polyplexes at varying N/P ratios prepared as described earlier in 10 μ L deionized water were dropped on a hydrophobic wax paper, then a carbon-coated copper TEM grid (Electron Microscopy Sciences [Hatfield, PA]) was placed on the sample droplet for 10 min at room temperature. Grid was then air-dried for 2 h at room temperature. The grids were imaged with a Philips/FEI (Hillsboro, OR) CM-20 Transmission Electron Microscope operated at 200 kV.

4.2.5. Transfection using ATC/pDNA polyplexes

Polyplexes were transfected into HeLa cells seeded in a 24 well plate at 20,000 cells/well. 100 μ L of polyplex solution was diluted with 300 μ L of 1X phosphate buffered saline (PBS) before it was added to the wells. The particles incubate in the wells for 4 hours without any serum. After 4 hours of transfection, the medium was removed, and the cells were washed with PBS, following this, media was replaced with 400 μ L of Dulbecco's Modified Eagle's Medium (DMEM) with 10% fetal bovine serum (FBS) and incubated at 37 °C with a 5% CO₂ atmosphere for 24 or 48 h. The analysis was performed 24 and 48 hours after transfection.

4.2.6. Silenced eGFP expression in HeLa cells by ATC/siRNA polyplexes

HeLa/eGFP cells were seeded overnight in a 24 well plate at a density of 20,000 cells/well. Prior to transfection, culture media was removed, and cells were washed once with PBS. siRNA-containing polyplexes were prepared by adding dropwise various volumes of polymer (200 µg/ mL in PBS) to eGFP siRNA or scrambled (scr) siRNA solutions (80 pM). Following 30 min incubation, polyplex solutions (100 µL in PBS) were diluted with 300 µL of FBS-free DMEM before it was added to the wells. The cells were incubated for 4 h with ATC/siRNA polyplexes at 37 °C with a 5% CO₂ atmosphere. After 4 h, the polyplex-containing medium was aspirated, and the cells were rinsed with PBS once, followed by the addition of 400 µL DMEM with 10% FBS and further incubation for 72 h. Fluorescence imaging and flow cytometry (Easycyte Plus, Guava) were performed to confirm eGFP silencing in the cells.

4.2.7. Cytotoxicity of ATC polyplexes on HeLa/eGFP cells

HeLa/eGFP cells were seeded at a density of 9,000 cells per/well in a 96-well plate and incubated overnight. The culture medium was replaced with 200 µL of ATC/siRNA polyplexes at various N/P ratios in FBS-free DMEM and incubated for 12 h at 37 °C. The medium was then replaced with 200 µL of MTT solution (1 mg/mL in FBS-free DMEM). After 2 h of incubation at 37 °C, the MTT solution was discarded from each well, and the cells were washed with PBS once. DMSO (200 µL) was added to each well to dissolve the MTT formazan crystals formed by live cells, and the plate was incubated at 37 °C for 5 min. The absorbance of formazan products was then measured at 561 nm wavelength using a microplate reader (Synergy HT, BioTEK).

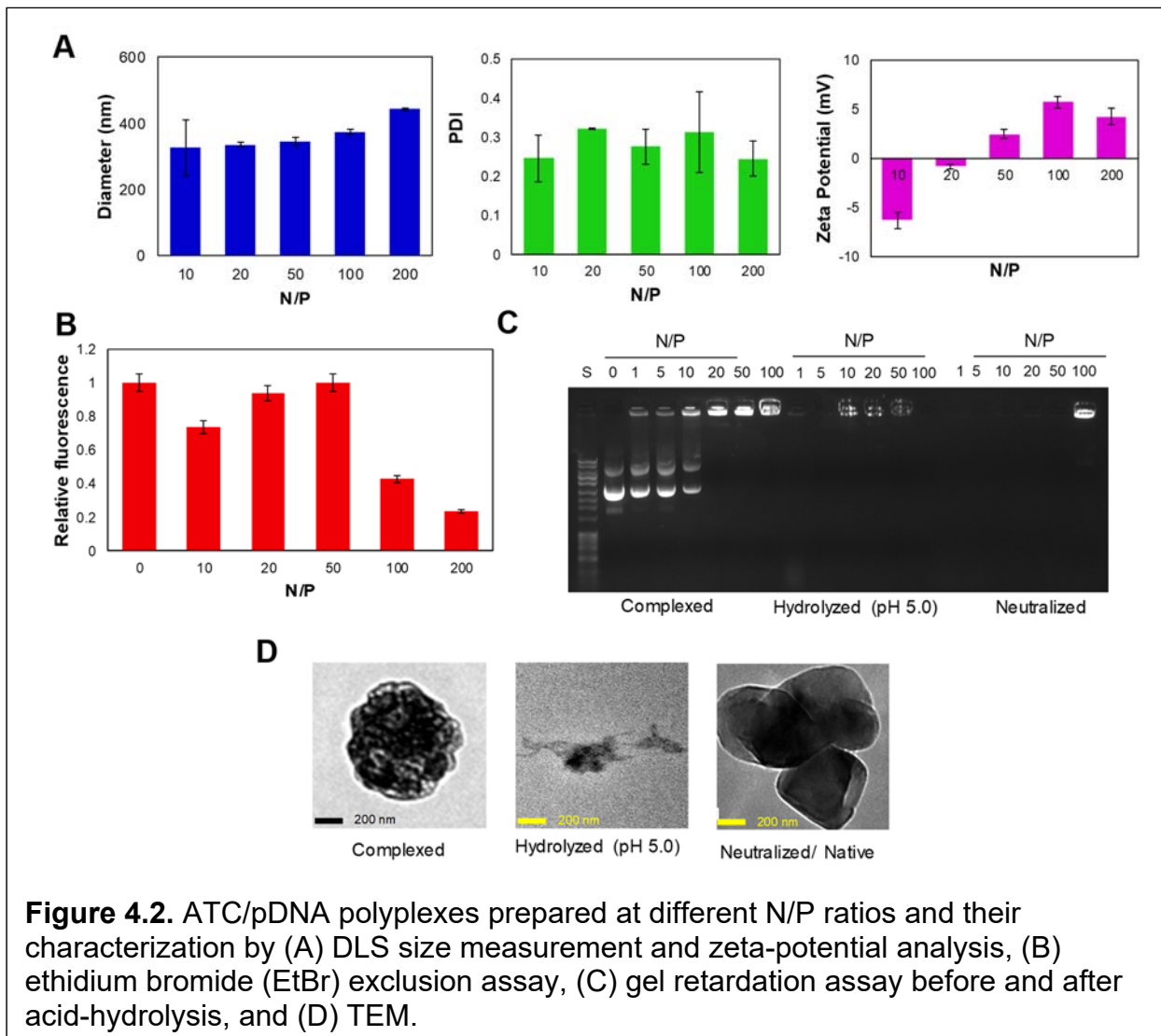
4.3. Results and discussion

4.3.1. Complexation of nucleic acids and the morphology of polyplexes

Since nucleic acids are hydrophilic, the improved aqueous solubility and flexible cationic side chains of ATC were speculated to contribute to efficient complexation via enhanced electrostatically-attractive molecular interactions. The particle size of ATC/pDNA polyplexes, prepared by simple complexation, increased gradually when the concentration of chitosan was increased from an N/P ratio of 1 to 10 in distilled water (Figure 4.2). However, there was a decrease in particle size from an N/P ratio of 10 to 100. Smallest particle sizes of ATC/pDNA polyplexes were obtained at N/P ratios 20 and 100. For ATC/siRNA polyplexes the size of the particles continued to gradually increase from N/P ratio of 1 to 100. Similarly, the PDI of the particles showed a similar trend, with PDI of N/P ratio of 50 was slightly higher than the N/P ratio of 100. The zeta potential of ATC/pDNA polyplexes increased with the increasing concentration of ATC at a constant nucleic acid concentration. The increment was due to the increase in the number of positive charges provided by ATC which counteracts with fixed negatively charged nucleic acid. When a polyplex was formed with ATC and large nucleic acid-like pDNA, a roughly spherical object was created with various contusions (Figure 4.2D). However, unmodified chitosan/DNA polyplexes formed cubic structures with defined edges. By adding 100 mM acetic acid to the polyplex, hydrolysis of the ketal group occurs, causing ATC to revert to native chitosan. When this occurred, there was the release of nucleic acid (Figure 4.2D), but additionally, the amine functionality on native chitosan became protonated as well.

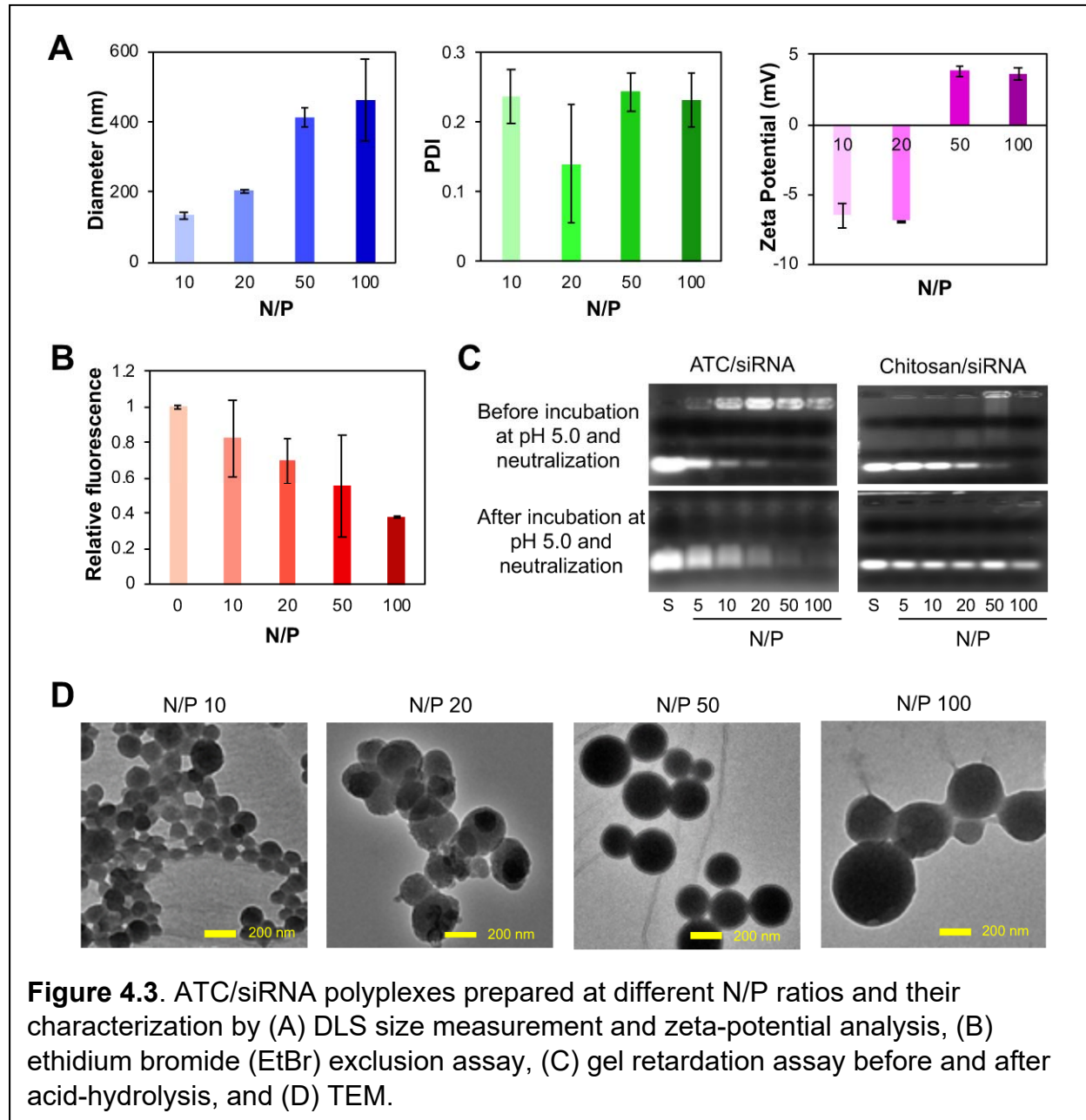
Thus, free nucleic acid reassembled into a polyplex with chitosan at pH 5. When returned to pH 8 there was the release of all the nucleic acids except at N/P of 100. Additionally, conditions at pH 7 ATC and N/P of 20 to 100 effectively complexed DNA (Figure 4.2C). At N/P ratios of 1 to 10 there was not enough polymer available to complex all the DNA in the solution, but some were still available to form a polyplex.

ATC complexed siRNA and formed ATC/siRNA polyplexes in a size range from 180 nm to 400 nm in a N/P ratio range of 10-100 within a consistent PDI of approximately 0.2 (Figure 4.3A). The zeta-potential transitioned from negative to positive between N/P



ratios of 20 and 50. This indicates a molecular ratio of ATC to siRNA was approaching the point where both molecules complement each other by attractive electrostatic interactions without shortage or excess between N/P 20 and 50. As expected, this is higher than the optimal N/P ratios known for complexing nucleic acids by PEI (i.e., N/P ratios of 5-10) due to the significantly lower cationic density of ATC than PEI. ATC has a total of two primary amines found on the pyranose backbone and another at the tip of aminoethoxy branch per repeating unit (MW 338 Da), while branched PEI has a total of four primary amines per repeating unit (MW 401 Da). In addition, the pyranose backbone of ATC makes it less flexible than PEI. Altogether, the electrostatic interactions with siRNA by ATC and PEI are different even for the same N/P ratios. The zeta potential of ATC/siRNA polyplexes became positive at N/P ratio of 50 and further increased at N/P of 100 (Figure 4.3A) or higher (data not shown) due to the significant excess of positive charges provided by ATC for a given number of negative charges of siRNA. Ethidium bromide (EtBr) exclusion assay (Figure 4.3B) showed the reduction in fluorescence intensity as ATC shielded siRNA at increasing N/P ratio as anticipated. The shielding of siRNA by ATC was similar to those reported for chitosan, PEI, and PLL³³. siRNA complexation by ATC was further qualitatively assessed by agarose gel electrophoresis (Figure 4.3C). ATC complexed siRNA via the increased charge density and close interaction with the cationic aminoethoxy branches more effectively than chitosan and was able to release siRNA upon acid hydrolysis. TEM showed consistent spherical morphology of ATC/siRNA polyplexes (Figure 4.3D) and their sizes increased as N/P ratios increased (Figures 4.3A and D).

Efficient delivery is dependent on the ability to efficiently protect siRNA, aid in cellular uptake, and ensure cytosolic release. While ATC demonstrated the capability of effectively complexing siRNA, the polyplex sizes as determined by DLS and TEM were

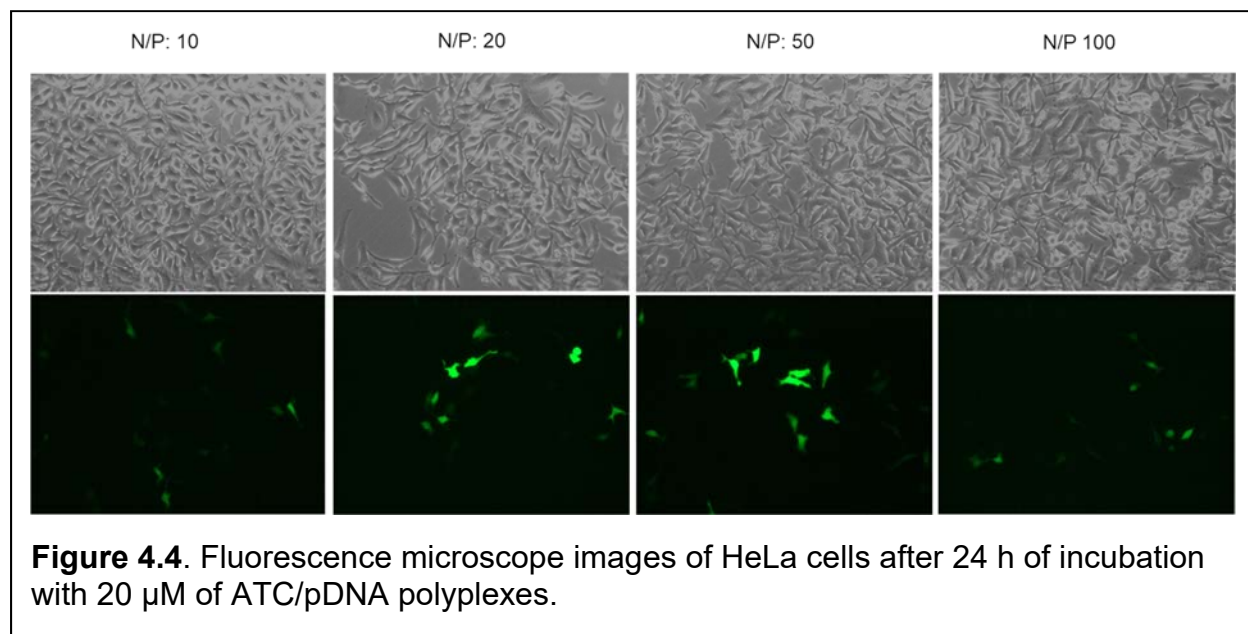


larger than a typical size range for endocytosis³⁴ but could be suitable for transfecting phagocytic cells³⁵, particularly *in vivo*. However, polyplexes in a similar size have also

been reported to efficiently transfect many kinds of cells *in vitro* as well as *in vivo* ^{36–40}. One advantage of transfecting larger gene carriers is to deliver a large number of nucleic acids to a cell ⁴¹, which seems to be crucial for gene silencing ^{42,43}.

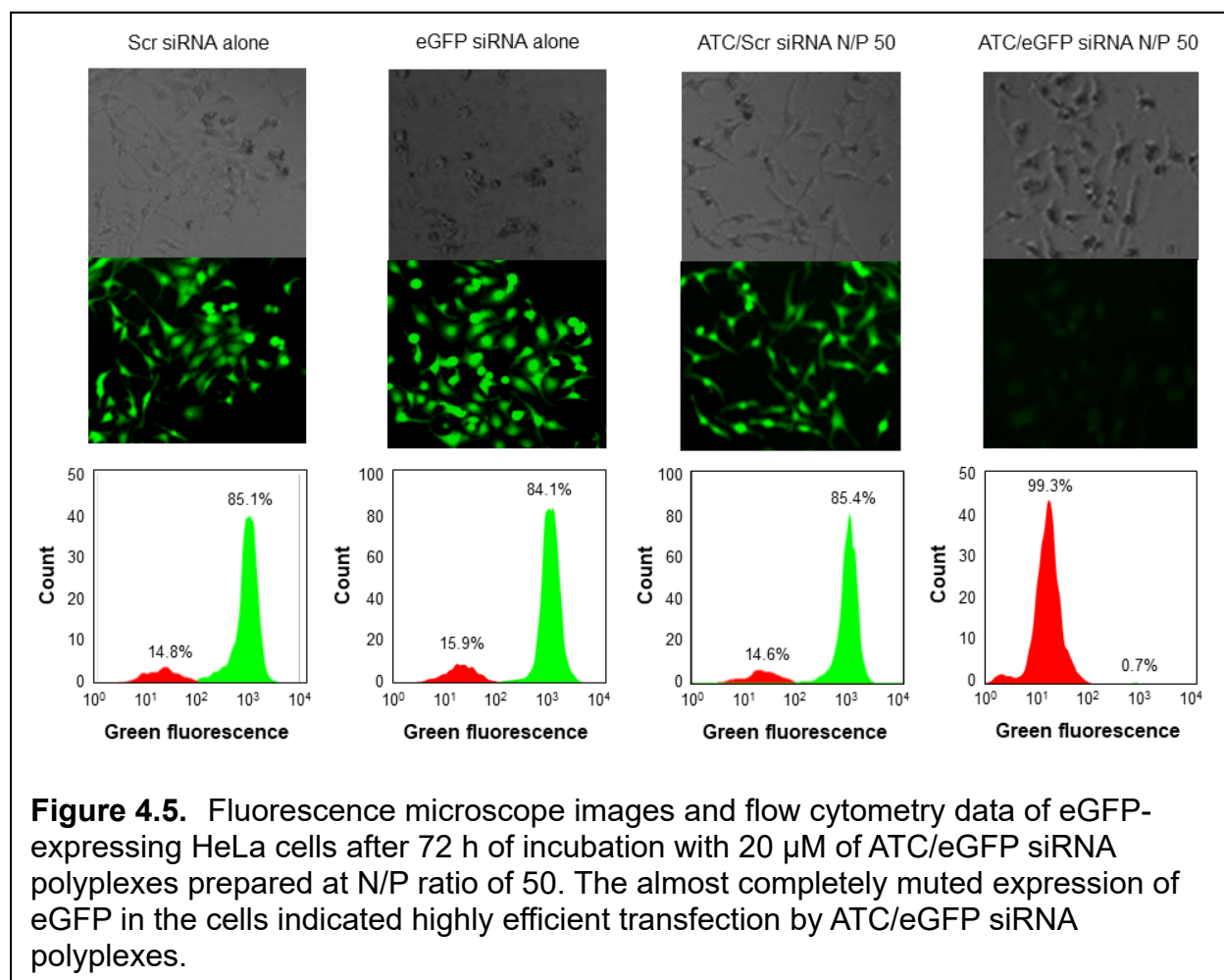
4.3.2. Efficient transfection of pDNA with low cytotoxicity

Transfections of HeLa cells with ATC/DNA polyplexes at different N/P ratios revealed that the highest transfection of a population of cells was observed at N/P ratios of 20 and 50 (Figure 4.4). After 24 hours of cell growth post transfection, about 20% of HeLa cells were producing GFP. Transfection was observed at other N/P ratios but at a smaller amount. In contrast, ATC/siRNA silencing is most optimal at higher N/P ratios. For N/P ratios of 100 and 200, an almost 100% reduction in expression is observed (Figure 4.6B). At higher N/P ratios of 300 and 400, the silencing efficiency decreases. Though there is a reduction in eGFP expression, there was some cell death observed.



Consequently, the death of some of the cells might have contributed to the increase silencing for N/P ratios of 300 and 400.

HeLa cell viability was accessed by MTT assay to investigate the potential cytotoxicity of ATC/DNA polyplexes. Over 95% average cell viability was observed for ATC/DNA polyplex and naked DNA at 40 μM concentrations. However, about 20-25% loss of cell viability was observed for polyplexes at 80 μM . Additionally, there was inherent toxicity of about 5% associated with a solution of pure material diluted in PBS. Free DNA



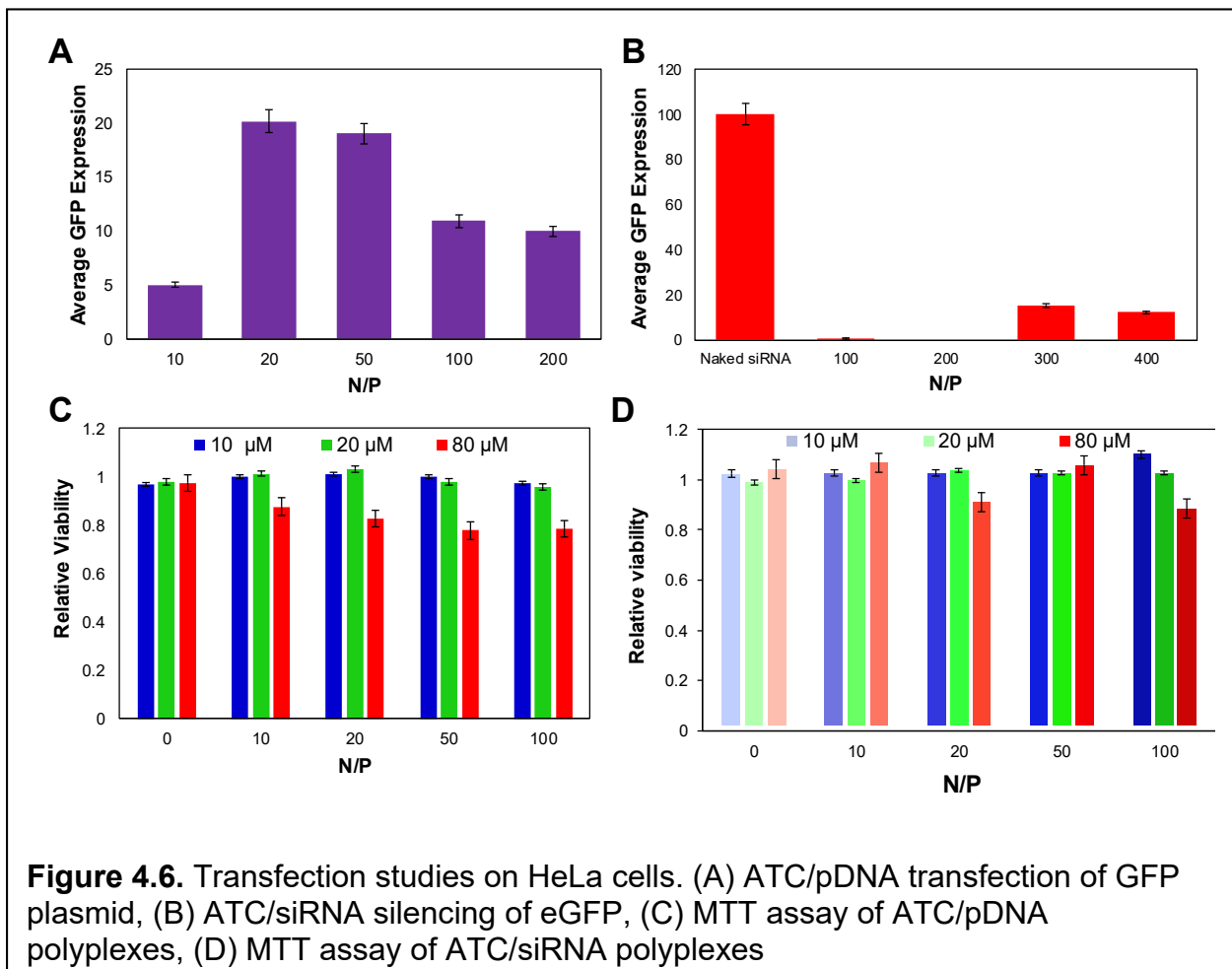
did not show toxicity at any concentration, while at the polyplexes at N/P of 50 appeared to be the most cytotoxic (25%) at 100% concentration, (Figure 4.6C). The apparent toxicity of the nanoparticles might be attributed to the release of acetone and methanol from the ketal linkage upon hydrolysis, or might also be an effect of the membrane

permeability properties of chitosan. Further studies are necessary to determine the appropriate pharmacokinetics of ATC.

4.3.3. Efficiently silencing eGFP expression by ATC/siRNA polyplexes with low cytotoxicity

The capability of ATC/siRNA polyplexes to silence the expression of a target gene was investigated by incubating them with HeLa cells expressing eGFP as a model gene. Polyplexes (20 μ M) prepared at N/P ratio of 50 demonstrated a very efficiently silenced eGFP expression from 85% to 0.7% without noticeable cytotoxicity (Figure 4.6D) after 72 h incubation, while eGFP siRNA alone or ATC/scr siRNA polyplexes did not affect eGFP expression (Figure 4.5). The polyplexes prepared at a higher N/P ratio also showed significant eGFP silencing: expression decreased from 85% to 0.67% (Figure 4.6B) at N/P ratio of 100. However, this was accompanied by moderate cytotoxicity (ATC/eGFP siRNA polyplexes in Figure 4.6D) as well as measurable non-specific gene silencing of 4.8% (ATC/scr siRNA polyplexes). In addition to poor solubility, limited endosomal escape before being cleared by endolytic recycling⁶ attributes to inefficient transfection by chitosan/siRNA polyplexes^{44,45}, despite chitosan's capability of generating the proton sponge effect⁴⁶. Acid-cleavage of ketal linkages in ATC in the mildly acidic endosome/lysosome greatly aided endosomal escape of siRNA via dissociation from hydrolyzed ATC and increased osmotic pressure via release of side branches^{27,31}. Acid-hydrolyzed ATC self-aggregates with low solubility at a neutral pH and releases free siRNA for binding to the RISC complex.

The acid-transformation of ATC in the endosome/lysosome to native chitosan makes it a promising carrier in treating intracellular infections. Intracellular bacteria are infectious microorganisms that replicate within host cells allowing the bacteria to evade host defense mechanisms and aids in its survival⁴⁷. ATC is capable of not only delivering antimicrobial agents such as antibiotics and nucleic acids but also directly act on microbes upon conversion to native chitosan⁴⁸. For example, ATC complexing siRNA against a resistant gene cannot only silence the expression of the target drug-resistance gene but also eradicates microbes upon acid-transformation. The relatively large size of ATC/siRNA polyplexes could be particularly suitable for treating microbial infections (e.g., salmonella) in phagocytic cells (e.g., macrophages)⁴⁹. Additionally, ATC can be used to



coat the hydrophilic surface of implantable devices for aseptic applications^{50,51}. The ketal linker and the aminoethoxy branch could be replaced by other stimuli-responsive linkers and side chains, depending on specific demands by other biomedical applications.

4.3.4. Use of ATC as a vector for other cargo

Effectively complexing other types of nucleic acids or larger cargo such as proteins demonstrate the versatility of a polymeric carrier. To this end, ATC was complexed with polydeoxyribonucleotide (pdrn). Pdrn is a mixture of nucleic acids with varying lengths. Due to the heterogeneity, and genetic non-specificity, it served as a suitable control to observe the versatility of ATC. Polyplexes created from ATC/pdrn at an N/P ratio of 100 had a diameter around 200 nm with a zeta potential of 12 mV. Interestingly, these polyplexes have a low polydispersity and are all almost completely the same size. This was partially observable in the TEM image. However, some polyplexes appeared to have shrunk during the drying process.

4.3.5. Use of ATC in combined therapeutic

This polyplex formed from ATC was especially unique due to the ability to revert to native chitosan in acidic conditions. Many chitosan's plethoras of uses are dependent on the free amine functionality, thus leaving that intact is ideal for maintaining those advantages. ATC, which maintains this free amine and is water soluble, can be an excellent asset in the treatment of intracellular bacterial infections. Intracellular bacteria are infectious microorganisms that replicate in host cells allowing the bacteria to evade host defense mechanisms and aids in its survival⁴⁷. Since ATC, composed of antimicrobial chitosan, already serves as an efficient vector, it can additionally act as an

antimicrobial agent. Additionally, ATC can be applied to implantable devices for applications of wound healing, and antimicrobial uses^{50,51}.

Furthermore, while the ketal linkage serves the purpose of providing hydrophilicity to chitosan and making it water-soluble future studies will take aim at changing this linker. While our current linker has no added toxicity, it does not serve any purpose. The current linker does act as an excellent working model for designing the synthesis scheme of ATC, in the long term it is cleaved as a byproduct once the polyplex has been endocytosed. To engineer a genuinely efficient and multipurpose vector, a drug with therapeutic significance would be an ideal molecule to conjugate to chitosan through the same pH-responsive linker.

4.4. Significance of findings

ATC is a water-soluble and acid-labile vector. When the acid-responsive group is gone, native chitosan is generated, allowing applications which utilize other properties of chitosan (e.g., antimicrobial and anti-inflammatory), an advantage that offers a gene therapy delivery vector with a dual-purpose. We have demonstrated the capability to synthesize a water-soluble chitosan, capable of complexing with nucleic acids at neutral pH and displaying release and delivery of payload intracellularly. In the future, it would be of interest to test linker molecules that play an active role in the therapeutic process. Polyplexes formed from ATC, can change morphology based on the environmental pH due to the pH-responsive acid-transforming linkage. The transformation permits the improved transfection efficiency without having to modify the material to high extremes. From our studies, we conclude that chitosan modified with a pH sensitive functional group

can efficiently deliver nucleic acids to HeLa cells *in vitro*. To engineer some novel therapeutics, studies that take advantage of the natural properties of chitosan as an antibiotic and inflammatory agent, combined with the improved transfection efficiency of ATC are warranted.

4.5. References

- (1) Kole, R.; Krainer, A. R.; Altman, S. *Nat. Rev. Drug Discov.* **2012**, *11* (2), 125–140.
- (2) Shi, J.; Kantoff, P. W.; Wooster, R.; Farokhzad, O. C. *Nat. Rev. Cancer* **2016**, *17* (1), 20–37.
- (3) Kim, H. J.; Kim, A.; Miyata, K.; Kataoka, K. *Adv. Drug Deliv. Rev.* **2016**, *104*, 61–77.
- (4) Kanasty, R.; Dorkin, J. R.; Vegas, A.; Anderson, D. *Nat. Mater.* **2013**, *12* (11), 967–977.
- (5) Yin, H.; Kanasty, R. L.; Eltoukhy, A. A.; Vegas, A. J.; Dorkin, J. R.; Anderson, D. G. *Nat. Rev. Genet.* **2014**, *15* (8), 541–555.
- (6) Sahay, G.; Querbes, W.; Alabi, C.; Eltoukhy, A.; Sarkar, S.; Zurenko, C.; Karagiannis, E.; Love, K.; Chen, D.; Zoncu, R.; Buganim, Y.; Schroeder, A.; Langer, R.; Anderson, D. G. *Nat. Biotechnol.* **2013**, *31* (7), 653–658.
- (7) Bobbin, M. L.; Rossi, J. J. *Annu. Rev. Pharmacol. Toxicol.* **2016**, *56* (1), 103–122.
- (8) Kean, T.; Thanou, M. *Advanced Drug Delivery Reviews*. 2010, pp 3–11.

- (9) Shu, X. .; Zhu, K. . *Eur. J. Pharm. Biopharm.* **2002**, *54* (2), 235–243.
- (10) Lee, M. K.; Chun, S. K.; Choi, W. J.; Kim, J. K.; Choi, S. H.; Kim, A.; Oungbho, K.; Park, J. S.; Ahn, W. S.; Kim, C. K. *Biomaterials* **2005**, *26* (14), 2147–2156.
- (11) Rinaudo, M.; Pavlov, G.; Desbrières, J. *Polym. J.* **1999**, *40* (25), 7029–7032.
- (12) Shepherd, R.; Reader, S.; Falshaw, A. *Glycoconj. J.* **1997**, *14* (4), 535–542.
- (13) Sugimoto, M.; Morimoto, M.; Sashiwa, H.; Saimoto, H.; Shigemasa, Y. *Carbohydr. Polym.* **1998**, *36* (1), 49–59.
- (14) Mourya, V. K.; Inamdar, N. N. *React. Funct. Polym.* **2008**, *68* (6), 1013–1051.
- (15) Ravi Kumar, M. N. . *React. Funct. Polym.* **2000**, *46* (1), 1–27.
- (16) Maurstad, G.; Danielsen, S.; Stokke, B. T. *Biomacromolecules* **2007**, *8* (4), 1124–1130.
- (17) Gan, Q.; Wang, T.; Cochrane, C.; McCarron, P. *Colloids Surf., B* **2005**, *44* (2), 65–73.
- (18) Francis Suh, J.-K.; Matthew, H. W. . *Biomaterials* **2000**, *21* (24), 2589–2598.
- (19) Wang, Q. Z.; Chen, X. G.; Liu, N.; Wang, S. X.; Liu, C. S.; Meng, X. H.; Liu, C. G. *Carbohydr. Polym.* **2006**, *65* (2), 194–201.
- (20) Becerra, J.; Sudre, G.; Royaud, I.; Montserret, R.; Verrier, B.; Rochas, C.; Delair, T.; David, L. *AAPS PharmSciTech* **2016**, *18* (4), 1070–1083.
- (21) Mourya, V. K.; Inamdar, N. N.; Tiwari, A. *Adv. Mater. Lett.* **2010**, *1* (1), 11–33.
- (22) Kim, T. H.; Jiang, H. L.; Jere, D.; Park, I. K.; Cho, M. H.; Nah, J. W.; Choi, Y. J.;

- Akaike, T.; Cho, C. S. *Prog. Polym. Sci.* **2007**, *32* (7), 726–753.
- (23) Rinaudo, M. *Prog. Polym. Sci.* 2006, pp 603–632.
- (24) Lee, D. W.; Lim, H.; Chong, H. N.; Shim, W. S. *Open Biomater. J.* **2009**, *1*, 10–20.
- (25) Ji, J.; Wang, L.; Yu, H.; Chen, Y.; Zhao, Y.; Zhang, H.; Amer, W. A.; Sun, Y.; Huang, L.; Saleem, M. *Polym. Plast. Technol. Eng.* **2014**, *53* (14), 1494–1505.
- (26) Shim, M. S.; Kwon, Y. J. *Biomacromolecules* **2008**, *9* (2), 444–455.
- (27) Kwon, Y. J.; Standley, S. M.; Goodwin, A. P.; Gillies, E. R.; Fréchet, J. M. J. *Mol. Pharm.* **2005**, *2* (1), 83–91.
- (28) Kwon, Y. J. *Acc. Chem. Res.* **2012**, *45* (7), 1077–1088.
- (29) Rehman, Z. ur; Hoekstra, D.; Zuhorn, I. S. *ACS Nano* **2013**, *7* (5), 3767–3777.
- (30) Kwon, Y. J.; Standley, S. M.; Goh, S. L.; Fréchet, J. M. J. *J. Control. Release* **2005**, *105* (3), 199–212.
- (31) Shim, M. S.; Kwon, Y. J. *Bioconjug. Chem.* **2009**, *20* (3), 488–499.
- (32) Kwon, Y. J.; Yu, H.; Peng, C.-A. *Biotechnol. Bioeng.* **2001**, *72* (3), 331–338.
- (33) Strand, S. P.; Danielsen, S.; Christensen, B. E.; Vårum, K. M. *Biomacromolecules* **2005**, *6* (6), 3357–3366.
- (34) Gary, D. J.; Puri, N.; Won, Y.-Y. *J. Control. Release* **2007**, *121* (1–2), 64–73.
- (35) He, C.; Hu, Y.; Yin, L.; Tang, C.; Yin, C. *Biomaterials* **2010**, *31* (13), 3657–3666.
- (36) Peng, Q.; Chen, F.; Zhong, Z.; Zhuo, R. *Chem. Commun.* **2010**, *46* (32), 5888.

- (37) He, Y.; Cheng, G.; Xie, L.; Nie, Y.; He, B.; Gu, Z. *Biomaterials* **2013**, *34* (4), 1235–1245.
- (38) Gao, Y.; Xu, Z.; Chen, S.; Gu, W.; Chen, L.; Li, Y. *Int. J. Pharm.* **2008**, *359* (1–2), 241–246.
- (39) Kunath, K.; von Harpe, A.; Fischer, D.; Petersen, H.; Bickel, U.; Voigt, K.; Kissel, T. *J. Control. Release* **2003**, *89* (1), 113–125.
- (40) de Wolf, H. K.; Luten, J.; Snel, C. J.; Oussoren, C.; Hennink, W. E.; Storm, G. *J. Control. Release* **2005**, *109* (1–3), 275–287.
- (41) Xiang, Y.; Oo, N. N. L.; Lee, J. P.; Li, Z.; Loh, X. J. *Drug Discov. Today* **2017**, *22* (9), 1318–1335.
- (42) Babaei, M.; Eshghi, H.; Abnous, K.; Rahimizadeh, M.; Ramezani, M. *Cancer Gene Ther.* **2017**, *24* (4), 156–164.
- (43) Chen, C.; Yang, Z.; Tang, X. *Med. Res. Rev.* **2018**.
- (44) Huang, M.; Fong, C.-W.; Khor, E.; Lim, L.-Y. *J. Control. Release* **2005**, *106* (3), 391–406.
- (45) Chang, K. L.; Higuchi, Y.; Kawakami, S.; Yamashita, F.; Hashida, M. *Bioconjug. Chem.* **2010**, *21* (6), 1087–1095.
- (46) Richard, I.; Thibault, M.; De Crescenzo, G.; Buschmann, M. D.; Lavertu, M. *Biomacromolecules* **2013**, *14* (6), 1732–1740.
- (47) Kaufmann, S. H. E. *Annu. Rev. Immunol.* **1993**, *11* (1), 129–163.

- (48) Verlee, A.; Mincke, S.; Stevens, C. V. *Carbohydr. Polym.* **2017**, *164*, 268–283.
- (49) Ribet, D.; Cossart, P. *Microbes and Infection*. Elsevier Masson March 1, 2015, pp 173–183.
- (50) Govindharajulu, J.; Chen, X.; Li, Y.; Rodriguez-Cabello, J.; Battacharya, M.; Aparicio, C. *Int. J. Mol. Sci.* **2017**, *18* (2), 369.
- (51) Poth, N.; Seiffart, V.; Gross, G.; Menzel, H.; Dempwolf, W. *Biomolecules* **2015**, *5*, 3–19.

Chapter 5. Summary and future directions

5.1. Summary of dissertation

Chapter 1 served as an introduction to the dissertation. This chapter highlighted the challenges with drug-resistant formation caused by conventional antibiotics, and to demonstrate a possible strategy to circumvent the current problems with antimicrobial resistance by using nanoantibiotics. Further discussions delved into the possibility of combining gene therapy with a nanoantibiotic vector. The combined therapeutic can aid in overcoming the threatening challenges ahead with respect to the increasing rate of drug-resistant microbes. The need for an antimicrobial material with gene delivery capabilities led to the use of chitosan as our selected polymer.

In Chapter 2, details of the synthesis of acid-transforming chitosan (ATC) were provided. Chitosan was selected as our vector because it had many of the desired properties for the therapeutic. However, the use of the polymer was met with various hurdles such as aqueous solubility, and challenges with endosomal escape. This chapter provided the synthesis scheme used to create the acid-responsive variant of chitosan. The modification of chitosan with an acid-responsive linker to form acid-transforming chitosan (ATC) was accomplished and fully characterized. This modification was shown to be temporary and chitosan is regenerated upon acid hydrolysis. While the synthesis worked, the efficiency was relatively low yielding with only milligram quantities of ATC recovered after each reaction process.

Chapter 3 explored the antimicrobial capabilities of ATC and determined the possible mechanism for the antimicrobial efficacy of ATC and chitosan. The efficacy was observed against the bacteria alone at varying pH conditions to see the effects it had on the polymer and microbe. Followed with the utility of ATC polyplexes in the eradication of an intracellular infection was also demonstrated. There were almost no surviving bacteria at 1000 $\mu\text{g/mL}$, and the amount surviving intracellularly in each cell is almost negligible. Moreover, the surviving colonies post cell lysis for 100 $\mu\text{g/mL}$ appears to be much less than was seen from the flow data or the fluorescence images which indicated polyplexes hindered the growth of *Salmonella* better intracellularly even at low concentrations of the polymer. Furthermore, the mechanism of action of ATC was hypothesized using preliminary data from transposon insertion sequencing. The preliminary data of sequenced samples highlighted a myriad of genes that could have some significance in the mechanism of action, however, to confirm the true significance, more replicates would be needed.

The motivation for Chapter 4 was to demonstrate the gene delivery capabilities of ATC polymer. While the previous chapter confirmed intracellular uptake of ATC polyplexes, these chapters elucidated on the efficient intracellular release of genetic components. Various polyplexes were created using different genetic materials pDNA, and siRNA. These polyplexes were characterized by morphology, surface charge, complexation and release efficiency. Additionally, in this chapter, the transfection efficiency was observed using flow cytometry.

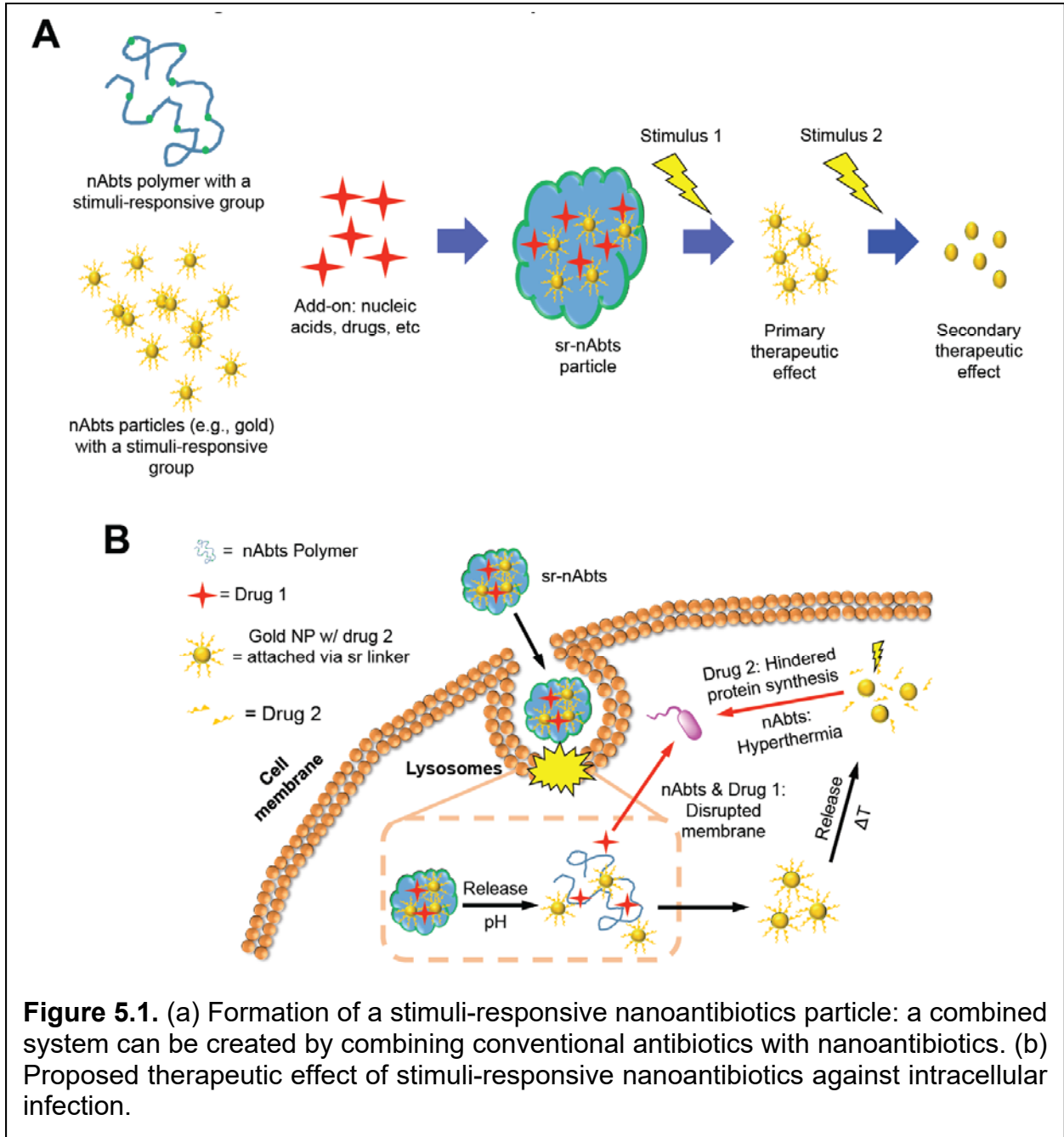
Chapter 5 describes the summary of the dissertation and concluded with perspectives and future directions of the work.

5.2 Future directions

5.2.1. Nanoparticles with multi-stimuli response

Another advantageous nAbts design is one that places various stimuli into one package. These will require the use of different stimuli-responsive linkers with two or more nAbts. For instance, a thermo-responsive group like NIPAM is combined with pH-responsive functionality for the purpose of designing a multi-environment NP¹. These could be very useful in topical applications where one release will happen at body temperature, followed by another stimulus-triggered release intracellularly or at an inflammatory site. Moreover, a multi-stimuli nAbts can be advantageous for treating difficult intracellular drug-resistant microbe as illustrated in Figure 5.1. Adding a stimuli-responsive functional group to a nAbts such as a gold nanoparticle or a carbon nanotube can be accomplished by different methods from surface coating using emulsion to reduction-driven synthesis ^{2,3}. For polymeric systems, the method that dictates the addition of stimuli-responsive functional group is determined by the specific group being conjugated. For example, conjugating a pH-responsive functionality such as succinyl or acetyl to chitosan has been done by various groups with relative ease ⁴⁻⁶. An alternative pairing is one that places a light-responsive nanoparticle with one that has a different antimicrobial mechanism. For example, doping TiO₂ with silver creates a particle that can destroy bacteria by photocatalytic inactivation and generation of silver ions ⁷⁻⁹. These particles have been shown to have excellent light-independent antimicrobial activities against *Escherichia coli* (*E. coli*), *Staphylococcus aureus* (*S. aureus*) and *Pseudomonas aeruginosa* (*P. aeruginosa*) ⁸. A similar interaction can be observed when gold is combined with TiO₂ NPs. While not necessarily used for antimicrobial therapy yet, various

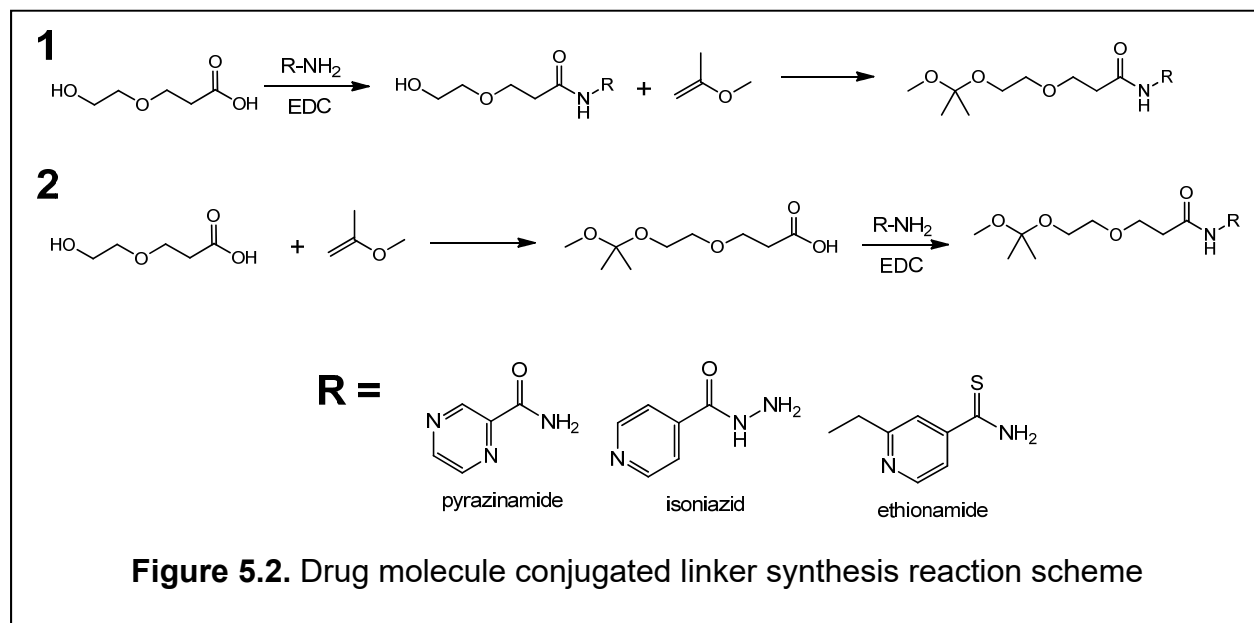
groups in the cancer research field are already applying the strategy of multi-stimuli-responsive particles ¹⁰.



5.2.2. Modification of Linker Molecule

The current linker molecule on ATC is 2-aminoethoxyethanol, which is a monomer of polyethylene glycol (PEG). While this material has no inherent toxicity, it does not serve any therapeutic process for the nanoantibiotic system. The current linker did serve as an excellent working model for designing of ATC, but in the long-term, it is cleaved as a byproduct once the polyplex has been endocytosed. To engineer an efficacious nanoantibiotic system, especially one that can hinder the growth or destroy intracellular bacteria, an antibiotic with therapeutic significance would be an ideal molecule to conjugate to chitosan through the same pH-responsive linker.

Various small drugs can be conjugated to chitosan that will adequately serve the purpose of eradicating intracellular bacteria. For example with *tuberculosis* three drugs that are given as frontline drugs for the treatment of persistent TB, infections could be the candidates. Pyrazinamide, isoniazid, and ethionamide^{11,12} are three drugs usually prescribed when an infection is detected. Pyrazinamide is a membrane damaging agent against tuberculosis. It acts as an ionophore and leads to cellular acidification. This disruption in pH is an important part of proton motive force, which also kills metabolically dormant cells at acidic pH under oxygen-limiting conditions. This type of microbe targeting is energy dependent metabolism disrupting. Isoniazid is along the same line of anti-TB drugs; the pathway leads to the inhibition of mycolic acid, which is required for synthesis of mycobacteria. Another of the first line of prescribed anti-TB drugs is ethionamide. However, ethionamide is uncommonly prescribed in the regiment of drugs used to treat multi-drug resistant (MDR) TB or extensively drug-resistant (XDR) TB¹² The mechanism of action is like that of isoniazid.



This modification could be easily accomplished by repeating the reaction mechanism detailed in a previous publication, in which anti-tuberculosis drugs were conjugated to chitosan^{13,14}. Briefly, the first step is the preparation of *O*-carboxymethylated (OCMC) chitosan which was accomplished with the reaction of 1 g of Chitosan suspended in 10 mL of 2-propanol, and chloroacetic acid is added. Reaction proceeds for 2 hours and the product is precipitated in acetone. Subsequently, 500 mg of OCMC is dissolved in water, and 200 mg of the appropriate drug (Pyrazinamide, Isoniazid, or Ethionamide) is added. The reaction mixture is cooled to 0 – 5 °C and 220 mg of *N*-(3-dimethylaminopropyl)-*N'*-ethylcarbodiimide (EDC) is added as a crosslinker. The reaction proceeds for 3 hours. After, the reaction is brought back up to room temperature, and the product precipitated with acetone. Upon confirmation of product by NMR, another material (Figure 5.2) will be made that maintains the acid-cleavable region. Starting with 3-(2-Hydroxyethoxy)propanoic acid, EDC and the appropriate drug can be conjugated at a 1:1-mole ratio at 0 – 5 °C in tetrahydrofuran. After 3 hours the reaction

can be stopped, and the crude ^1H NMR will be checked to confirm the generation of desired product. The product will be purified using column chromatography. That product will then be reacted with 2-methoxypropene, in anhydrous THF and 5 Å sieves to remove water and methanol. The TLC of the product will be checked, along with a crude ^1H NMR, followed by purification on a column depending on whether the final product is recovered. After synthesis of the new drug conjugated linker molecule, a modified ATC will be generated. An alternate route of synthesis will consist of using protected half acetal (HA) deprotecting it in 1M NaOH, followed by reaction with EDC, and drug molecule¹⁵ at a 1:1-mole ratio. The product can be collected and purified by column chromatography.

5.2.3. Designing nucleic acid targets against drug-resistance enablers

The final piece in the engineering of a multi-faceted nanoantibiotic drug that will specifically target drug-resistant intracellular bacteria is the use of genetically specific nucleic acids. The provided genetic specificity will increase the antibiotic capability of the system. To achieve efficient treatment of prokaryotic infections, engineering specific crRNA sequences that facilitate the silencing of drug-resistance enablers is indispensable. There are various facilitators of drug resistance in microbes (Table 5.1). Designing the genetic sequences that can silence just one of the common facilitators would be highly advantageous and beneficial to the design of the nanoantibiotic. Recent studies have shown the capabilities of sensitizing drug-resistant bacteria by silencing the expression using CRISPR RNA (crRNA)¹⁶.

Ideally, purchasing crRNA that silence the drug-resistant proteins in the microbes directly would be the course of action, but considering crRNA use and understanding is still in infancy there is a likelihood of not finding the specific sequences necessary for that drug resistance protein. Therefore, in this case, the well-understood siRNA-mediated RNAi in eukaryotes can be a good model to mimic. Eukaryotic siRNA can be prepared by chemical synthesis and transcription *in vitro*, or used as longer dsRNA for delivery followed by further intracellular processing (diced to shorter siRNA). Chemical synthesis of siRNA starts with the sequence selection in a target cDNA complementary to 5'-AA(N19)UU-3' (N to be any nucleotide) in the mRNA with desirably about 50% G to C content ¹⁷. Then the sense RNA 5'-(N19)TT-3' and antisense RNA 5'-(N'19)TT-3' are synthesized, where N'19 is the reversely complementary to N19. The confirmed

Table 5.1. Drug-resistance enablers for MDRMOs (common in bold) ¹⁸

MDRMO	Alterers	Blockers	Expellers	Ref.
<i>S. aureus</i>	MphC, VatA-E	MecA, dhfr , mupA, fucA, gyrA, gyrB, fabI , VanA , rpoB	MSF (NoA, TetK-L , MdeA) QacA, MepA, ABC (MsrA)	9,14,17,19, 21, 22, 24
<i>Enterococci faecium</i>	VatA-E	PBP, VanA , VanC->E VanG	MSF (Mef, TetK-L , EmeA) ABC (Lsa)	19, 21, 24
<i>Neisseria gonorrhoeae</i>	Not Available	ponA	MtrD	9, 19, 21, 24
<i>M. tuberculosis</i>	ARR, katG, inhA, embB, BlaC	pncA, rpoB , GyrA , gyrB	MSF (TetK-L), ABC (DrrB), Mmr	18,19, 21, 24, 27
<i>Klebsiella pneumoniae</i>	KPC2, SFC1	Mosaic PBP, dhfr	MSF (MefE, PmrA, TetK-L)	19, 21, 24
<i>E. coli</i>	MphB, ereA, ereB, TEM1, TEM2, SHV1, CTX-M	Erm, fabI	MSF (TetA-E, BCr, MDfA, YceL, Emr), ABC (MacB, Lmr), RND (AcrD, MexAR-OrnM)	9,18,19, 21, 22, 24, 26

sequences, confirmed by Basic Local Alignment Search Tool (BLAST) will be annealed to produce siRNA duplexes. The process contains some flexibility in meeting these exact sequence specifications. Similarly, *in vitro* siRNA preparation, an 18mer oligonucleotide along with a T7 promoter sequence is annealed to form 38mer oligonucleotides containing the sequence complementary to the target ¹⁹. The transcribed 19mer RNA includes 2 extra nucleotides. The sense and antisense transcripts are then annealed and precipitated in ethanol to recover the resulting siRNAs. An approach similar to the siRNA preparation has been explored for obtaining crRNAs. Briefly, a target RNA is extracted, sequenced, and amplified by T7 RNA polymerase. Then pre-crRNA with a complementary sequence to the amplified RNA is generated and recovered by ethanol precipitation, followed by annealing with a complementary crRNA to generate duplexes ^{20,21}.

5.2.4. Challenges for nanoantibiotics

With all the promise of nAbts comes challenges that must be addressed before widespread clinical use can be adopted. The two main challenges of nanomaterials in biological applications are toxicity of the material and large-scale manufacturing of those materials.

5.2.4.1 Toxicity

Various nAbts, particularly metallic and carbon-based ones, have severe toxicity generated from prolonged exposure. Although silver NPs provide many benefits, prolonged exposure to soluble silver-containing compounds may produce an irreversible

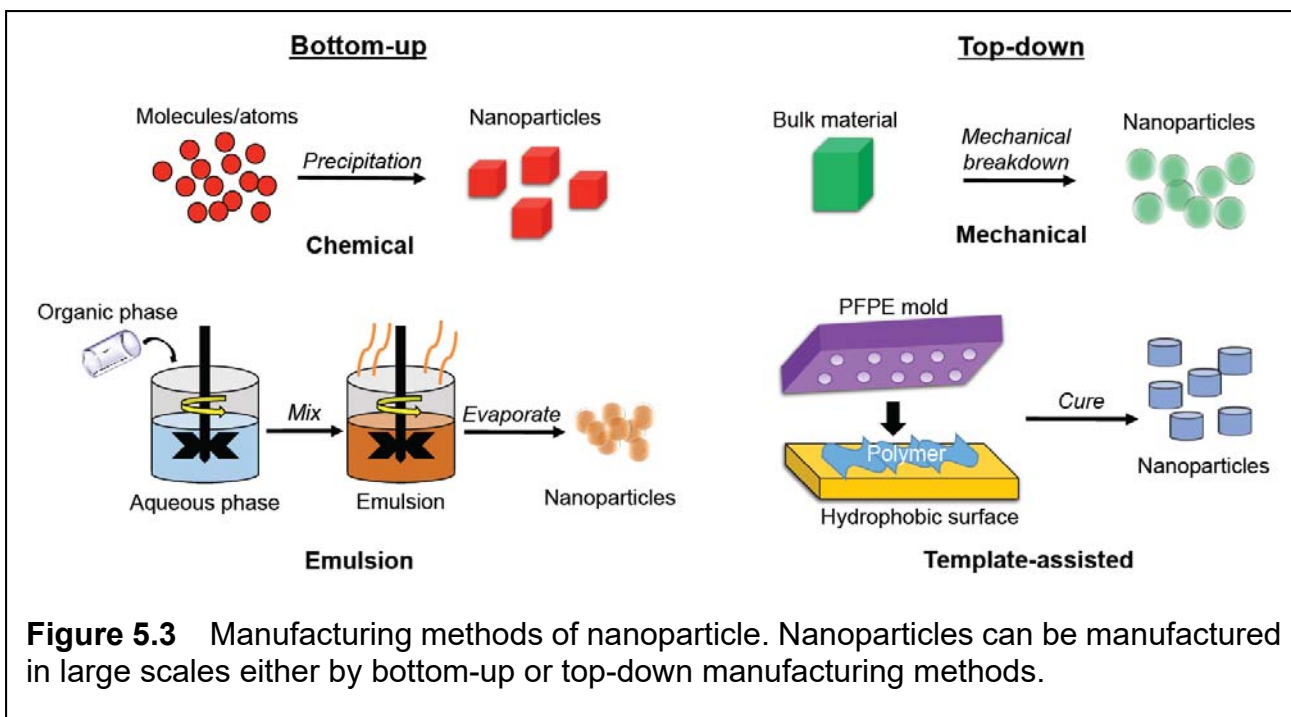
pigmentation in the skin (argyria) and the eyes (argyrosis) in addition to other toxic effects²². Some studies provide a direct contradiction to this, claiming minimal concentration-dependent toxic effects^{22,23}. These concentration-dependent toxicities in mammalian cells have been shown in other studies using metallic nanoparticles^{24,25}. Similarly, while nanotubes and fullerenes have been shown to be potentially toxic, there are some contradictions which suggest that the toxicity may be due to solvent contaminants during preparation^{26,27}. For one, a suspension of nC₆₀ prepared without THF lacked toxicity²⁸. Moreover, nC₆₀ prepared without using any polar organic solvent lacked any acute or subacute toxicity in rodents²⁹. And although these potential side-effects limit their applications, their use should not be disregarded entirely. A complete elucidation of nanoparticle toxicity needs to be ascertained before extensive manufacturing induced exposure.

In general, there has been increased scrutiny over the toxicity of nanoparticles due to increased use in various industries. Not only in the application, but also in the manufacturing of nanoparticles as those who manufacture the nanoparticles will experience the most exposure. Silver NPs have been analyzed to determine their toxicity when manufactured. Based on a continuous 3-day exposure assessment, it was evident that workers were exposed to high levels of nanoparticles on a day-to-day basis; similar results were also found for other metallic and carbon NP manufacturing³⁰. While the exact toxicities of long-term overexposure are still completely unknown, a recent study by Das et al.³¹ looks at the potential toxicity to mammalian germ cells and developing embryos from engineering nanoparticles such as gold, silver, fullerenes, and chitosan. They summarize various toxicities based on nanoparticle uptake and internalization

mechanisms. The major emphasis of the study is that while some nanoparticles may not have any acute toxicity, there is a possibility that there is some long-term toxicity or effect to germ lines to consider. The authors disclose that a large percentage of these toxicities are mostly dependent on NP size and surface modifications. Taking those variables into consideration when designing and engineering nAbs can aid in ameliorating the possible toxicities that may arise.

5.2.4.2 Large-scale manufacturing

Scale-up for creating nanoparticles requires sophisticated techniques.³² Two key pathways to generate nanoparticles are through chemical or mechanical routes³³; these can also be considered as bottom-up or top-down manufacturing approaches respectively (Figure 5.3)³⁴. A bulk material may be dissolved chemically into molecular entities to yield a distinct molecular intermediate form of the material. That intermediate is then reacted kinetically or processed further using stabilizing agents such as emulsifiers. Generation of silver nanoparticles from silver nitrate is an excellent example of a chemical route³³. Alternatively, mechanical energy can also be applied to a bulk material to split it into smaller particles. This usually requires heavy machinery such as a mill. Regardless of the chosen pathway, most particles are modified, whether by some type of surface modification or another type of customization, before further use³³.



Another method used to industrially generate nanoparticles is an emulsion type system^{35,36}. This is a bottom-up synthesis approach that has some similarity to chemical synthesis route. Instead of distinct intermediates being formed, the emulsion route allows for the formation of nanoparticles based on an oil-water system. The versatility of the reactor system, where starting materials may simply be mixed, serves as an advantage for this system. A disadvantage of the emulsion system is that it will be limited to only certain types of nanoparticles made with materials that are soluble in an organic phase or an aqueous layer, and thus, it cannot be widely used.

The other end of the spectrum for scaling and manufacturing is the top-down approach of templated systems^{37,38}. Using cast molding generated from polydimethylsiloxane (PDMS), different shapes and sizes can be generated for a material that can be cured and dried, usually a polymeric material. While most nAbts are not applicable to this technique, there might be a way of combining the stimuli-responsive

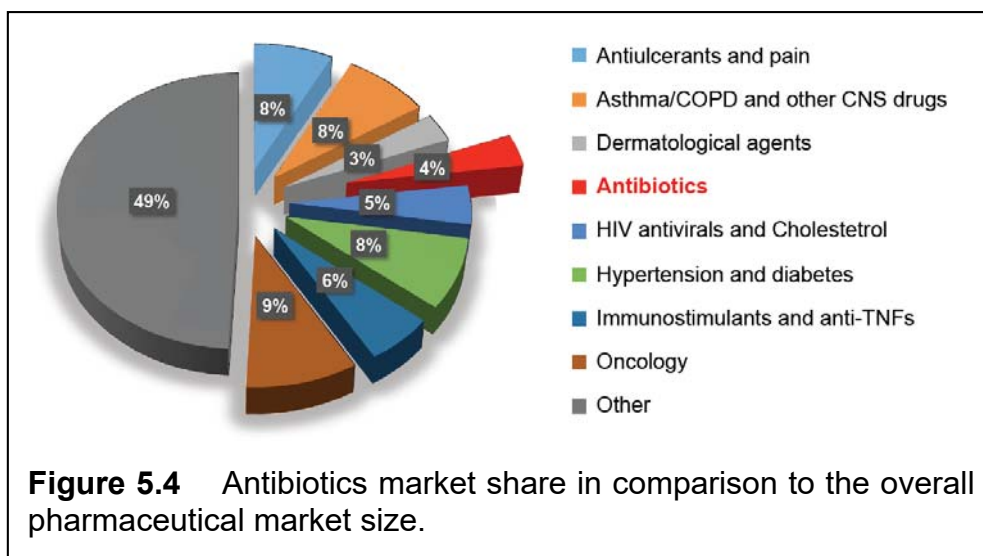
linkers or polymers that will allow for the template-assisted system to be leveraged. The main advantage of using a template-like system is the ability to make many uniform nanoparticles very rapidly. This would reduce the cost of manufacturing for pharmaceutical applications while being able to maintain consistent quality. This consistency is something that the bottom-up approach may lose. The downside is the limited source materials that can be used in the template-assisted systems.

One thing is certain, when industrial scale manufacturing of nAbts comes into question, attempting to use just one system may not be adequate to serve a broad therapeutic need. Entities that decide to venture into commercializing nAbts for therapeutic applications need to consider which systems they are trying to target, and what would be the safest and most economical way to accomplish that goal.

5.2.5. Future directions for nanoantibiotics

Worldwide, scientists are scrambling to discover and uncover new ways to fight off infections. The rate of drug-resistant formation is frightening, and while there are many promising new compounds and products being introduced, unfortunately, that is still not enough. The major problem lies in the fact that we are stalled in this persistent paradigm of discovering new antibiotics. Of the few pharmaceutical companies that invest money into the discovery of new antibiotics, most do not see a return on their investment. This makes the prospect of developing new antibiotic highly unattractive from that standpoint.

However, the difficulty in developing new antibiotic compounds stems from the fact that most new antibiotic compounds are found from another, competing microbe^{39,40}. nAbts circumvent that system by using a completely different mechanism of action; moreover, they are also highly versatile and tunable. This allows for the ubiquitous use of nAbts. Antimicrobials are used in a multitude of industries such as livestock and agriculture, water treatment, military, and clinics; however, sr-nAbts will most likely thrive in industries that require the precise release of certain antibiotic effect after certain conditions are met. One possible application is to apply it to on-site or field-based medical devices, where autoclave or sterilization is not easily accessible. This will allow for situations where temperature, light, or pH-responsive nAbts coated materials can react to sterilize an environment. The same system can also be used in the design of a water treatment system where the filter self-cleans and sterilizes itself. Another possible direction would be a theranostic system for antimicrobial infections. This is a relatively



direct venture if the nAbts system is stimuli-responsive. The timing of such a system would be most useful in topical applications, or applications where an infection status may be uncertain. These types of nAbts theranostic system could also be very useful in curbing

the spread of sexually transmitted infections, such as *Neisseria gonorrhoea*, by applying them to contraceptives. Bacteriophages, though excluded can be classified as bio-active nanoantibiotics. These phages are virus-like particles that selectively kill bacteria when they infect them, without any damage to the eukaryotic cell ⁴¹. Furthermore, phages can be modified with stimuli-responsive functionalities that allow for added efficacy and capabilities ⁴². Additionally, non-lytic phages can be engineered to permit use as vaccines or diagnostic tools against specific bacterial infections ⁴³.

It is important to note, fortunately, that the antibiotic industry is gaining some steam. Aside from the obvious need, this renewed interest in antimicrobial discovery is

Table 5.2 Examples of commercial nanoantibiotics products				
Company	Product	Composition	Current application	Development stage
Insmed	Arikace	Liposomal amikacin	Chronic <i>P. aeruginosa</i> Infection	Clinical trial (phase 3)
Staten Serum Institute	CAF09	Cationic liposome-based adjuvant	Tuberculosis, HIV	Preclinical
Smith & Nephew	Acticoat	Ag NP coated polyethylene mesh	Wound dressing	Marketed
I-Flow	ON-Q Silver Soaker	Ag NP coated polyvinylchloride	Catheter for delivery of local anesthetics	Marketed
Benanova	EbNP	Ag ions embedded in lignin	Nanosilver substitute	Marketed
INGMedical	Antimicrobial textiles	Electrospun textiles with metallic NPs	Medical devices	Marketed
NanoBio	NanoStat	Nanoemulsion based carrying various adjuvants	Intranasal/intramuscular vaccine delivery	Completed phase 1
IBM	-----	Stimuli-responsive polymer hydrogel	Antimicrobial	Pre-clinical

likely due to the expected increase in the value of the industry. BCC Research reports the market to be worth about 40.6 billion in 2015 with an expected compound annual growth rate of 2.0% within the next 5 years ^{44,45}. Regardless of the source, whether it is IBIS World Industry Report, Statista, or BCC Research Reports, there is a general agreement over the size of the current antimicrobial market. However, the forecasted direction of the market is still uncertain. This uncertainty might be caused by the upcoming patent cliffs, production of cheaper generics, or the loss of efficacy due to the drug-resistance formation. Irrespective of that, about 3.7% of the over 1 trillion-dollar pharmaceuticals industry ⁴⁴ is focused on antibiotics(Figure 5.3). While it may not be the largest sector, it has been drawing increased interest. Interestingly enough, the number of clinical devices focusing on some sort of nAbts application that has received approval for use continues to increase (Table 5.2) ⁴⁶.

The ability to directly target drug-resistant strains of various microbes can provide a vital impact on the state of global medicine. The use and availability of a natural nanomaterial that can innately affect the growth of various strains of microbes will increase access, especially for those in various socioeconomic classes and developing countries that may not necessarily have traditional antibiotics readily available. Aside from direct use, nanoantibiotics can also be used to treat water systems all over the world, which will make help microbe polluted waters drinkable. There can also be additional use in agriculture and livestock.

5.3. References

- (1) Schmaljohann, D. *Adv. Drug Deliv. Rev.* **2006**, *58* (15), 1655–1670.
- (2) Fayaz, A. M.; Balaji, K.; Girilal, M.; Yadav, R.; Kalaichelvan, P. T.; Venketesan, R. *Nanomedicine Nanotechnology, Biol. Med.* **2010**, *6* (1), 103–109.
- (3) Rai, A.; Prabhune, A.; Perry, C. C. *J. Mater. Chem.* **2010**, *20* (32), 6789.
- (4) Oliveira, J. R.; Cristina, M.; Martins, L.; Mafra, L.; Gomes, P. *Carbohydr. Polym.* **2011**, *87*, 240–249.
- (5) Zhang, C.; Ping, Q.; Zhang, H.; Shen, J. *Eur. Polym. J.* **2003**, *39* (8), 1629–1634.
- (6) Lillo, L. E.; Yamamoto, B. M. *Carbohydr. Polym.* **1998**, *34* (4), 397–401.
- (7) Smith, M. A.; Barnard, C. A.; Ladner, D. A. *ACS Symp. Ser.* **2013**, *1123*, 189–203.
- (8) aureus aeruginosa, S. P.; coli Kiran Gupta, E.; Singh, R. P.; Pandey, A.; Pandey, A. *Beilstein J. Nanotechnol* **2013**, *4*, 345–351.
- (9) Ivanova, T.; Harizanova, A.; Koutzarova, T.; Vertruyen, B. *Opt. Mater. (Amst)*. **2013**, *36* (2), 207–213.
- (10) An, X.; Zhu, A.; Luo, H.; Ke, H.; Chen, H.; Zhao, Y. *ACS Nano* **2016**, *10*, 5947–5958.
- (11) Pálfi, G.; Dutour, O.; Perrin, P.; Sola, C.; Zink, A. *Tuberculosis*. 2015, pp S1–S3.
- (12) Cynamon, M. H.; Sklaney, M. *Antimicrob. Agents Chemother.* **2003**, *47* (8), 2442–2444.

- (13) Fan, L.; Du, Y.; Zhang, B.; Yang, J.; Zhou, J.; Kennedy, J. F. *Carbohydr. Polym.* **2006**, *65* (4), 447–452.
- (14) Vavříková, E.; Mandíková, J.; Trejtnar, F.; Horváti, K.; Bösze, S.; Stolaříková, J.; Vinšová, J. *Carbohydr. Polym.* **2011**, *83* (4), 1901–1907.
- (15) Hurdle, J. G.; O'Neill, A. J.; Chopra, I.; Lee, R. E. *Nat. Rev. Microbiol.* **2011**, *9* (1), 62–75.
- (16) Yosef, I.; Manor, M.; Kiro, R.; Qimron, U. *Proc. Natl. Acad. Sci.* **2015**, *112* (23), 7267–7272.
- (17) Elbashir, S. M.; Harborth, J.; Weber, K.; Tuschl, T. *Methods* **2002**, *26* (2), 199–213.
- (18) Edson, J. A.; Kwon, Y. J. *Journal of Controlled Release*. Elsevier 2014, pp 150–157.
- (19) Donzé, O.; Picard, D. *Nucleic Acids Res.* **2002**, *30* (10), e46.
- (20) Richter, H.; Zoepfel, J.; Schermuly, J.; Maticzka, D.; Backofen, R.; Randau, L. *Nucleic Acids Res.* **2012**, *40* (19), 9887–9896.
- (21) Richter, H.; Randau, L.; Plagens, A. *Int. J. Mol. Sci.* **2013**, *14* (7), 14518–14531.
- (22) Huh, A. J.; Kwon, Y. J. *J. Control. Release* **2011**, *156* (2), 128–145.
- (23) Ivask, A.; Kurvet, I.; Kasemets, K.; Blinova, I.; Aruoja, V.; Suppi, S.; Vija, H.; Käkinen, A.; Titma, T.; Heinlaan, M.; Visnapuu, M.; Koller, D.; Kisand, V.; Kahru, A. *PLoS One* **2014**, *9* (7), e102108.

- (24) Ning, C.; Wang, X.; Li, L.; Zhu, Y.; Li, M.; Yu, P.; Zhou, L.; Zhou, Z.; Chen, J.; Tan, G.; Zhang, Y.; Wang, Y.; Mao, C. *Chem. Res. Toxicol.* **2015**, *28* (9), 1815–1822.
- (25) Li, M.; Ma, Z.; Zhu, Y.; Xia, H.; Yao, M.; Chu, X.; Wang, X.; Yang, K.; Yang, M.; Zhang, Y.; Mao, C. *Adv. Healthc. Mater.* **2016**, *5* (5), 557–566.
- (26) Lyon, D. Y.; Adams, L. K.; Falkner, J. C.; Alvarez, P. J. J. *J. Environ. Sci. Technol.* **2006**, *40* (14), 4360–4366.
- (27) Xia, X. R.; Monteiro-Riviere, N. A.; Riviere, J. E. *Toxicol. Lett.* **2010**, *197*, 128–134.
- (28) Maeda-Mamiya, R.; Noiri, E.; Isobe, H.; Nakanishi, W.; Okamoto, K.; Doi, K.; Sugaya, T.; Izumi, T.; Homma, T.; Nakamura, E. *Proc. Natl. Acad. Sci. U. S. A.* **2010**, *107* (12), 5339–5344.
- (29) Gharbi, N.; Pressac, M.; Hadchouel, M.; Szwarc, H.; Wilson, S. R.; Moussa, F. *Nano Lett.* **2005**, *5* (12), 2578–2585.
- (30) Lee, J. H.; Ahn, K.; Kim, S. M.; Jeon, K. S.; Lee, J. S.; Yu, I. J. *J. Nanoparticle Res.* **2012**, *14* (9), 1134.
- (31) Das, J.; Choi, Y.-J.; Song, H.; Kim, J.-H. *Hum. Reprod. Update* **2016**, *22* (5), 588–619.
- (32) Roco, M. C. In *Nanostructured Materials*; Springer Netherlands: Dordrecht, 1998; pp 71–92.
- (33) Stark, W. J.; Stoessel, P. R.; Wohlleben, W.; Hafner, A. *Chem. Soc. Rev.* **2015**,

- 44 (16), 5793–5805.
- (34) Rossi, G. B.; Beaucage, G.; Dang, T. D.; Vaia, R. A. *Nano Lett.* **2002**, 2 (4), 319–323.
- (35) Zhou, Z. H.; Wang, J.; Liu, X.; Chan, H. S. O. *J. Mater. Chem.* **2001**, 11 (6), 1704–1709.
- (36) Brunel, F.; Veron, L.; David, L.; Domard, A.; Delair, T. *Langmuir* **2008**, 24 (20), 11370–11377.
- (37) Morton, S. W.; Herlihy, K. P.; Shopsowitz, K. E.; Deng, Z. J.; Chu, K. S.; Bowerman, C. J.; Desimone, J. M.; Hammond, P. T. *Adv. Mater.* **2013**, 25 (34), 4707–4713.
- (38) Kuznetsov, A. I.; Evlyukhin, A. B.; Gonçalves, M. R.; Reinhardt, C.; Koroleva, A.; Arnedillo, M. L.; Kiyan, R.; Marti, O.; Chichkov, B. N. *ACS Nano* **2011**, 5 (6), 4843–4849.
- (39) Lewis, K. *Nat. Rev. Drug Discov.* **2013**, 12 (5), 371–387.
- (40) Payne, D. J.; Gwynn, M. N.; Holmes, D. J.; Pompliano, D. L. *Nat. Rev. Drug Discov.* **2007**, 6 (1), 29–40.
- (41) Sunderland, K.; Yang, M.; Mao, C. *Angew. Chemie Int. Ed.* **2016**, epub ahead of print.
- (42) Cao, B.; Yang, M.; Mao, C. *Acc. Chem. Res.* **2016**, 49 (6), 1111–1120.
- (43) Huai, Y.; Dong, S.; Zhu, Y.; Li, X.; Cao, B.; Gao, X.; Yang, M.; Wang, L.; Mao, C. *Adv. Healthc. Mater.* **2016**, 5 (7), 786–794.

- (44) BPI; IMS Health. *Revenue of the worldwide pharmaceutical market from 2001 to 2014 (in billion U.S. dollars)*; New York, NY, 2016.
- (45) BCC Research. *Antibiotics: Technologies and Global Markets - PHM025D*; Wellesley, MA, 2016.
- (46) Zhu, X.; Radovic-Moreno, A. F.; Wu, J.; Langer, R.; Shi, J. *Nano Today* **2014**, *9* (4), 478–498.